UNIVERSITÀ DEGLI STUDI DI PADOVA

SEDE AMMINISTRATIVA: UNIVERSITÀ DEGLI STUDI DI PADOVA

DIPARTIMENTO DI BIOLOGIA

SCUOLA DI DOTTORATO DI RICERCA IN BIOSCIENZE E BIOTECNOLOGIE

INDIRIZZO: BIOTECNOLOGIE

CICLO XXIV

PLANT DERIVED SWEET AND ICE STRUCTURING PROTEINS AS NEW TOOLS IN FOOD PROCESSING

Direttore della Scuola: Ch.mo Prof. Giuseppe Zanotti

Coordinatore d'indirizzo: Ch.mo Prof. Giorgio Valle

Supervisore: Ch.mo Prof. Luigi Bubacco

Dottoranda: Elena Reghelin

Table of contents

CHAPTER 3

RESULTS - Expression, purification and characterization of the sweet protein brazzein 81

ABSTRACT

Among bioindustries, agribusiness is one of the most important application of biotechnology. The aim of this work is the design and production of recombinant proteins to improve food quality. Food quality comprises various aspects such as the conservation process, generally understood as shelf-life, the physical (e.g. color, texture, taste) and nutritional properties of food or the ability to produce food suitable for people with food intolerances or specific diseases.

Since sucrose over-intake has been implicated in different pathologies such as obesity, caries, and diabetes mellitus, our first research topic was a non-calorigenic protein sweetener. Among the sweet-tasting proteins isolated until now, brazzein seems to be the most promising one. The limited availability of the natural brazzein source has rendered large-scale production of brazzein from its natural source not viable. Recombinant DNA technology provides a feasible and cheaper alternative for mass production. Therefore, we develop an efficient method for brazzein inducible or constitutive expression in the GRAS (Generally Recognized As Safe) yeast *Pichia Pastoris*; about 200 mg of brazzein was obtained from a 1.5 liter fermentation volume. A safe and low cost purification process was optimized taking advantage of cation exchange chromatography, resulting in a final brazzein purity of 99.98 %. The purified protein was then characterized by several techniques: mass spectrometry, calorimetry and NMR analysis were performed to evaluate respectively the mass/post-translational modifications present in the final product, and the thermal stability of brazzein; NMR experiments were also performed to confirmed the structural similarity of the recombinant brazzein with the wild-type brazzein extracted from the natural plant; a taste panel assay for sweet taste control allowed us to determine the sweetness potency of the produced recombinant protein; finally, we evaluated the allergenic potential of brazzein by sequence analysis and pepsin digestion.

With regard to an improvement of the shelf-life and of the physical properties of food we focused our attention on a protein suitable for frozen food applications. In particular we are interested in the inhibition of ice recrystallization, a phenomenon by which larger ice crystals grow at the expense of smaller ones at temperature close to 0 °C. The ability of ISPs (Ice Structuring Proteins; that protect organisms that live in sub-zero environments from the deleterious effects of ice crystals' formation in cells) to retard ice recrystallization makes them suitable for the food industry as natural ice

modulators for cold storage of frozen products such as ice cream. In particular, plant ISPs are good inhibitors of the ice-recrystallization process compare to other ISPs (e.g. fish and insect ISPs). Therefore, we identified a promising wheat (*Triticum aestivum*) ISP and we did the first steps towards the development of an expression method for its industrial production. To perform preliminary studies we expressed this ISP in different *Escherichia coli* strains, obtaining a very low quantity of the recombinant protein, which precipitated in the pellet during the purification process. Hence, in order to obtain high levels of soluble recombinant ISP, we moved to the *P. pastoris* expression system. We constitutively expressed different form of this protein: with or without an histidine tag at the C-terminus, and with or without the *Saccharomyces cerevisiae* α-factor secretion signal. Thanks to experiments on a small scale we determined that only the wild type protein with the α-factor was expressed, and that its observed molecular weight is comparable with the expected one. Future development will be the scale-up of the process, the optimization of a purification protocol, and the characterization of the produced protein. Finally, in order to study the possible applications of an ISP as ingredient in the food industry or as cryoprotectant in medicine (another scope for ISPs application), we set up an experimental approach to evaluate the ice recrystallization inhibition activity and the cryopreservation ability of different ISP sources (wheat extract, and type I and II fish ISPs).

RIASSUNTO

Tra le bioindustrie quella agroalimentare rappresenta uno dei campi più importanti di applicazione delle biotecnologie. Obiettivo di questo lavoro è la progettazione e produzione di proteine ricombinanti al fine di migliorare la qualità del cibo. La qualità può interessare diversi aspetti come ad esempio il processo di conservazione intesa come *shelf-life* ('vita di scaffale', ossia il periodo durante il quale un prodotto può essere tenuto presso un punto vendita al dettaglio senza che vengano alterate le sue qualità), le proprietà fisiche (es. colore, consistenza, sapore) e nutrizionali dell'alimento, o la possibilità di produrre cibi adatti a persone con intolleranze alimentari o con particolari malattie.

Dato che un eccessivo consumo di saccarosio è implicato in varie patologie come ad esempio l'obesità, le carie e il diabete, il nostro primo tema di ricerca si è focalizzato su una proteina dolcificante non-calorica. Tra le proteine dolcificanti isolate finora, la brazzeina sembra essere la più promettente. La disponibilità limitata della fonte naturale di brazzeina ha reso economicamente non sostenibile la sua produzione su scala industriale a partire dalla fonte naturale. La tecnologia del DNA ricombinante costituisce un'alternativa praticabile e più economica per la produzione su ampia scala. Abbiamo pertanto sviluppato un metodo efficiente per l'espressione inducibile o costitutiva della brazzeina nel lievito GRAS (*Generally Recognized As Safe*) *Pichia Pastoris*; circa 200 mg di brazzeina sono stati ottenuti da un volume di fermentazione pari a 1.5 litri. Abbiamo inoltre ottimizzato un processo di purificazione sicuro ed economico mediante cromatografia a scambio cationico, ottenendo la brazzeina con una purezza finale pari al 99.98 %. La proteina purificata è stata poi caratterizzata mediante divere tecniche: spettrometria di massa, analisi calorimetriche e NMR sono state effettuate per valutare rispettivamente la massa e le modifiche post-traduzionali presenti nel prodotto finale, e la stabilità termica della proteina; analisi NMR sono state effettuate anche per confermare la similarità di struttura della proteina prodotta per via ricombinante, con quella della proteina *wild-type* direttamente estratta dalla pianta; un saggio per determinare l'intensità del gusto dolce ci ha permesso di definire la '*sweetness potency*' della brazzeina ricombinante; abbiamo infine analizzato il potenziale allergenico della brazzeina mediante analisi della sua sequenza amminoacidica e digestione con l'enzima gastrico pepsina.

Per quanto riguarda il miglioramento della *shelf-life* e delle proprietà fisiche dei cibi, abbiamo concentrato la nostra attenzione su una proteina

interessante per l'applicazione in prodotti surgelati. In particolare siamo interessati all'inibizione della ricristallizzazione, fenomeno che causa la formazione di grandi cristalli di ghiaccio a spese di cristalli piccoli a temperature vicine ai 0 °C. L'abilità delle ISPs (*Ice Structuring Proteins*; proteine che proteggono gli organismi che vivono a temperature inferiori allo zero dagli effetti deleteri della formazione di cristalli di ghiaccio nelle cellule) di inibire il fenomeno della ricristallizzazione le rende interessanti per l'industria alimentare come naturali modulatori del ghiaccio per la conservazione di prodotti surgelati come ad esempio il gelato. In particolare, è stato visto che le ISPs di pianta sono degli ottimi inibitori della ricristallizzazione del ghiaccio. Abbiamo pertanto identificato una promettente ISP di grano (*Triticum aestivum*) e abbiamo fatto i primi passi verso lo sviluppo di un metodo di espressione per la sua produzione a livello industriale. Al fine di effettuare degli studi preliminari abbiamo espresso la ISP in diversi ceppi di *Escherichia coli*, ottenendo però una piccolissima quantità di proteina ricombinante che, oltretutto, precipita nel *pellet* durante il processo di purificazione. Quindi, al fine di ottenere alti livelli di ISP solubile, siamo passati al sistema di espressione costitutiva in *P. pastoris*. La proteina è stata espressa in diverse forme: con e senza coda di istidine al C-terminale, e con e senza il fattore di secrezione *α-factor* di *Saccharomyces cerevisiae*. Grazie a esperimenti su piccola scala abbiamo determinato che solamente la proteina *wild type* con l'*α-factor* viene espressa, e che il suo peso molecolare osservato è comparabile con quello atteso. Sviluppi futuri riguarderanno lo *scale-up* del processo di espressione, l'ottimizzazione di un protocollo di purificazione e la caratterizzazione della proteina prodotta. Per concludere, al fine di studiare la possibile applicazione di una ISP come ingrediente nell'industria alimentare o come crioprotettore in medicina (altra possibile applicazione delle ISPs) abbiamo messo a punto un protocollo sperimentale per valutare l'attività di inibizione della ricristallizzazione e l'abilità di criopreservazione di differenti fonti di ISPs (estratto di grano, ISPs di tipo I e II di pesce).

Chapter 1

INTRODUCTION

1.1. Brazzein as low-calorie sweetener

1.1.1. Sucrose intake and related diseases

Sucrose over-intake has been implicated in different pathologies such as obesity, caries, cardiovascular disease, hypertension, certain type of cancer and diabetes mellitus.

The global epidemic of overweight and obesity, and the other consequences of sugar over-consumption, is rapidly becoming a major public health problem in many parts of the world (see Figure 1.1). Therefore, the demand for non-calorigenic protein-based sweeteners with taste proprieties resembling those of sucrose is very high.

The generally accepted mechanism responsible for the epidemic increase of obesity and related disease is the thrifty gene hypothesis proposed by James V. Neel in 1962. Before the agricultural and industrial revolutions, availability of food was subjected to seasonality and so the evolution of thrifty genes allowed the maximization of nutrient intake and energy storage when food was available. With the agricultural and industrial progress the availability of (refined) foodstuffs has become virtually unlimited; moreover, motorization of industrial equipment and transportation, and advancements in heating technology and clothing (which diminishes the energy requirements for adaptive thermogenesis), push energy balance upward in many individuals. For all these reasons, individuals genetically predisposed to survive in harsh circumstances have become particularly susceptible to gain weight. Thus, the thrifty gene hypothesis proposes that people that carry a hereditary trait to maximize ingested calories are the one who run the greatest risk to grow obese in the contemporary industrial civilization (Pijl, 2011).

In this context, the necessity of non-calorigenic sweeteners doesn't represent only the simply creation of a sugar substitute, but focuses to the development of a strategy to fool the human psyche: the sweetness perception satisfy hungry people, but actually, the sweet taste doesn't correspond to a calories intake.

1.1.1.1. Obesity

With more than 1 billion overweight adults, obesity represents a major health problem not only in high income countries, but also in low- and middle-income ones (Figure 1.1).

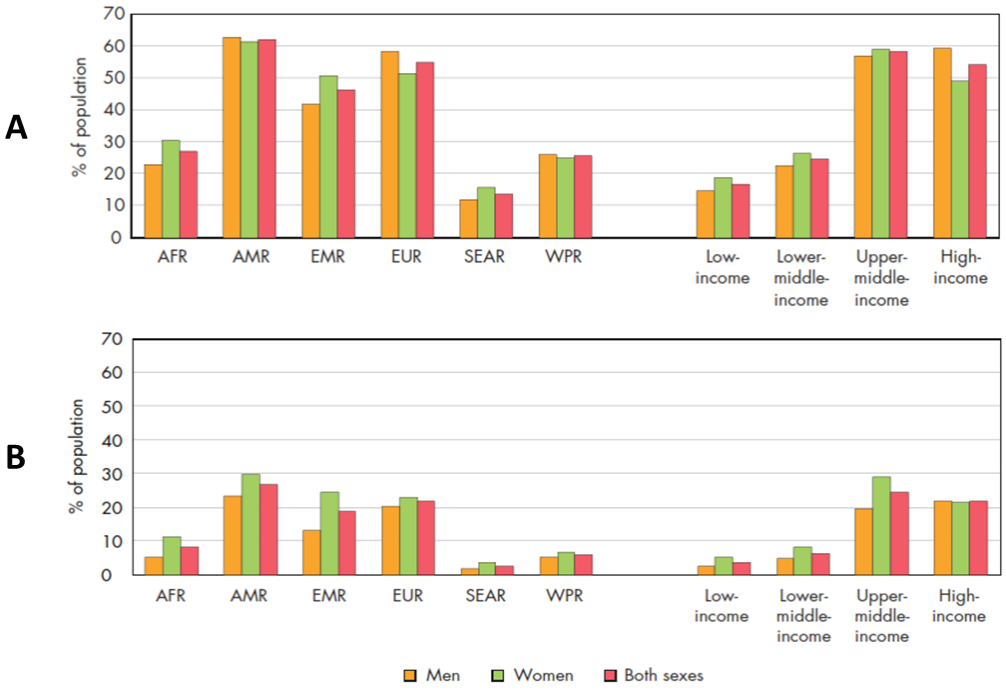

Figure 1.1 - Age-standardized prevalence of overweight (A) and obesity (B) in adults aged 20+ years, by WHO Region and WorldBank income group, comparable estimates, 2008. AFR=African Region, AMR=Region of the Americas, EMR= Eastern Mediterranean Region, EUR= European Region, SEAR=South-East Asia Region, WPR=Western Pacific Region (adapted from Global Status Report on Noncommunicable Disease, WHO, 2010)

The most used criteria to classifying overweight and obesity in adult populations and individuals is the Body Mass Index (BMI). BMI is defined as a person's weight in kilograms divided by the square of their height in meters (kg/m^2). According to this definition overweight is defined as BMI $\geq$ 25 kg/m^2 while obesity is defined as BMI $\geq$30 kg/m^2.

Overweight and obesity represent a major risk factors for chronic disease such as cardiovascular disease (mainly heart disease and stroke), diabetes and cancer (endometrial, breast and colon). Worldwide, 2.8 million people die each year as a result of being overweight (including obesity) (Global Status Report on Noncommunicable Disease, WHO, 2010).

Therefore, it is important to consider the potential impact of diet, and in particular of dietary sugar, on weight management.

Vermunt and coworkers (2003) indicated that the use of low-energy sweeteners instead of sugars might result in lower energy intake and reduced body weight. In 2007 Bellisle and Drewnowsky suggested that diet beverages and foods may help people to reduce their calorie intake, but the effects on weight loss will depend on their integration within a reduced energy diet. Mattes and Popkin (2009) shown that when low calories sweetener are used as substitutes for higher energy sweeteners, they have the potential to aid in weight management, but that there is a need of more information about their use in a long-term study.

Therefore, in a weight-loss program, the use of low calories sweetener can help people to reduce their energy intake contributing to weight loss or weight maintenance. Moreover, it is important to underline that a complete and effective weight-loss program has to focus not only on a reducing energy intake, but also to an increasing energy expenditure through a regular physical activity.

1.1.1.2. Caries

In regard to contributions to dental caries, there is convincing evidence derived from human intervention studies, epidemiological studies, animal studies and experimental studies, that suggests an association between the amount and frequency of sugars consumption and the development of caries (Moynihan *et al*., 2004). In the mouth sugars such as glucose, fructose and sucrose may be convert by α-amylase and bacteria into acid (e.g. lactic acid) which increases the risk of caries due to tooth demineralization. However, the impact of carbohydrates on caries development is dependent on several factors including the amount and frequency of sugars consumption, degree of oral hygiene performed, fluoride availability, salivary function, and genetic factors.

1.1.1.3. Diabetes

To date, nearly 300 million people in the world are affected by diabetes (IDF, International Diabetes Federation, 2010). The top ten countries, in number of people with diabetes, are: India, China, USA, Indonesia, Japan, Pakistan, Russia, Brazil, Italy and Bangladesh. As a general definition, diabetes could be recognized as a chronic disease caused by insulin deficiency, impaired effectiveness of insulin action,

or both (Diabetes Atlas website). The diet of diabetic patients for the control of blood glucose requires the consumption of low-calories, possibly sugar-free, foods and drinks. Therefore, for diabetic patients, the development and use of low calories sweeteners is a valid alternative to maintain the pleasure of the sweet taste without raising blood glucose.

1.1.2. Artificial sweeteners

Since the most widely used natural sweetener, sugar, has problems associated with its use (as reported in 1.1.1), several artificial low calories sweeteners have been developed. However, as reported below for each single compound, these sweet molecules have undesirable side effects or are deficient in certain respects. Two of the most important problems are the different temporal sweetness profiles of artificial sweeteners which do not exactly match that of sugar, and the presence of off-taste. For these reasons all the known non-caloric sweeteners fail to mimic the real sugar taste. Therefore, it is a common practice to mix two different artificial sweetener having a different temporal profile, in order to create a sweetener blend that matches more closely the temporal and sweetness profile of sugar. Moreover, since their discovery the safety of artificial sweeteners has been controversial: while some research has associated artificial sweeteners with cancers, hepatotoxicity, migraines, and low birth weight, other studies have demonstrated the safety of these sweeteners (Whitehouse *et al.*, 2008). Hence, further investigations are required not only on animal models, but also on large-scale studies in human (Tandel, 2011).

The most used artificial sweeteners in Europe are: Acesulfame potassium, Aspartame, Saccharin and Sucralose.

Acesulfame potassium (E950[1]), also known as Acesulfame K, was approved for food use by the US Food and Drug Administration in 1988 (Food and Drug Administration, 1988) , and its safety was reaffirmed in 2000 by the EU's Scientific commission on Food (European commission opinion, 2000). In chemical structure, it is the potassium salt of an organic acid (6-methyl-1,2,3-oxathiazine-4(3H)-one 2,2-dioxide). It is 180-200 times sweeter than sucrose and it is very soluble in water (270 g/l at 20°C) (Clauss *et al.*, 1976). Moreover, it is stable at high temperature, and so it can be used in backed foods (Klug *et al.*, 1992). As all existing non caloric

[1] E numbers are number codes for food additives that are considered safe for human consumption within the European Union (the "E" prefix stands for "Europe")

sweeteners it presents an off-taste, especially at high concentrations, and therefore, it is often blended with other sweeteners (usually sucralose or aspartame) (Clauss *et al.*, 1976).

Aspartame (E951) was for the first time approved in 1983 by the UK's Committee on Toxicity, Consumer products and the Environment, and reaffirmed the last time in 2011 by the European Food Safety Authority (EFSA). It is a methyl ester of the L-aspartic acid/L-phenylalanine dipeptide and it was shown that upon digestion, it breaks down to the 2 single amino acids and a small amount of methanol (Ranney *et al.*, 1976); all of these compounds are normally metabolized, thereby delivering calories. It has a sweetness approximately 180 times that of sucrose; therefore, the quantity of aspartame needed to elicit a sweet perception is so small that its caloric contribution is negligible (Cloninger *et al.*, 1970). It has no noticeable off-taste, but its temporal sweetness profile differs from sucrose since it has a slower onset and a lingering sweet taste (Ager *et al.*, 1998). Unlike Acesulfame K, Aspartame loses its sweetness at high temperatures (American Dietetic Association report, 2004), and so it is unsuitable for use in baking applications.

Saccharin (E954) is a calorie-free sweetener widely used to sweeten foods and beverages. It has been approved by the Scientific Committee on Food (SCF) of the European Commission in 1984 and reaffirmed in 1995. It is 300-500 times sweeter than sucrose and its sweetening power is not reduced with heating (American Dietetic Association report, 2004). In its acid form, saccharin is not water-soluble; therefore, it is usually used as sodium salt. The calcium salt is also available, and it is used by people needing a low dietary sodium intake (Ager *et al.*, 1998). Saccharin has a metallic aftertaste, especially at high concentrations, and so it is often used together with aspartame or cyclamate.

Sucralose (E955) is a disaccharide 600 times sweeter than sucrose. This sweetener is stable under a broad range of pH and temperature conditions. Moreover, it has a taste profile very close to that of sucrose (Jenner *et al.*, 1982). Sucralose was approved as a general-purpose sweetener by FDA (Food and Drug Administration) in 1999, and by the EU's Scientific Commission on Food in 2000.

Other artificial sweetener commonly used are Cyclamate (E952) and Neotame (E961). Concerning cyclamate, it was approved by the EU's scientific commission on Food in 1984 but, due to its suspected cancer-promoting activity (Price *et al.*, 1970), it is banned in the United States. Neotame is the newest discovered artificial sweetener. Neotame is about

8000 times sweeter than sugar and has no calories (Whitehouse *et al.*, 2008). It has been approved by FDA in 2002 and by EFSA in 2007.

1.1.3. Sweet proteins

The high interest for non-calorigenic protein-based sweeteners is confirmed by an increasing number of publications in sweet proteins characterization and expression (Figure 1.2).

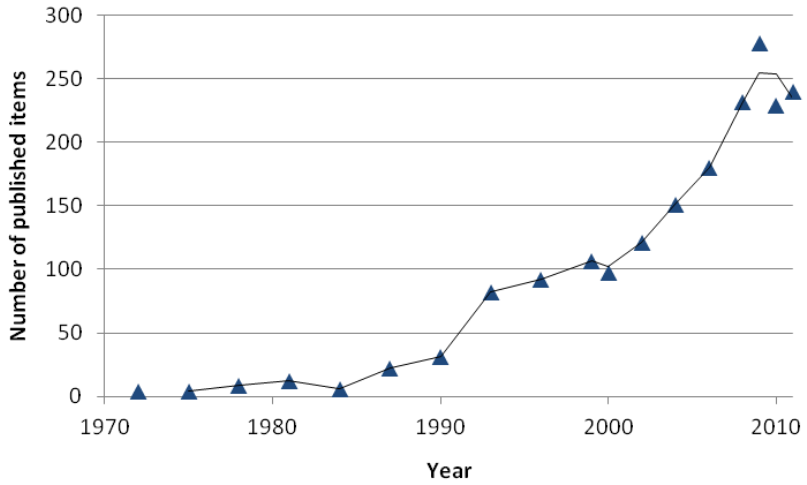

Figure 1.2 – Citation report adapted and modified from ISI web of knowledge: published items in each year (from 1972 to the present) for the topic "sweet protein"

Until now, only six sweet-tasting proteins have been isolated: thaumatin, monellin, mabinlin, brazzein, egg white lysozime, and neoculin (Masuda, 2005) (Table 1.1). These proteins are several thousand or hundred times sweeter than sucrose on a weight basis (Kant, 2005). Moreover, compared to synthetic sweeteners, sweet-tasting proteins are of less concern from a toxicological point of view and they present a long history of human consumption (Faus, 2000).

Thaumatin was isolated from the tropical West African plant *Thuamatococcus daniellii* Benth in 1972 (van der Wel *et al.*, 1972). It is composed by 207 amino acids residues and its structure comprises eight disulfide bonds and no free cysteine residues. It is 1600 times sweeter than sucrose on a weight basis. The difficulty in obtaining the natural source of thaumatin, lead to the development of different method to produce the protein in a recombinant organism. Thaumatin has already been produced in different microorganisms such as bacteria (e.g. *Escherichia coli* and *Bacillus subtilis*), filamentous fungi (*Aspergillus oryzae* and *Aspergillus*

niger), yeast (e.g. *Saccharomices cerevisiae*, *Kluyveromyces lactis* and *Pichia pastoris*), and transgenic plants (e.g. potatoes, tomatos, and strawberries) (Masuda *et al.*, 2006). Thaumatin has been approved for use as sweetener and flavor enhancer in many countries and therefore, it has become a marketed product. However, up to now none of this expression methods is economically feasible (Faus, 2000). Thaumatin sweetness disappear, due to aggregation process, at 70 degrees and pH 7.0. Because of its lingering after-taste, thaumatin is often used as a flavour modifier and not as a sweetener (Masuda *et al.*, 2006).

Monellin was originally purified in 1972 by Morris and Cagan from the berries of the West African plant *Dioscoreophyllum cumminisii* Diels. It consists of 2 polypeptides of 44 and 50 amino acids residues associated via non-covalent interaction. It is 3000 times sweeter than sucrose on a weight basis, but it loses its sweetness at above 50°C and at acidic pH. This represents a problem to the commercial application of monellin as a sweetener for baked goods and beverages such as fruit juice and cola.

Mabinlin, first characterized by Liu and coworkers (1993), is isolated from the mature seed of *Capparis masaikai*, a Chinese plant. It is an heterodimer composed of two polypeptides of 33 and 72 amino acids residues associated via non-covalent interaction. It is 400 times sweeter than sucrose on a weight basis. Mabinlin has an high thermostability: it retains its sweet taste even after 48 hours incubation at boiling point. However, until now it was no developed a method for its high level expression.

Hen Egg white Lysozyme (HEL) is a single chain protein constituted by 129 amino acid residues. It's sweet taste was for the first time claimed in 1998 by Maehashi and Udaka, and was determined to be 700 times than that of sucrose (Ide *et al.*, 2009). Due to its antimicrobial proprieties, it is used in food industry (Ibrahim *et al.*, 2002; Masschalck *et al.*, 2003). HEL can be directly extracted from egg white; moreover, it was already been produced in a sweet-retaining form in the yeast *S. cerevisiae* (Oberto *et al.*, 1985) and *P. pastoris* (Masuda *et al.*, 2005).

Neoculin is a protein with a sweetness approximately 500-fold that of sugar, extracted from the pulp of the *Curculigo latifolia* fruits. It is the only known protein with both sweet-tasting and taste-modifying activity (it converts sourness to sweetness) (Yamashita *et al.*, 1990). In fact, until now, only Miraculin (protein extracted from the fruit of *Synsepalum dulcificum*) had been found to has the interesting propriety of modifying a sour taste into a sweet taste; however, Miraculin itself has no sweet taste (Theerasilp *et al.*, 1988). On the other hand, the sweet proteins previously described have no

taste modifying activity. Neoculin was been produced in *E. coli* (Suzuki *et al.*, 2004) and *A. oryzae* (Nakajima *et al.*, 2006).

	Thaumatin	**Monellin**	**Mabinlin**	**Hen Egg Lysozyme**	**Neoculin**	**Brazzein**
Source	*T. danielli*	*D. cumminsii*	*C. masakai*	*Egg white*	*C. latifolia*	*P. brazzeana*
Geographic distribution	West Africa	West Africa	China	World over	Malaysia	West Africa
Sweetness factor (weight basis)	1600	3000	400	700	500	2000
Molecular mass (kDa)[a]	22.2	10.7	12.4	14.5	20	6.5
Amino acids	207	45 (A chain) 50 (B chain)	33 (A chain) 72 (B chain)	129	113 (A chain) 114 (B chain)	54
Active form	Monomer	Dimer (A+B)	Dimer (A+B)	Monomer	Dimer (A+B)	Monomer

Table 1.1 – Six different sweet protein identified until now: Thaumatin, Monellin, Mabinlin, Egg white Lysozyme, Neoculin, and Brazzein. [a]Molecular mass relative to the active form. Adapted from Kant (2005)

1.1.3.1. Brazzein

Proprieties

Brazzein was first isolated from the fruit of the West African plant *Pentadiplandra brazzeana* Bailon in 1994 (Ming *et al.*, 1994). The occurrence of *P. brazzeana* is reported in Figure 1.3.

Figure 1.3 – Geographical distribution of *Pentadiplandra brazzeana* bailon. It occurs from Nigeria east to the Central African Republic and south to DR Congo and Angola

P. brazzeana fruits are so sweet that African locals call them “Oubli”, or "Forgetting", because once nursing infants eat them, they forget their mothers' milk (Stein, 2002). The extreme sweetness of the pulp of the fruit and the unpleasant bitter taste of seeds cause consumers to spit out the seed, facilitating seed dispersal. In natural habitats the distribution of the seed is carried out by squirrels, monkeys, apes, and local people (Dounias, 2008).

No function of brazzein has been reported, but the structural similarity with plant defensins suggests a possible role as a serine protease inhibitor (Temussi, 2006).

Brazzein is a monomer protein, consisting of 54 amino acid residues (Figure 1.4); with a molecular weight of 6.5 kDa it is the smallest of the known sweet proteins (Ming *et al.*, 1994).

```
         10         20         30         40         50
QDKCKKVYEN YPVSKCQLAN QCNYDCKLDK HARSGECFYD EKRNLQCICD YCEY
```

Figure 1.4 - Amino acids sequence of the sweet-tasting protein brazzein

Brazzein exists in three different forms in the native fruit, differing only at the N-terminal amino acid residue. The first one corresponds to the predicted 54 amino acids form (Figure 1.4), containing glutamine at its N-terminus. This form has a short life since the N-terminal glutamine undergoes natural conversion to pyroglutamate (Figure 1.5), resulting in the second form. This form represents the major form of brazzein in the native fruit, and it was determined that it is 2000 times sweeter than a 2% sucrose solution and 500 times sweeter than a 10% one (Ming *et al*., 1994). Nevertheless, the minor form resulting from the loss of the N-terminal pyroglutamate (des-pGlu1), is twice as sweet as the major form (Izawa *et al.*, 1996).

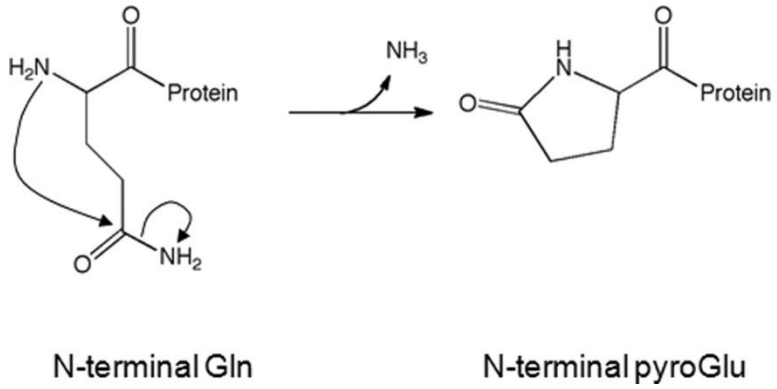

Figure 1.5 - Pyroglutamate formation mechanism. The mechanism of pyroglutamate (pyroGlu) formation from Glutamine is shown. Adapted from Liu *et al.*, 2011

Among the six sweet tasting protein isolated, brazzein seems to be the most promising one (Faus, 2000). In fact, its sweet perception is more similar to sucrose than that of the other sweet proteins (Pfeiffer *et al.*, 2000). Furthermore, it possesses better pH and thermal stabilities in comparison to the other sweet-tasting proteins. It was demonstrated that its sweetening power does not diminish after incubation at 98°C for 4 hours; moreover, it is stable over a broad pH range (2.5 to 8). It was also demonstrated that brazzein is very soluble in water (>50 mg/ml) (Ming *et al.*, 1994). These proprieties made the protein suitable for many industrial food manufacturing processes as a low-calorie sweetener.

The three-dimensional structures of brazzein have been determined by Nuclear Magnetic Resonance (NMR) spectroscopy (Caldwell *et al.*, 1998; Gao *et al.*, 1999). Such NMR studies have revealed that brazzein contains one short α-helix and three strands of antiparallel β-sheets. Brazzein also possesses three loops (loop I,

residues 9–19; loop II, 30–33; loop III, residues 38–45). Brazzein structure is characterized by the presence of four evenly spaced disulfide bonds, that are responsible for the high stability of this small protein (Figure 1.6). Izawa and coworkers (1996) demonstrated that reduced brazzein refolded spontaneously *in vitro* into the native, sweet conformation. This suggests that the four disulfide bonds correct formation is dictated by the driving force toward an energetically favorable structural organization.

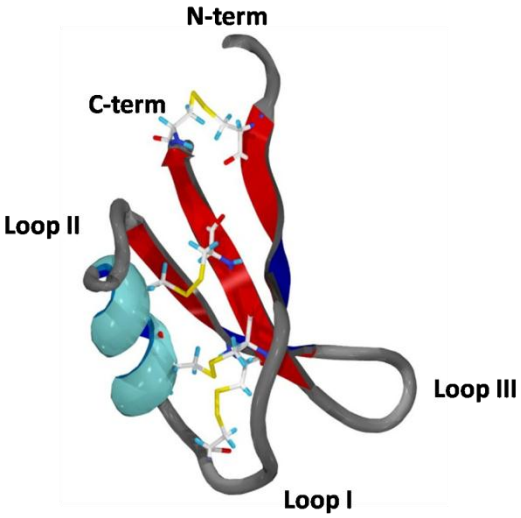

Figure 1.6 – Solution NMR structure of the brazzein protein. Brazzein is constituted by one α-helix and three strands of antiparallel β-sheets; it also possess three loops. Brazzein structure is stabilized by the presence of four disulfide bonds

Limited availability of the fruit and complications associated with large-scale production of the native plant are the reasons for which large-scale production of brazzein from natural sources is not affordable. Recombinant DNA technology provides an alternative more economic and reliable option for mass production.

Developed expression methods

Brazzein can be chemically synthesized (Izawa *et al.*, 1996), which is useful for its production in small scale for structure-function studies, but not suitable for large scale production.

Although suitable for the production of small quantities of protein, chemical synthesis is expensive. Therefore, in order to perform mutagenesis and structural studies, in 2000 Assadi Porter and collaborators developed a method for the recombinant production of

des-pGlu1 brazzein in *Escherichia coli*. They obtain a low level expression of a protein with sweetness similar to that of brazzein isolated from the plant. To improve the production yield they express the target protein as a fusion with the staphylococcus nuclease protein, that exhibits a high expression level. Considering that the 60% of the fusion protein so produced was deposited in inclusion bodies, it had to be solubilized and refolded. After cyanogen bromide cleavage of the fusion protein, brazzein was isolated by a single cation exchange chromatography step. In conclusion, this protocol involved several steps with a low overall yield. Therefore, in 2008 Assadi Porter and coworkers developed an alternative method: they express the protein as a fusion with SUMO[2]. The major advantage of this system is that it yields brazzein in folded and soluble form with less time and lower cost. Using these expression systems, the structure-sweetness relationships in the brazzein molecule have been investigated in detail (Assadi Porter *et al.*, 2000; Assadi Porter *et al.*, 2003; Assadi Porter *et al.*, 2005; Assadi Porter *et al.*, 2010; Jin *et al.*, 2003; Jin *et al.*, 2003I).

However, even if the bacterial system is ideal for its ease of rapid genetic manipulation as well as isotopic labeling for structural investigation, it is unsuitable for the production of protein for human consumption.

In 2006 Berlec and collaborators express brazzein in the "Generally Recognize As Safe" (GRAS) Lactic Acid Bacteria (LAB) *Lactococuss lactis*. They propose the use of LAB in order to express the protein directly in the diary products, removing the need for the addition of sugar. Brazzein was expressed using Nisin-Controlled Expression system (NICE)[3] (de Ruyter *et al.*, 1996) in low yield, detectable only with anti-brazzein antibodies. Yields was later increased by optimizing fermentation condition (Berlec *et al.*, 2008), but was still relatively low. In 2009 Berlec and Strukelj obtained an improvement of brazzein expression yield (maximum production in *L. lactis* yielded 1.65 mg of soluble brazzein per liter of fermentation broth) by using a new plasmid/strain combination of the NICE system. However, the

[2] SUMO (Small Ubiquitin-related Modifier). In *E. coli* recombinant proteins expressed as SUMO fusions have demonstrated enhanced stability and solubility, leading to greatly increased yields (5 to 20-fold) over constructs lacking this tag. Furthermore, efficient removal of the SUMO tag by SUMO protease allows the generation of a native N-terminus of the target protein (Yan *et al.*, 2009)

[3] The nisin controlled gene expression system of *L. lactis* is one of the most commonly used regulated expression system of Gram positive bacteria. Sub-toxic amounts of nisin in the ng/ml range are sufficient to fully activate the otherwise tightly closed promoter (Mierau *et al.*, 2005)

increased expression of brazzein resulted in a slight improvement of the secretion to the medium; moreover, the resulting brazzein had low-intensity sweetness, which could be due to absence of correct folding.

The production of recombinant brazzein has also been attempted in maize seed (Lamphear *et al.*, 2005). An high yield of brazzein expression was achieved (400 µg of brazzein per gram seed), with accumulation of approximately 4% of total soluble protein in a seed. Lamphear and coworkers reported that brazzein-containing maize germ flour could be used directly in food, providing a sweet product without the addition of sugar. However, this expression method involves the creation and introduction in the environment of transgenic maize line, with the associated environmental and health risks.

Brazzein mutations and their effect on sweetness

Brazzein can be produced in its natural (wild type) form, or in a mutated and recombinant form in order to enhance its sweet proprieties. With the aim to identify critical regions important for sweetness, several brazzein mutants have already been generated by genetic engineering (Table 1.2).

Jin and collaborators in 2003 shown that, between 25 brazzein mutants tested, four mutants (D29A, D29K, D29N, and E41K) were significantly sweeter than wild-type brazzein, while three mutants (A2ins, D2N, and Q17A) were as sweet as the wild-type brazzein. Mutants in the K6, K30, R33, E36, R43 position, and the deletion of the C-term Y54 amino acid, caused a decrease of the protein sweetness, that did not different significantly from that of water. Also mutation of the K5, Y8, K15, H31, and D50 residues, resulted in a decrease of the brazzein sweetness, but the score was different from that of water. Therefore, they concluded that residues 29-33 and 39-43, plus residue 36 between these starches, as well as the C-terminus are the critical regions of the molecule responsible for elicitation of the sweetness. Moreover, since mutations of the negatively charged D29 to neutral or positively charged residues markedly increase sweetness, while similar mutation at the E36 site caused a significantly decrease of sweetness to the level of no taste, they suggested that charge has an important role in the sweetness perception mechanism. These results were later supported by Yoon and coworkers (2011) that demonstrated the importance of the

positive charge in the 29-33 region, and in particular the fundamental role of K30 and R33 to maintain full sweetness.

Assadi Porter and collaborators performed extensive studies on the structure-activity relationship of brazzein (Assadi Porter *et al.*, 2003; Assadi Porter *et al.*, 2005; Assadi Porter *et al.*, 2010). They confirmed the importance of the 29-33 and 39-43 regions in the sweetness of brazzein. Moreover, by saturation transfer difference NMR spectroscopy, they suggested that also the 9-19 region between the β-strand I and α-helix, is involved in sweetness elicitation (Assadi Porter *et al.*, 2010). In particular, it was then founded (Walters *et al.*, 2006; Yoon *et al.*, 2011) that the size of the side chain of the Q17 residues is fundamental for the overall structural integrity, and so for the sweet taste. In fact, mutation of the Q17 to N17 resulted in significantly decreased sweetness (Yoon *et al.*, 2011).

It was also demonstrated that brazzein had to be correctly folded in order to elicit the sweet taste (Izawa *et al.*, 1996). Moreover, it was found that modifications of the cysteinic residues of brazzein resulted in the loss of sweetness (Ming *et al.*, 1994; Assadi Porter *et al.*, 2000).

These results are interesting not only from an industrial point of view, i.e. the production of the sweetest form of the protein, but also for the investigation of the residues responsible for the sweetness taste (see 1.1.4.2). In fact, understanding the mechanism by which brazzein and the other sweet proteins elicit the sweet taste represents a step towards the development of a new non-caloric sweetener, and towards a better knowledge of biological systems.

WILD TYPE BRAZZEIN AMINO ACIDS		NS	RS	NC	IS	Max
1	Q				del	
2	D				E	
4	C	A				
5	K		A	R		
6	K	D	A			
8	Y		A			
15	K		A			
16	C	A				
17	Q	C	N	A		
29	D				A - K - N	
30	K	D	R A			
31	H		A			R
32	A					
33	R	A	D K			
36	E	A - K - Q				
37	C	A				
39	Y		A			
40	D					K
41	E				Q - R	K A
42	K		A			E
43	R	A	K E - N			
47	C					
48	I					
49	C					
50	D		A		N	
54	Y	del	H		W	

Table 1.2 – Summary of brazzein mutation investigated until now and their effect on sweetness. NS = completely non-sweet; RS = reduced sweetness; NC = no change; IS = increased sweetness; Max = maximally increased sweetness. Color legend: pink = deletion of the N- or C-terminus; orange = larger residue change to alanine; light blue = change of side-chain size; yellow = change of charge; green = removal or shift of disulfide bond. In red are the amino acid residues identified as most important for the sweetness elicitation

Commercial applications

In order to reach the market brazzein must overcome many technical, regulatory, and market barriers.

From a technical point of view, it is necessary to develop an efficient and low-cost method for brazzein production. In fact, extraction of the protein from its natural source is not affordable since plants shown difficulties in bearing fruit outside their natural habitats. Therefore, a method for the expression of the protein in a recombinant host has to be optimized.

Once an efficient, cost-competitive biotechnological process has been developed, produced brazzein will have to be approved by

regulatory authorities (EFSA[4] in Europe, FDA[5] in USA). In order to obtain the regulatory approval several toxicological and allergological studies will be performed. Moreover, to demonstrate that the recombinant protein is identical to the natural one, an extensive comparison between the two form have to be done.

Once the process has been validated and the product approved, market forces will dictate the final success of the new product.

Brazzein should be added as sugar substitute to consumable food, beverage, and medication products for human consumption to impart a sweet flavor. Typical application include baked goods such as breads, cookies, cakes, etc.; beverages such as coffee, tea and soft drinks; chewing gum; dairy products such as ice cream, yoghurt, cheesecake, etc., confectionaries such as chocolates and candies; unpalatable pharmaceutical products; etc.

Among the several interesting application the addition of brazzein to baked goods is very attractive because the amount of sugar added to the dough to reach the required sweetness often hinders the capacity of the dough to leaven. Due to its pH stabilities brazzein can also be used to impart sweet flavour to acid beverage such as cola or fruit juice.

Brazzein should also be blended with other sweeteners, e.g. with aspartame, to reduce side aftertaste and complement flavor of such other sweetener(s).

1.1.4. Sweet taste receptor

The mammalian sweet taste receptor is a heterodimer of two subunits belonging to the G-Protein Coupled Receptor (GPCR) family: hT1R2 and hT1R3 (human Taste type 1 Receptor 2 and 3). Each T1R chain has a large extracellular ligand-binding region linked to a heptahelical Transmembarane Domain (TMD). The extracellular region is composed of 2 domains: a Venus Flytrap Module (VFTM), and a Cysteine-Rich Domain (CRD). The VFTM that has 2 large lobes that close around the bound ligand, resembling the carnivorous Venus flytrap plant, *Dionacea*

[4] EFSA: European Food Safety Authority. EFSA's role is to assess and communicate on all risks associated with the food chain in Europe

[5] FDA: U.S. Food and Drug Administration. FDA is responsible for protecting the public health by assuring the safety, effectiveness, and security of human and veterinary drugs, vaccines and other biological products, medical devices, USA food supply, cosmetics, dietary supplements, and products that give off radiation

muscipula. The CRD linked the Venus flytrap domain with the transmembrane one (Morini *et al.*, 2005); recent crystallographic studies (Muto *et al.*, 2007) suggest that it plays a major role in transmitting the conformational change in the ligand-binding domain to the TMD helical bundle, and prevents a direct interaction between the ligand-binding and TMD regions (Figure 1.7).

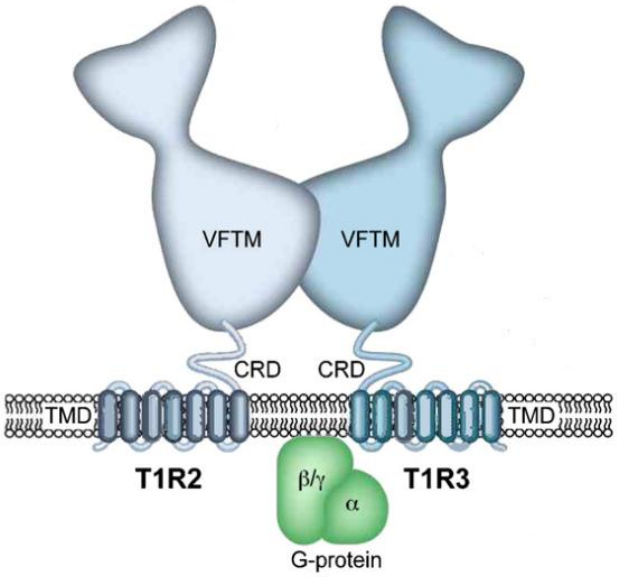

Figure 1.7 – Schematic representation of the human sweet taste receptor. The human sweet taste receptor is a heterodimer of two subunits belonging to the G-protein coupled receptor (GPCR) family: T1R2 and T1R3 (Taste type 1 Receptor 2 and 3). Like all GPCRs, it is characterized by a seven-helix transmembrane domain (TMD). In addition, it presents a large extracellular domain called the Venus Flytrap module (VFTM), which is linked to the TMD domain by a Cys-rich domain (CRD). Adapted and modified from Assadi Porter *et al.*, 2010

The tridimensional structure of the human sweet taste receptor has been built by homology modeling with the neurotransmitter glutamate receptor, which belong to the same class C of G protein-coupled receptors. However, the glutamate receptor is a homodimer and the sequence identity between the two receptor is about 23%, with only approximately 40% of sequence similarity (Wintjens *et al.*, 2011). Therefore, it is important to consider with caution results from modeling.

It was suggested that, similarly to the glutamate receptor, the sweet receptor might exist as an equilibrium between a resting, inactive form (Resting open-open) (Figure 1.8A_Roo), and an active (open-close) form (Figure 1.8A_Aoc), even in the absence of ligands (Morini *et al.*, 2005; Temussi, 2009).

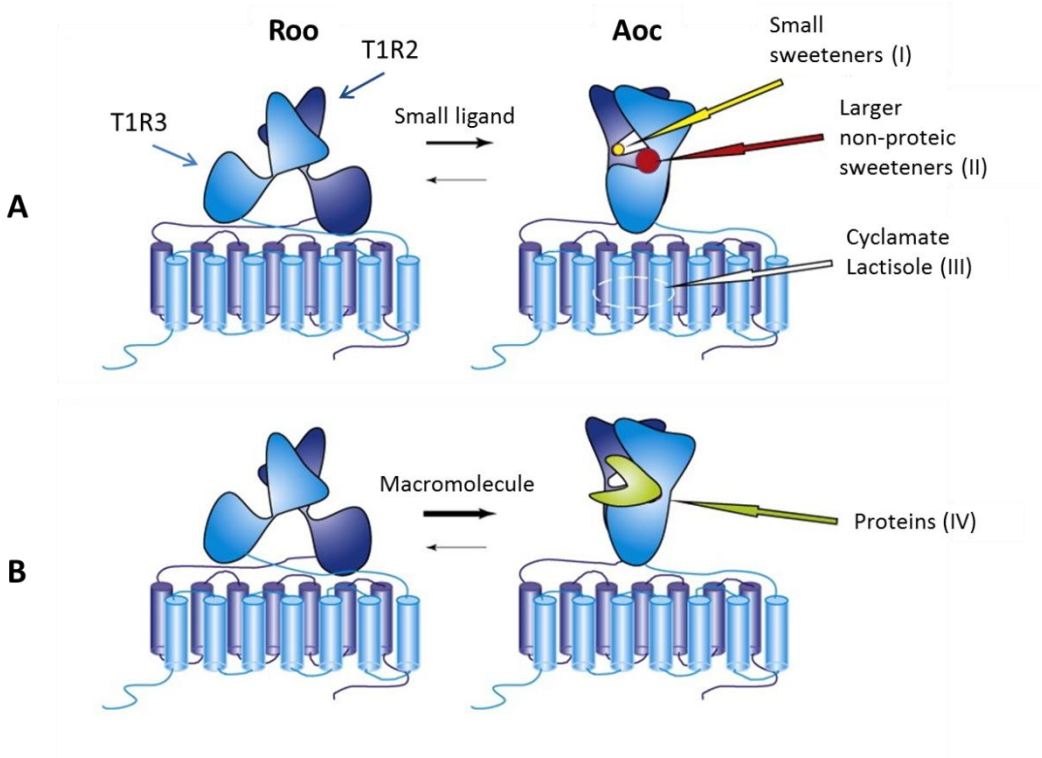

Figure 1.8 – Active sites of the T1R2-T1R3 sweet taste receptor. A) Small molecular weight sweeteners bind to the inactive form (Roo) shifting the equilibrium to the active one (Aoc). Smaller ligands (yellow ball) are hosted by the closed site within T1R2 (I) of Aoc; larger ligands (red ball) are hosted by the open cavity of T1R3 (II) of Aoc. Cyclamate and Lactisole bind to a third site located in the TM domain. B) Macromolecules, such as sweet proteins (in green), stabilize the Free form II (identical to the Aoc active form) by binding to a large and deep cavity on the receptor surface (IV). Adapted and modified from Temussi (2009)

It was proposed that the ability of the sweet receptor to recognize many structurally different sweet compounds (carbohydrates, amino acids, peptides, protein and synthetic sweeteners) is due to the presence of multiple different active sites (Morini *et al.*, 2005).

The comprehension of the structure-function relationships that trigger the sweetness response would be useful not only for the optimal design of a new non-caloric sweetener, but also for our basic knowledge of biological systems.

1.1.4.1. Interaction with sucrose and other small molecules

The equilibrium between the inactive and active form of the sweet receptor can be shifted by binding small molecules in the binding sites of the VFTM (Temussi, 2002) (Figure 1.8A). It was suggested that most of small sweet molecules bind in the cavities hosted by the N-terminal VTFM domains. These observations provide a possible

explanation for the phenomenon of sweetness synergy[6]: the binding in a single T1R subunit is sufficient for receptor activation, the binding of a ligand in the second subunit increase the response (Morini *et al.*, 2005). An additional site located in the C-terminal TMD of T1R3 is required for recognizing the artificial sweetener cyclamate and the sweet taste inhibitor lactisole (Xu *et al.*, 2004).

In conclusion, there are three different binding site for small molecular weight molecules: cavity of the T1R2 (I) and T1R3 (II) VFTDs, and a site of the T1R3 TMD (III) (Figure 1.8A). However, the existence of further binding sites cannot be excluded. For instance, is actually not know the binding site for stevioside, sweet molecule of *Stevia rebaudiana* Bertoni plant.

1.1.4.2. Mechanism of interaction with sweet proteins

Sweet proteins have dimensions completely different from those of all other sweet molecules, and they have a sweet potency that is a thousand times greater than that of small sweet compounds (Temussi, 2011). Therefore, in relation to their large size, it is not possible to foresee that sweet proteins can interact with one of the three small molecules binding sites.

From some preliminary studies, such as mutagenesis studies, it was proposed that sweet proteins may interact with the Free form II of the receptor, that corresponds to the Aoc active form, and presents a wide and deep cavity that can host the tips of sweet proteins (Temussi, 2011) (Figure 1.8B). The surface of the active form is prevalently negative (Temussi, 2011; Morini *et al.*, 2005) but, inside the binding site there isn't a uniform distribution of charged residues. Therefore, also the tip of a sweet macromolecule must have an irregular distribution of key charged residues (Temussi, 2011). The binding of a sweet protein "freeze" the active form of the receptor, leading to the sweet taste response. This mechanism, named 'wedge model', was for the first time proposed by Temussi in 2002 on the basis of docking calculation (Temussi, 2002) (Figure 1.8B).

The sweet taste response is generally thought to involve the formation of hydrogen bonds between protein and receptor residues.

[6]A molecule exhibits a sweetness synergy effect if, when used in combination with other sweeteners, the relative sweetness of the mixture is perceived to be greater than the sweetness calculated from individual components

Therefore, even if sweet proteins present a low sequence and structure similarity, it has been proposed that they share a common mechanism for receptor activation (Temussi, 2006).

Also the synergy between sweet proteins and several sweet compounds could be explained by the wedge model, since sweet proteins don't occupy any of the three ligand binding sites for small molecular weight sweeteners (Morini *et al.*, 2005).

Thanks to the great number of known mutants affecting sweetness (Table 1.2), brazzein represent a helpful model to study the interaction with the sweet receptor.

Recent studies (Assadi Porter *et al.*, 2010; Temussi, 2011; Yoon *et al.*, 2011) suggest that brazzein interact with a non-continuous, multisite, multidomain surface that includes the "hinge" region of T1R2 and the CDR of T1R3. The most important regions for brazzein sweetness are the flexible loop 29-33 which has a high positive charge (Figure 1.9 and

Figure 1.10, Loop II), and the flexible loop 38-45 (Figure 1.9, Loop III), containing Glu41 and Arg43 (in the middle of the β-turn between strands II and III) which are essential for the sweet taste.

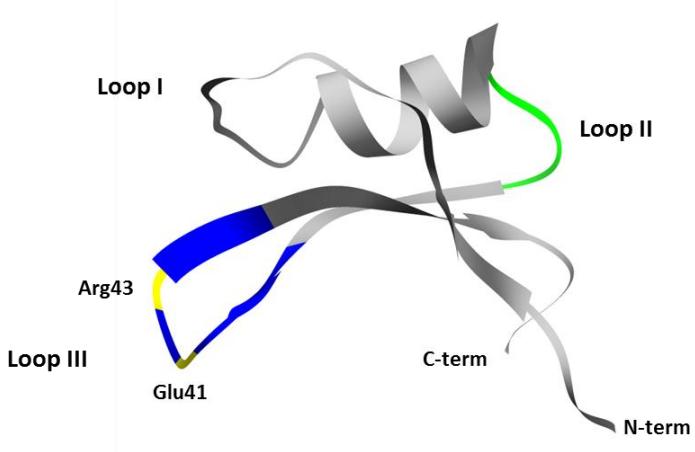

Figure 1.9 – Diagram showing the three-dimensional backbone of brazzein with the position of the most important regions for its sweetness: Loop II (in green) and Loop III (in blue); the yellow indicates Glu41 and Arg43, amino acids essential for brazzein sweet taste

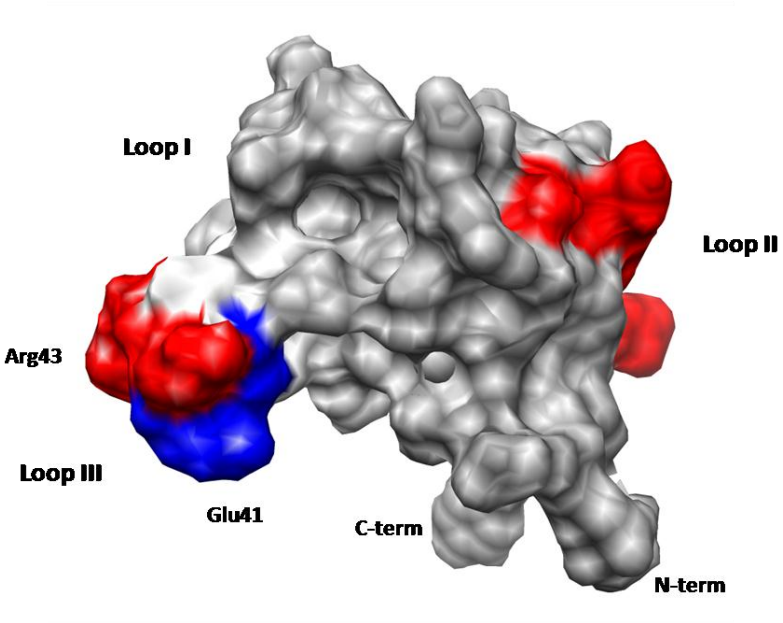

Figure 1.10 – Molecular model of brazzein. Loop II and Loop III positive residues are colored in red, whereas negative residues are colored in blue

Moreover, by docking calculation Temussi (2011) shown that residues 40-43 have a one-to-one correspondence to T1R2 residues of opposite charge or to a residue with which it can form an hydrogen bond (Table 1.3).

Receptor residues (T1R2)	Brazzein residues	Type of interaction
R457 – K174	D40	Electrostatic
S458	E41	Hydrogen bond
D456	K42	Electrostatic
Q441	R43	Hydrogen bond

Table 1.3 – One-to-one contacts between receptor T1R2 and brazzein residues. Adapted from Temussi, 2011.

Since the sweet taste receptor is constituted by proteins, the receptor site is chiral. Consequently, also the native conformation of a sweet protein is important for its sweet taste. This hypothesis was confirmed by Izawa and coworkers (1996) that chemically synthesized

both the L and D enantiomer of brazzein, demonstrating that only the L-form is sweet, while D-brazzein is essentially tasteless.

1.2. Ice Structuring Proteins (ISPs)

Water in the liquid phase is essential to all living cells and, therefore, freezing is detrimental to most organisms. In fact, the freezing process causes the concentration of electrolytes and other solutes in the unfrozen part and subtracts liquid water necessary for biological reactions, solute transport and interaction, regulation of intracellular pH, and stabilization of macromolecules structures (Hew *et al.*, 1992). Moreover, the formation of ice damages cell components such as membrane and proteins (Brockbank *et al.*, 2011).

Many organisms have evolved different mechanisms to survive at subzero temperature. These includes seasonal migration, hibernation[7], synthesis of colligatively[8] cryoprotectant molecules such as sugars or salts and, the synthesis of Ice Structuring Proteins (ISPs) (Bouvet *et al.*, 2003).

ISPs were identified for the first time by DeVries and collaborator just over 40 years ago in the blood of Antarctic fishes (*Nototheniidae*) (DeVries *et al.*, 1969). The freezing point of Arctic and Antarctic ocean water is around -1.9 °C; fishes living in such environments have a blood freezing temperature slightly lower than the freezing temperature of the sea water (-2.0/-2.1 °C). The analysis of the blood of these fishes shown that colligative effects of electrolytes such as sodium chloride is responsible for less than 50% of the freezing point depression of the blood; the non-colligative depression of the blood freezing point was found to be due to the presence of small proteins identified as ISPs (DeVries *et al.*, 1970).

Shortly after their discovery, ISPs were found in various organisms that live in sub-zero environments, including insects, plants and polar bacteria.

ISPs protect organisms from the deleterious effect of ice crystals' formation in cells thanks to their two related effects on aqueous solutions: thermal hysteresis (TH) and ice recrystallization inhibition (RI) (see 1.2.2). In brief, TH is the non-colligative depression of the freezing temperature of solutions below their melting temperature[9]; ice recrystallization is the growth of large ice crystals at the expense of smaller ones in partially frozen solutions. ISPs inhibit both processes.

Moreover, it was shown that ISPs are able to protect cells membrane during the cooling process (Hays *et al.*, 1996; Tomczak *et al.*, 2001; Wu *et al.*,

[7] Hibernation is a state of inactivity and metabolic depression in animals, characterized by lower body temperature, slower breathing, and/or lower metabolic rate

[8] A colligative phenomenon depends on the molar concentration of the solute, regardless of its chemical propriety (it was shown that for every molar of free ions, the melting temperature is depressed by 1.86°C, regardless of the ion type; Yeh et al., 1996)

[9] The melting point is the warmest temperature at which an ice crystal can be stably held without melting

2001; Tomczak *et al.*, 2002; Beirão *et al.*, 2011), thus inhibiting the leakage across the membrane and so the cell damage and death (see 1.2.5.2).

Analysis of these different ISPs has shown that there is no consensus sequence or single structure for an ice-binding domain and that some ISPs undergo structural changes at low temperatures. Currently, it is not possible to identify a novel ISP using an approach based on structural models interrogation of available database; the only way to identify an ISP is by directly assaying its ability to interact with ice inhibiting the recrystallization process or by assaying the freezing point depression of a solution (Griffith *et al.*, 2004).

From an industrial point of view, the ability of ISPs to hinder ice recrystallization makes them particularly suitable in food industry as natural ice modulators for cold storage of frozen products such as ice cream (see 1.2.5.1). Instead, the cells membrane protection during cooling makes ISPs interesting for the cryopreservation or low-temperature storage of cells, tissues, and organs (see 1.2.5.2).

The high interest for ISPs characterization and commercial application is confirmed by an increasing number of publications on this field of research (Figure 1.11).

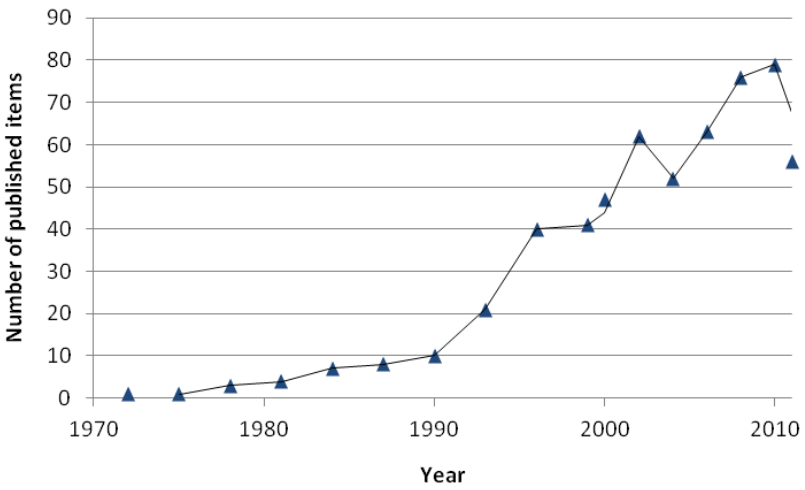

Figure 1.11 - Citation report adapted and modified from ISI web of knowledge: published items in each year (from 1972 to the present) for the topic "antifreeze protein"

1.2.1. Ice structure and growth

The phase diagram for the equilibrium between ice, liquid and vapor phases is reported in Figure 1.12. Pure water freezes at 0 °C and 1 atm (Smolin *et al.*, 2008); however, even if at freezing temperature, water will not start the freezing process unless a small amount of solid material (seed) is present. When the seed is formed, water molecules can attach to it to rapidly form ice. In the absence of a seed, the water will remain liquid to a temperature below the freezing point (supercooled water) before crystal nucleation spontaneously begins (Hew *et al.*, 1992)

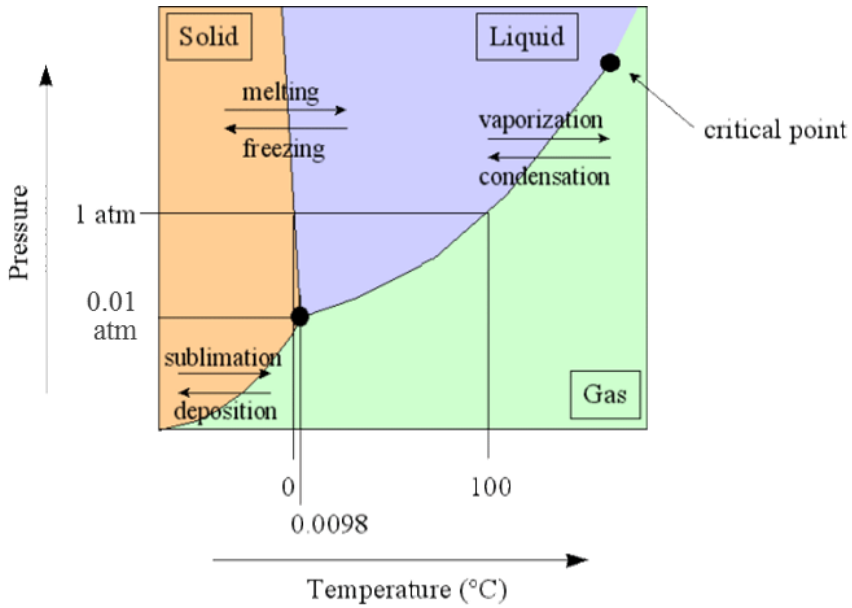

Figure 1.12 – Schematic phase diagram of water. Adapted and modified from http://www.its.caltech.edu/~atomic/snowcrystals/ice/ice.htm

The structure of ice around 0 °C is hexagonal ice crystal; ice grows as hexagonal sheets lying on top of each other (Figure 1.13, a) (Deng *et al.*, 1997). During the freezing process, a water molecule forms hydrogen bonds to three of its neighbors in the same plane, and one hydrogen bond that crosslinks the different sheets as shown in Figure 1.13, b (tetrahedral arrangement).

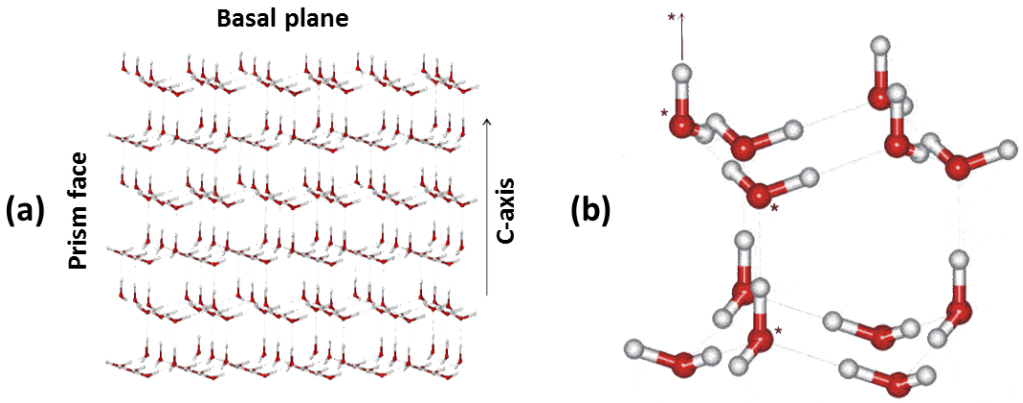

Figure 1.13 – (a) Ice structure: the crystals may be thought as hexagonal sheets lying on top of each other. (b) One water molecule forms three hydrogen bonds to other water molecules in the same plane, and one hydrogen bond that crosslinks the different sheet. Adapted and modified form http://www.lsbu.ac.uk/water/ice1h.html

The ice structure forms two hexagonal basal planes, and six equivalent prism planes. The direction normal to the basal planes is called c-axis, while the three symmetric axes lying in the basal planes are called α-axes (Griffith *et al.*, 2004) (Figure 1.14, a).

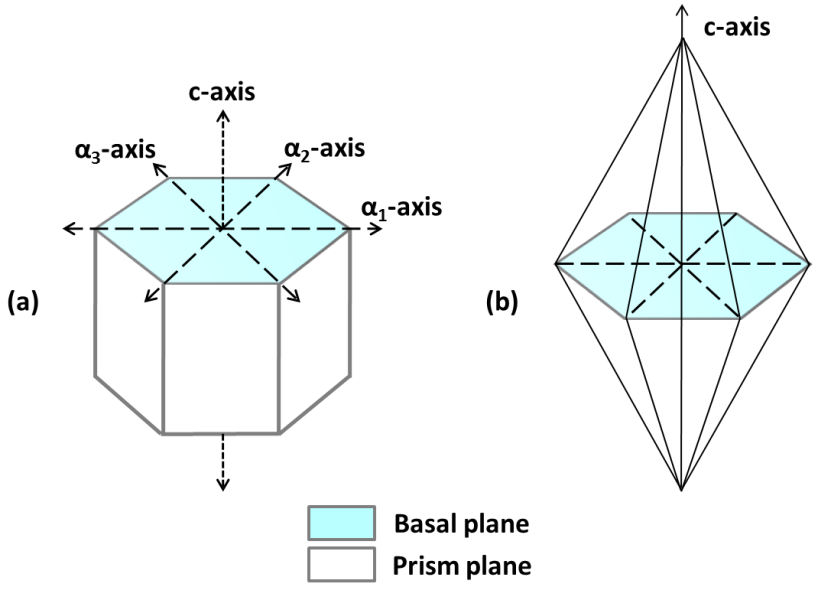

Figure 1.14 – Ice structure. (a) Hexagonal ice structure: in this crystal form, the three symmetric α-axes lay in the basal plane, and the c-axis lay in the prism plane, perpendicular to the basal plane. (b) Ice crystal morphology in presence of ISPs: bypiramidal crystallites and columnar spicules are formed instead of sheets

Ice crystal grows in water at different rate in each plane. The fastest growth occurs from the prism plane direction (α-axis), which makes the ice crystal wider, while the slower growth occurs along the basal plane

direction (c-axis) making the ice crystal longer. Due to this difference ice crystals form disc-like sheet (Wathen *et al.*, 2004).

In the presence of ISPs, the ice growth changes from the normal disc-like sheet to bipyramidal crystals and columnar spicules (Figure 1.14, b) (Barret *et al.*, 2001; Jia *et al.*, 2002). For instance, it was demonstrated that a fish ISP interact with the prism plane of ice crystals, inhibiting the growth along the prism faces; this cause the formation of the hexagonal bypiramidal structure (Jia *et al.*, 1996).

1.2.2. Thermal hysteresis and recrystallization inhibition activity

As reported in 1.2, ISPs was initially identified thanks to their ability to lower the freezing point[10] of the Antarctic marine teleost blood (Duman *et al.*, 1975). The unique ISPs propriety of generating a difference between the melting and the freezing point is termed thermal hysteresis activity (TH) (Barret *et al.*, 2001). During the thermal hysteresis gap (temperature interval between the melting and freezing point due to the presence of an ISP) the shape of ice crystals remains unchanged, and ice doesn't grow. When the temperature is lowered to the hysteresis freezing point, ice starts to grow (Figure 1.15).

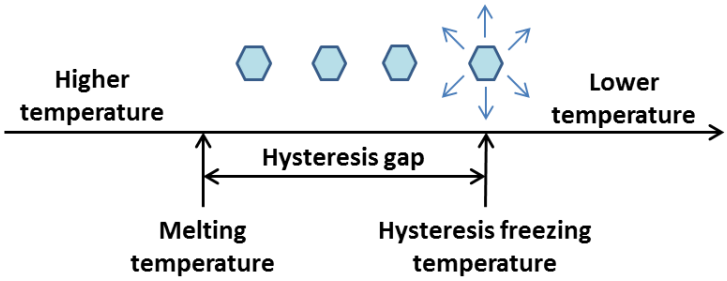

Figure 1.15 – Schematic representation of the ISP thermal hysteresis activity: the adsorption of ISP to the ice crystals surface lowers the freezing temperature of the solution below its melting point. The temperature interval between the melting and freezing point is called hysteresis gap, and the temperature at which the ice growth occurs is named hysteresis freezing point

The generally accepted mechanism by which ISPs cause thermal hysteresis is the so-called adsorption-inhibition mechanism (see 1.2.3) (Knight *et al.*, 1991; Barret *et al.*, 2001; Kristiansen *et al.*, 2005).

ISPs cause thermal hysteresis in a non-colligative manner: the TH activity of those proteins is far greater than expected for their molar

[10] The freezing point is the temperature at which uncontrollable or spicular crystals growth

concentration in the solution, and depends on the physical proprieties of the ISPs (Raymond *et al.*, 1977). This allows them to be 300-500 times more effective (on a molar basis) at lowering the freezing temperature than other dissolved solutes, thereby minimizing their effect on the osmotic pressure of cells or plasma (Fletcher *et al.*, 2001, Crevel *et al.*, 2002). It has also been reported that ISPs thermal hysteresis activity is additive to the colligative effects caused by solutes such as sugars and salts (Yeh *et al.*, 1996; Jia *et al.*, 2002) (Figure 1.16).

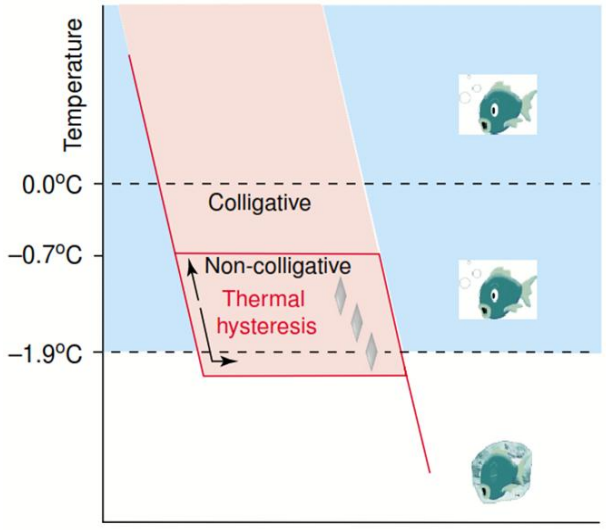

Figure 1.16 – Fishes are protected from freezing by a combination of colligative and non-colligative mechanisms. The blue areas represent seawater, which freezes at −1.9°C (indicated by the transition to white). Pink area indicates fish blood, which freezes just below −1.9°C (marked by the lower horizontal red line). The depression of the freezing point from 0 to -0.7 °C is due to colligative phenomenon, while the further depression to -1.9°C is caused by the non-colligative ISP interaction with ice. Adapted and modified from Jia *et al.*, 2002

Thermal hysteresis is used to detect and quantify antifreeze activity of ISPs by using a nanoliter osmometer or a differential scanning calorimeter (Griffith *et al.*, 2004). Based on their TH activity, ISPs can be divided in two groups: moderate active (fish and plant ISPs), and hyperactive ISPs (insects). The moderate active group comprises fish ISPs with a thermal hysteresis of 1-1.5 °C, and plant ISPs where TH activity is between 0.2-0.4 °C. Instead, insect ISPs are considered hyperactive, since their TH activity is between 5-10 °C (Urrutia *et al.*, 1992; Venketesh *et al.*, 2008; Griffith *et al.*, 2004).

Ice crystallization refers to ice crystals formation upon the seed formation. Instead, recrystallization is the phenomenon of existing large ice crystals growth at the expense of disappearing small ice crystals, without the

seed formation process involved. In comparison to smaller ice crystals, larger ones increase freezing-related tissues and cells damage (Griffith *et al.*, 1995).

Recrystallization of ice, also referred as migratory recrystallization, occurs when the temperature fluctuates in the subzero range. When temperature increases, the smallest ice crystals melt increasing the amount of water in the liquid phase. On the contrary, when temperature decrease, water refreeze but does not re-nucleate: water from liquid phase deposits on the surface of larger crystals, therefore, the number of ice crystals decreases and the mean crystal size increases (Goff, 2005).

In ISPs related literature, it was demonstrated that these proteins possess an ice Recrystallization Inhibition activity (RI activity) at extremely low concentrations (nanomolar concentrations) (Breton *et al.*, 2000; Griffith *et al.*, 2004). Moreover, since RI activity unlike TH activity was found in all cold-resistant organisms (fishes, insects, plants, etc.), it is considered as the common characteristic between all ISPs; therefore, monitoring the rate of recrystallization of ice has become a common, quantitative, tool to measure antifreeze activity (Atici *et al.*, 2003; Griffith *et al.*, 2004).

RI activity measurement is very useful for plant ISPs (see 1.2.4.3), since their TH activity level is relatively small compared to that of fish and insect ISPs (Urrutia *et al.*, 1992; Venketesh *et al.*, 2008), but they are more effective at preventing the ice recrystallization process (Griffith *et al.*, 1995; Sidebottom *et al.*, 2000, Regand *et al.*, 2006). This characteristic makes plant ISPs very interesting for the food industry, since for the long-term food preservation the decrease of recrystallization rate (RI activity) is more important than the freezing point depression (TH activity); in fact, the temperature usually employed during food freezing (-30 to -40 °C) and storage (-18 to -25 °C) are far below the freezing point of any food (Kontogiorgos *et al.*, 2007).

1.2.3. Ice Structuring Proteins' mechanism of action

Crystal growth inhibition by ISPs is assumed to result from the binding of ISPs to the surface of an ice crystal; this interaction interfere with the normal expansion of ice by inhibiting the growth in the areas where ISPs cover the water-accessible surfaces of ice. The growth inhibition in such restricted area (in other regions, where there are no ISP molecules, ice continue to grow) cause the ice front to growth as convex shape ("adsorption-inhibition model"); this local curvature increased as the ice

grows (Figure 1.17) (Knight *et al.*, 1991; Barret *et al.*, 2001; Kristiansen *et al.*, 2005).

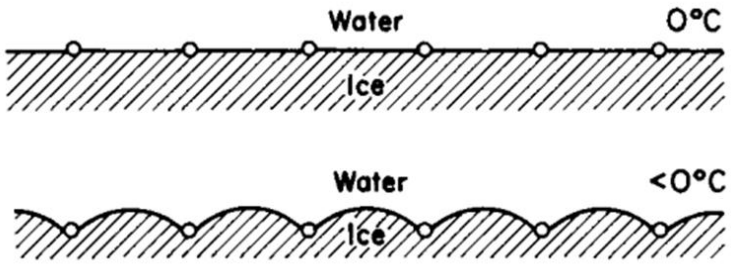

Figure 1.17 – The adsorption-inhibition model of ISPs interaction with ice. Where the ISPs bind to the ice surface they inhibit the ice growth; this caused the growth of the ice surface between two ISP molecules as convex shape. Adapted and modified from Kinght *et al.*, 1991

The surface curvature of the ice crystal results in an increased surface_area/volume ratio, beyond the point that is thermodynamically unfavorable for spontaneous ice growth to occur (Barret *et al.*, 2001; Kristiansen *et al.*, 2005). Therefore, ice crystals propagation stops. This generally accepted model is called "Kelvin (Gibbs-Thomson) effect" (Yeh *et al.*, 1996).

The mechanism by which ISPs bind to ice has been debated for over 30 years. In fact, the possible Ice Binding Site/s (IBS) of an ISP (determined for example by mutagenesis studies) is characterized by the presence of hydrophilic and hydrophobic amino acids (Yang *et al.*, 1998; Harding *et al.*, 1999; Madura *et al.*, 2000; Jia *et al.*, 2002; Jorov *et al.*, 2004), indicating that both hydrophobic and hydrophilic interaction contributed to ice binding. In a recent work, Garnham and coworkers (2011) resolve the first crystal structure of an Antarctic bacterial (*Marinomonas primoryensis*) ISP showing the contribution of both the hydrophobic effect and hydrogen bonding during ISP adsorption to ice. They demonstrated that the relative hydrophobicity of an ISP IBS causes the ordering of water molecules into an ice-like-lattice; these ordered water molecules are anchored to the protein via hydrogen bonds, and allow the ISP binding to ice by matching a specific plane (or planes) of the ice crystal (Figure 1.18).

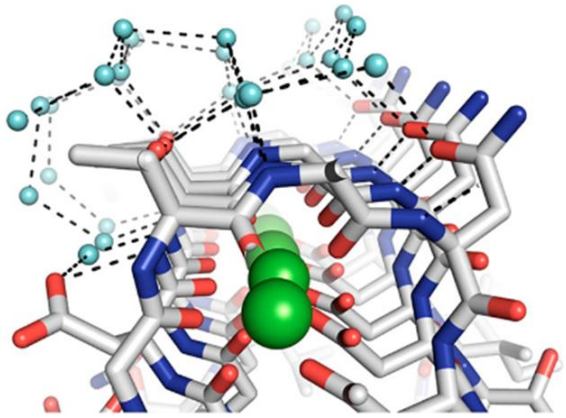

Figure 1.18 – Ordered surface water (blue spheres) hydrogen bonded directly to the IBS of the Antarctic bacterial (*Marinomonas primoryensis*) ISP; green spheres are the calcium molecules necessary for the correct folding of this protein. Adapted and modified from Garnham *et al.*, 2011

This mechanism, called "anchored clathrate" mechanism, can be applied to all the known ISPs and is able to explain the different ISP activity level: hyperactive ISPs (i.e. insect ISPs, see 1.2.4.2) will be able to bind to multiple plane (one is the basal plane, and one or more are prism planes) of ice through their ability to order water molecules; instead, moderate active ISPs (i.e. fish and plant ISPs, see 1.2.4.1 and 1.2.4.3) will be capable to bind to one or more prism plane, but not to the basal one. This explanation is consistent with previous studies in which the preferential ISP affinity for a particular plane of ice was demonstrated through ice-etching experiments (Knight *et al.*, 1991; Antson *et al.*, 2001; Mao *et al.*, 2006). Therefore, while moderate active ISPs inhibit the growth of ice along the α-axis, the hyperactive ISPs inhibit the ice crystal growth from both the α-axis and the c-axis. As a consequence, when temperature is lowered (and so the ISPs is no longer able to inhibit the ice growth), ice crystals grow in two different ways: in presence of moderate active ISPs the ice crystal will grow along the c-axis allowing an elongation of the ice crystal but not a widening (i.e. there is the formation of bypiramidal crystals and columnar spicules) (Figure 1.19); in presence of hyperactive ISPs ice crystals will growth in all directions (crystals initially growth as hexagonal shape), resulting in the freezing of the entire sample at once (Figure 1.20).

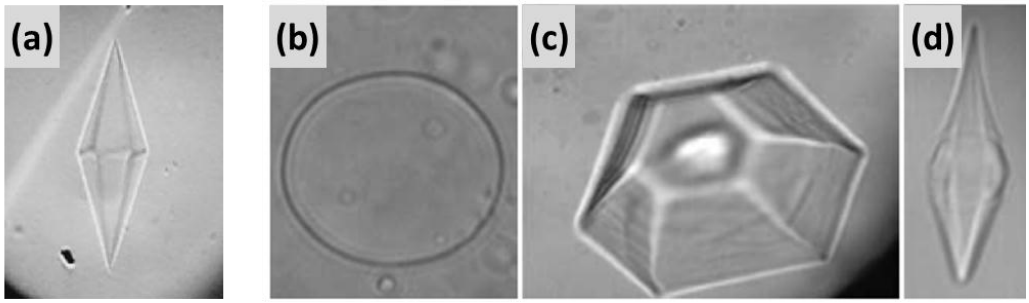

Figure 1.19 – Ice crystal morphology in the presence of (a) type IV fish ISP (Deng *et al.*, 1997), (b) water without ISPs, and (c,d) plant ISPs (Griffith *et al.*, 2004). In water (b) ice growth as a round and flat ice crystal, while in presence of fish (a) or plant (c-d) ISPs crystal growth along the c-axis forming bypiramids

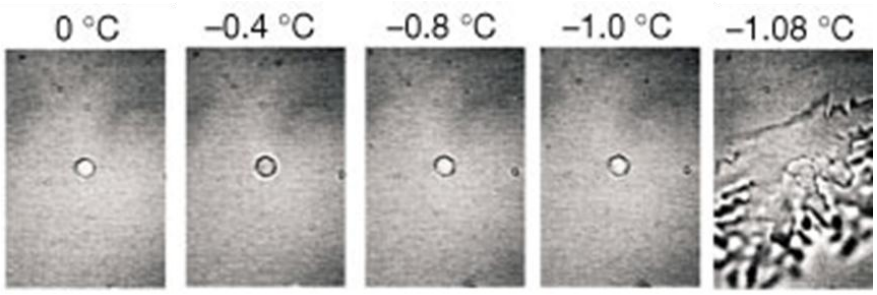

Figure 1.20 – Ice crystal morphology in the presence of insect (*Spruce budworm*) ISP; below the non-equilibrium freezing point, there is an uncontrolled growth of the crystal. Adapted and modified from Greather *et al.*, 2000

The anchored-clathrate mechanism also explains the concentration dependence (Kristiansens *et al.*, 2005) of antifreeze activity. In fact, ordered water molecules have a sort life time (also reported by Modig *et al.*, 2010); in other words, water molecules on the IBS of the ISP exchanged with bulk water very quickly. This rapid exchange results in a small fraction of ISPs presenting a sufficient percentage of water molecules in the correct orientation for ice binding, at a given moment. Rising the protein concentration would result in an increasing number of protein molecule available to bind to ice, and consequentially to a greater antifreeze activity (Garnham *et al.*, 2011)

1.2.4. Evolution and diversity of Ice Structuring Proteins

ISPs are proteins widely found in nature: fishes, insects, plants, bacteria, and other organisms that are able to survive at harsh temperatures, have evolved this strategy (i.e. the production of ISPs) which help them to maintain their body fluid in the liquid state at subzero temperatures.

Thanks to their characteristics (i.e. thermal hysteresis and ice recrystallization inhibition activity), ISPs allow organisms survival in freezing environments.

Despite their common mechanisms of action, the different ISPs present a great diversity in their primary, secondary and tertiary structure.

ISPs are generally divided into different groups according to their discovery, origin, and/or structure.

1.2.4.1. Fish ISPs

Fish ISPs may be divided in five different classes: ISGPs (Ice Structuring Glycoproteins), Type I, II, III and IV ISPs (Table 1.4).

ISGPs are found in Antarctic notothenioids (*Dissostichus mawsoni*) and northern cods (*Boreogadus saida*). They present a molecular mass ranging from 2.6 to 33 kDa. ISGPs are characterized by the presence of a repeated glycopeptide, Ala-Ala-Thr-galactosyl-N-acetyl galactosamine (Morris *et al.*, 1978) (Figure 1.21, a).

Type I ISPs are found in Winter flounder (*Pseudopleuronectes americanus*), Yellowtail flounders (*Limanda ferruginea*), Shorten sculpins (*Myoxocephalus scorpius*), and Grubby sculpins (*Myoxocephalus aenaeus*). They are the best documented ISPs because they were the first to have their tridimensional structure determined. Type I ISPs are rich in alanine and consist of a single, long, amphipathic alpha helix (Figure 1.21, b). They are approximately 3.3-4.5 kDa in size. They are characterized by 11 amino acid repeats of $ThrX_2$-$AsxX_7$, where X is usually alanine (Duman *et al.*, 1976).

Type II ISPs are found in Sea raven (*Hemitryptrrus*), Smelt (*Osmerus mordax*) and Atlantic herring (*Clupeah harentus harengus*). They are globular, cysteine rich proteins characterized by a high content of disulfide bonds (Ng *et al.*, 1992). In contrast to type I ISPs they present a limited α-helix content (Figure 1.21, c). They can be divided in two different subgroups: type II ISPs from smelt and herring require Ca^{2+} for they activity, while that form Sea raven are not Ca^{2+} dependent (Ewart *et al.*, 1999).

Type III ISPs are found in both Northern (*Macrozoarces americanus*) and Antarctic Eelpout (*Lycodichthys dearborni*). They are globular proteins characterized by a β-sandwich structure consisting of eight β-strend (Figure 1.21, d). Type III ISPs have a molecular weight ranging from about 6.5 kDa to about 14 kDa, and their amino acid

compositions do not have an imbalance of any one amino acid (Davies *et al.*, 1990).

Type IV ISPs are discovered in Longhorn sculpin (*Myoxocephalus octodecimspinosis*). They are alpha helical proteins characterized by a high (17%) content of glutamine. Type IV ISPs are approximately 12.3 kDa in size and consist of a 4-helix bundle (Deng *et al.*, 1997) (Figure 1.21, e). The only post-translational modification present in Type IV ISP is a N-terminal cyclized glutamine residue, i.e. a pyroglutamate residue (Deng *et al.*, 1998).

Type	Size (kDa)	Primary structure	Secondary structure	Tertiary structure	Natural source
ISGP	2.6 - 33	$(Ala\text{-}Ala\text{-}Thr)_n$	Expanded	Not determined	Antarctic notothenioids, Northern cods
I	3.3 - 4.5	11 aa repeats of $ThrX_2\text{-}AsxX_7$	α-helix	100% helical	Winter flounder, Yellowtail flounders, Shorten sculpins, Grubby sculpins
II	11 - 24	Cysteine rich	β-sheet	Globular	Sea raven, Smelt, Atlantic herring
III	6.5-14	No dominant aa or repeat units	β-sandwich	Globular	Northern and Antarctic Eelpout
IV	12.3	Glutamine rich	α-helix	Four-helix boundle	Longhorn sculpin

Table 1.4 – Characteristics of the five ice structuring proteins from fish. Table adapted and modified from Crevel *et al.* (2002) and Jia *et al.* (2002)

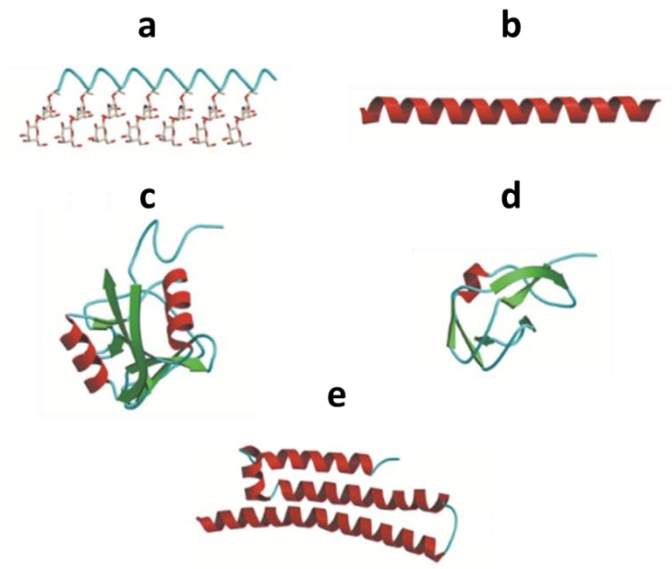

Figure 1.21 – Fish ice structuring proteins structures; α-helices are drawn in red, β strands in green and coil in cyan. a) ISGP (drawn as an extended left-handed helix with disaccharides displayed), b) Type I ISP from winter flounder, c) Type II ISP from sea raven, d) Type III ISP from ocean pout, e) Type IV ISP. Adapted and modified from Jia *et al.* (2002)

1.2.4.2. Insect ISPs

There are four different known insect ISPs: the sprouce budworm, the pyrochroid beetle, the yellow mealworm, and the snow flea ISPs. Insect ISPs are called 'Hyperactive ISPs' since they are 10-100 times more active than fish ISPs in terms of thermal hysteresis activity (-5/-10°C) (Graham *et al.*, 2005). They are relative small with a molecular mass ranging from 8.3 to 12.5 kDa. Insect ISPs are rich in threonine and cysteine residues, and none of them contain carbohydrates (Duman *et al.*, 1991). The yellow mealworm (*Tenebrio molitor*) and the pyrochroid beetle (*Dendroides canadensis*) ISP structure consists of a right-handed β-helix with 12 residues per coil (Yue *et al.*, 2009) (Figure 1.22, a), while the sprouce budworm *(Choristoneura fumiferana*) one is characterized by a left-handed β-helix (Duman *et al.*, 1998) (Figure 1.22, b). Instead, the main structural elements of the snow flea (*Hypogastrura harveyi*) ISP are six left-handed helices, stacked in two groups and joined by five reverse turns and interlocked by a complex hydrogen bond network (Pentelute *et al.*, 2008) (Figure 1.22, c).

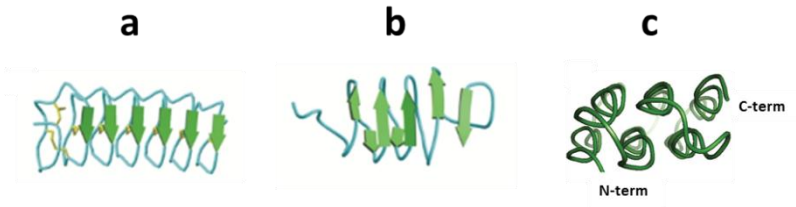

Figure 1.22 – Insect ice structuring proteins structures. a) Yellow mealworm ISP, b) Sprouce budworm ISP, c) Snow flea ISP. Adapted and modified from Jia *et al.* (2002) (a, b), and from Pentelute *et al.* (2008) (c)

1.2.4.3. Plant ISPs

Plant ISPs were identified for the first time by Griffith and coworkers (1992) in extracts obtained from winter rye (*Secale cereale*).

Many species of over-wintering plants have been investigated for their ISPs content (Table 1.5) (Atici *et al.*, 2003; Griffith *et al.*, 2004), and it was shown that they contain ISPs in different parts such as seeds, stems, crowns, barks, branches, buds, petioles, leaf, flowers, berries, roots and tubers (Griffith *et al.*, 2004).

COMMON NAME				
Aarrow leaf plantain	Antarctic hairgrass	Bamboo	Barley	Beech
Bittersweet nightshade	Bluegrass	Brown rush	Buttercup	Butterfly bush
Cabbage	Carrot	Chickweed	Crack willow	Creeping bentgrass
Dandelion	Daylily	Douglas fir	Dutchman's breeches	Eastern cottonwood
Elder	Evergreen legume	Fescue	Garlic mustard	Geranium
Grape berries	Heath rush	Heather	Jacob's ladder	Japanese radish
Maple	Oat	Peach	Perennial ryegrass	Periwinkle
Potato	Prickly burr	Shasta fern	Sheep sorrel	Snow lotus
Spurge	Spruce	Timothy	Tussac grass	Violet
Virginia waterleaf	Water sedge	Weeping forsythia	White oak	Winter & spring canola
Winter & spring rye	Winter & spring wheat	Winter cress	Wood aster	Wood sorrel

Table 1.5 – Plants exhibiting antifreeze activity in soluble extract obtained from cold-acclimated plants. Adapted and modified from Atici *et al.* (2003) and Griffith *et al.* (2004)

Plant ISPs have a moderate thermal hysteresis activity (-0.2/-0.4 °C) compared to that of fish (-1.5 °C) and insect (-5/-10°C) ISPs (Urrutia *et al.*, 1992; Venketesh *et al.*, 2008), but they are better at preventing the ice recrystallization process (RI activity) (Griffith *et al.*, 1995; Sidebottom *et al.*, 2000, Regand *et al.*, 2006). For example, sucrose solution containing *Lolium perenne* (perennial ryegrass) ISPs, exhibited RI activity at concentrations below 10 μg protein/ml, which is at least 200 times less in molar terms than the type III ISP from ocean pout (Sidebottom *et al.*, 2000). Regand and Goff (2006) reported that in a sucrose solutions containing 0.13% total protein from cold-acclimated winter wheat grass extracts, the ice recrystallization rate was significantly reduced compared to the control after temperature cycling.

This suggests that the physiological function of plant ISPs is likely the inhibition of the ice crystals growth in tissues rather than the prevention of ice formation (Atici *et al.*, 2003; Griffith *et al.*, 2004).

Until now, no plant has been reported to have constitutive RI activity; in fact, RI activity was found in over-wintering plants only after they have been exposed to low temperatures (Griffith *et al.*, 2004). In other words, if plants are not cold acclimatized they don't regulate and express ISPs, and so, they don't present RI activity. Three main factors are involved in cold acclimation of plant, and in particular in ISPs regulation and expression: low temperature itself, dehydration due to the cold stress (formation of ice crystals in the apoplast resulted in export of water from protoplast; dehydration causes an increase in the concentration of solutes inside the cells and rupture of membrane bilayer due to the resulting changes in membrane potential. Beck *et al.*, 2007), and light decline. These environmental cues lead to the activation of gene regulation and expression, including the synthesis of ISPs (Griffith *et al.*, 2004; Winfield *et al.*, 2010). Griffith and Yaish (2004) shown that winter rye (*Secale cereale*) subjected to low temperature synthetize ethylene, which induces ISPs expression. They also found that plant ISPs are homologous to Pathogenesis-Related (PR) proteins. PR proteins include different members that have evolved to perform more than one biological role in plants: β-1,3-Glucanases (GLU), Chitinases (CHT), Thaumatin-Like Proteins (TLP), and a polygalacturonase inhibitor protein (Bishop *et al.*, 2000; Griffith *et al.*, 2004). In response to snow mold infection, Salicylic Acid (SA) or Abscisic Acid (ABA) treatment (also at warm temperature, i.e. 18-20 °C), all these proteins accumulate in the apoplast where they inhibit the

growth of fungal pathogens (Figure 1.23, b). Instead, if one of the cold stimuli is present, PR-ISPs were expressed, some of them presenting a dual role: they are able to inhibit both the ice recrystallization and the growth of low temperature pathogens such as snow molds (Figure 1.23, a) (Kuwabara *et al.*, 2002; Griffith *et al.*, 2004; Moffatt *et al.*, 2006; Yaish *et al.*, 2006). Therefore, it was hypothesized that PR and PR-ISP proteins are likely to be different members of gene families that are differentially regulated by cold and by pathogens (Griffith *et al.*, 2004).

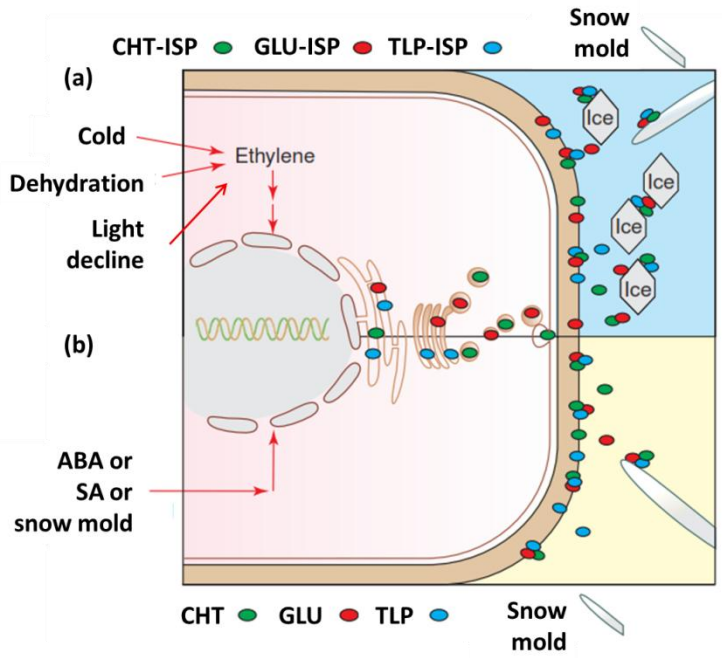

Figure 1.23 – Regulation of PR and PR-ISP proteins in winter rye (*Secale cereale*). (a) When subjected to environmental cues (cold, dehydration or light decline), winter rye synthetized ethylene, which induces the expression of chitinase-ISPs (CHT-ISP, in green), glucanase-ISPs (GLU-ISP, in red), and thaumatin-like-ISPs (TLP-ISP, in blue). These proteins are secreted in the apoplast where they act as inhibitor of the ice recrystallization; they can also have the dual role of ice and pathogens growth inhibitors. (b) When subjected to snow mold infection, salicylic acid (SA) or abscisic acid (ABA) treatment (also at worm temperatures), winter rye secrete PR proteins into the apoplast (CHT, GLU, and TLP), where they inhibit the growth of fungal pathogens; these PR proteins don't present the antifreeze activity. Adapted and modified from Griffith *et al.* (2004)

Wheat ISPs

Among plant ISPs, wheat (*Triticum aestivum*) ISPs present interesting proprieties. Regand and collaborators (2005 and 2006) shown that the ISPs present in the winter wheat extract have an interesting potential for the food industry, in particular for the ice cream production. They demonstrated that in a sucrose solutions or in an ice cream formulation containing 0.25% total protein from cold-acclimated

winter wheat grass extracts, the ice recrystallization rate was significantly reduced compared to the control after temperature cycling. In other words they reported that the addition of the winter wheat extract containing the ISPs resulted in the formation of a population of smaller ice crystals in both sucrose solution and ice cream. In 2007 Kontogiorgos and coworkers confirmed the previous results and isolated the protein responsible for the recrystallization inhibition activity: after heat treatment, alcohol precipitation and separation on a size exclusion chromatography, they were able to identify by an image analysis protocol (see 1.2.5.1) a ~22 kDa ISP protein (Figure 1.24).

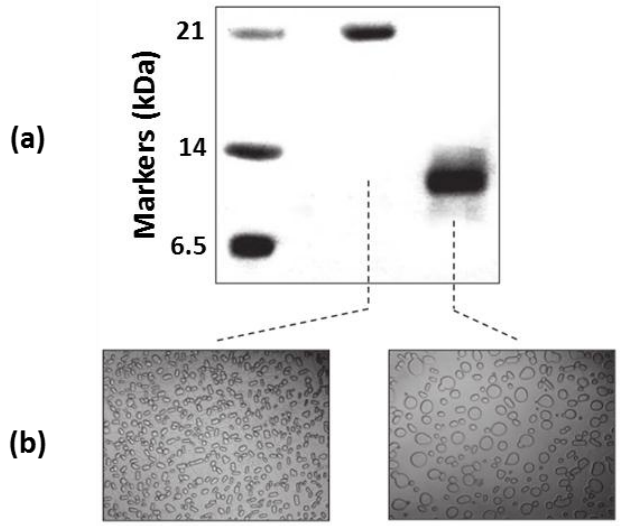

Figure 1.24 – (a) Electrophoretic profiles of the heat stable isolated proteins. (b) Qualitative comparison between the images at the end of a temperature cycling protocol for each of the isolated proteins in 23% w/w sucrose solution. Only the ~22 kDa protein exhibit a recrystallization inhibition activity. Adapted and modified from Kontogiorgos *et al.*, 2007

Circular dichroism indicated that the protein was mainly β-sheet and random coil. They also demonstrate that this protein are heat stable, a propriety very important for an industrial application; in fact many industrial processes require heat-treatment before freezing, such as ice-cream (pasteurization), ready meals (pre-cooking), or frozen vegetables (blanching). By a staining protocol (Yeh *et al.*, 1996) researchers also shown that the isolated wheat ISP was not glycosylated. Finally they determined the sequence of the ISP protein by peptide mass fingerprinting and sequencing (Figure 1.25): results indicate homology to a thaumatin-like protein of 225 amino acids, among which 16 are cysteine residues. Therefore they attributed the heat stability of the protein to the formation of 8 disulfide bridges; moreover, the protein

has a low molecular weight and attains a β-sheet conformation that is generally more heat-stable (Chakravarty *et al.*, 2000).

```
1   MASTRVLHLI ALVLAVATAA DAATITVVNR CSYTVWPGAL PGGGVRLDPG
51  QSWALNMPAG TAGARVWPRT GCTFDGSGRG RCITGDCGGT LACRVSGQQP
101 TTLAEYTLGQ GGNKDFFDLS VIDGFNVPMN FEPVGGSCRA ARCATDITKE
151 CLKELQVPGG CASACGKFGG DTYCCRGQFE HNCPPTNYSK FFKGKCPDAY
201 SYAKDDQTST FTCPAGTNYQ IVLCP
```

Figure 1.25 – Amino acid sequence of isolated ISP form *Triticum aestivum*. The boxed peptides are those that matched to the isolated ISP; the total sequence coverage was 47%. Kontogiorgos *et al.*, 2007

Furthermore, in 2002 Kuwabara and collaborators isolated a thaumatin-like protein from cold acclimated *Triticum aestivum*, identical to the ISP later isolated by Kontogiorgos and coworkers (2007). In this study it was found that the wheat ISP present an antifungal activity against the pink snow mould, *Microdochium nivale*. This result is consistent with the dual-role of some plant ISPs, which are able to inhibit both the ice and the fungal pathogens growth (see 1.2.4.3).

ISPs from winter wheat also became interesting for the biomedical industry as a non-toxic, natural and cost-affordable cryopreservation agent (see 1.2.5.2). In fact, recent studies (Hamel *et al.*, 2006; Grondin *et al.*, 2008) shown the ability of wheat extract to preserve the hepatocytes viability, attachment efficiencies, and hepatospecific functions during cryopreservation. However, protein/s or substance/s responsible for the protective effect were not isolated.

Therefore, it would be of interest to obtain a large amount of a single and pure ISP; this will be one of the objectives designed for this project.

1.2.5. Industrial applications

The discovery of ISPs is interesting not only from a biological point of view (i.e. the comprehension of their mechanism of action and of the interaction with ice), but also for their possible application in agricultural/food and medical fields.

Application of ISPs has already been studied as additives for frozen meet and frozen desserts. Payne and collaborators (1994) shown that cryopreserved (-20 °C) beef and lamb presented smaller ice crystals if soaked in presence of type I ISP from Winter Flounder or ISGP from the Antarctic Cod; moreover, meat treated with ISGP and stored at -20 °C for 8 weeks presented less drip with no effects on the overall quality of the product (e.g. flavour, texture, etc.). In frozen desserts such as ice lollies and ice cream, ISP shown to inhibit the recrystallization of ice allowed for the preservation of the smooth and creamy texture of a high quality product (see 1.2.5.1). Despite the good results obtained with fish IS(G)Ps as food additives, the use of these proteins in frozen food has encountered both ethical and market problems. From the ethical point of view vegetarian people are not willing to eat products containing fish proteins, such as ISPs. Moreover there is a market problem concerning the consumers acceptance, because consumers think that food with the fish IS(G)Ps may taste "fishy". Therefore the use of ISPs from other sources such as plants represents a valid alternative to overcome these problems.

Aquaculture is another field interested in the application of ISPs. In fact, in the northern parts of the Atlantic region, the harsh climatic conditions represent a problem for aquaculture. Some attempts have been made in order to create a transgenic freeze-tolerant fish carrying an ISP gene. One of the first attempts concerned the injection[11] of the ISP gene from the winter flounder into the rainbow trout; the direct injections resulted in the survival of the transgenic fish at temperature as low as -1.4 °C (Hew *et al.*, 2002). Also fruit and vegetables (e.g. strawberries, raspberries, tomatoes, etc.) are subjected to injuries due to freezing temperature. Insertion of an ISP gene from winter flounder in a tomato plants resulted in a recrystallization inhibition activity in the transgenic tissue, indicating a possible application of this technique in fruit and vegetables (Hightower *et al.*, 1991).

However, there are three major problems related to the creation of a transgenic organism: I) stable gene integration and inheritance through

[11] Injection: the gene of interest is injected into the pronuclear of a fertilized ovum by a capillary needle

generations; II) expression and correct post-translational modification of the gene product; III) introduction of a transgenic organism in the environment and in the human diet. Moreover, as for the use of ISPs as food additive, the production of a transgenic food will encountered both ethical and market problems.

Another application of ISPs could be their introduction in baker's yeast cells in order to improve their vitality in frozen dough products (Panadero *et al.*, 2005).

1.2.5.1. Ice cream

It is well known that quality of ice cream depends on its physical structure, which consists of air bubble, fat globules, ice crystals, and an unfrozen serum phase. Among them, ice crystals seem to play the most important role in storage stability and texture (Alelong *et al.*, 2008). In fact, ice crystals larger than 40 μm are perceived from the tongue and, therefore, if present in sufficient number, they result in a coarse and grainy texture (Donhowe *et al.*, 1991). For this reason, one of the main problems of ice cream manufacturing is the recrystallization process caused by temperature fluctuation during production phases, transportation and storage.

Manufacturing of ice cream consists on the formulation, weighting of ingredients, mixing, pasteurization and homogenization. The homogenization step is fundamental to obtain a more uniform and stable emulsion, thus limiting ice crystallization during the freezing process. After homogenization, the ice cream mixture is cooled down to 0-5°C and then subjected to freezing (-5 °C). Freezing is important in determining the mean size and the size distribution of ice crystals: an optimal freezing process resulted in a large number of small ice crystals. Lowering the freezing temperature (e.g. -9 °C) allows the production of smaller ice crystals (Julien, 1985), but requires higher costs due to greater energy expenditure. The obtained semi-frozen product, is then frozen rapidly down to -25 °C by the use of a liquid nitrogen cooled airflow (hardening) (Huang *et al.*, 1992). Temperatures and times of cooling depend on the type of storage freezer; rapid cooling will promote quick freezing of water and create small ice crystals. The product is finally packed and stored at -18/-22 °C, temperature that resulted in a little increase in mean ice crystal size and so in the product quality maintenance (Hagiwara *et al.*, 1996). During

transportation, retailing and home storage, temperature is well above -20 °C and fluctuates because of automatic defrost cycles and mishandling of the product (e.g. transportation in a shopping cart); these great number of temperature fluctuation cause the formation of large ice crystals and the deterioration of textural characteristics of ice cream (and in general of frozen foods) (Damodaran, 2007).

In this context, ISPs hold the great potential to act as recrystallization control agents, thus providing smoother ice creams and higher quality products compared to the current available products (Regand *et al.,* 2006). ISPs can be added to the ice cream mixture during the semi-frozen stage, eliminating the necessity for rapid freezing during the hardening step and minimizing the rate of recrystallization caused by temperature fluctuation (Warren *et al.*, 1992).

Regand and Goff in 2006 shown that a winter wheat grass extract containing an ISP significantly decrease the mean size of ice crystals in sucrose solution containing ice cream ingredients (Figure 1.26); in the same work they presented an efficient and quantitative method to evaluate the ice crystals size and distribution using a cold-stage optical microscopy device. In brief, they investigated the effect of the ISP in a solution containing only sucrose (Formulation A) and in a solution containing ice cream ingredients (Formulation D). 0.25% Total Protein (TP) from winter wheat extract was added to the solutions; this was compared to the respective samples without the extract. The ice crystals analysis protocol was performed taking advantage of a cold stage attached to a light microscope: after a temperature cycling protocol a picture was taken every 80 minutes, in order to follow the process of crystallization in the different solutions (see Chapter 2.9.1 for a more detailed protocol) (Figure 1.26).

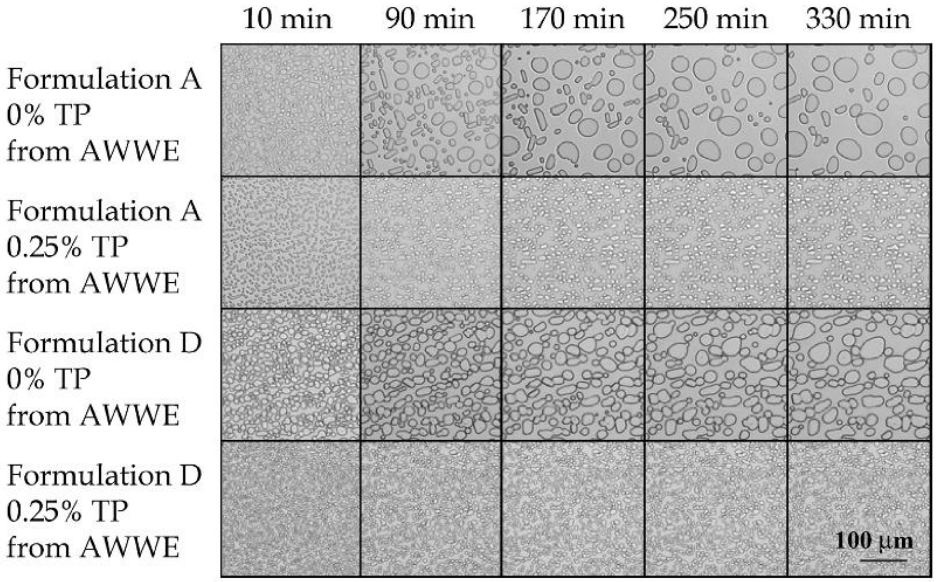

Figure 1.26 – Bright field images acquired every 80 minutes (starting after 10 minutes) at -5 °C from sucrose (Formulation A) and ice cream (Formulation D) solution with and without 0.25 % total protein (TP) from winter wheat extract (AWWE) (Regand *et al.*, 2006)

As reported in Figure 1.26, the addition of the winter wheat extract containing the ISP resulted in the formation of a smaller population of ice crystals in both formulations.

Therefore, the addition of an ISP to frozen dessert (and in general, to frozen food) could answer the need to develop an alternative ingredient for controlling ice crystal growth during the manufacturing and storage processes. Moreover, the ISPs exploitation will not involve the expensive improvement of the cold chain or the unhealthy incorporation of chemical additives to food.

1.2.5.2. Biomedical area: cell cultures and organs preservation

The cryopreservation or low-temperature storage of cells, tissues, and organs has an important impact on medical and veterinary purposes, particularly on cell culture maintenance, organ transplantation, and reproduction.

Until now, the developed cold-preservation technique requires the use of chemical substances as protective agents, e.g. dimethyl sulfoxide (DMSO), glycerol, and sucrose. Since these substances prevent ice crystals injury in a colligative manner, they have to be used at high concentration that may cause toxicity and side effects (Breton *et al.*, 2000).

Due to their protective effect on organisms that survive at subzero temperature, and to their non-colligative mechanism of action, ISPs represent a potential alternative to the available protective agents. Numerous studies have been performed, ranging from platelets and human hepatoma cells, to oocytes and whole organs.

Human platelets could be stored at 22 °C for a maximum of 5 days, because of their chilling sensitivity. Therefore, since platelets are routinely used for blood clotting and transfusion to needy patients, it would be of enormous interest the development of an efficient and long-term platelet preservation method. Carpenter and collaborators (1992) shown that the addition of 150 µg/ml of recombinant ISP type I from winter flounder allowed for an optimal protection (measured as reduction of hemolysis[12] percentage) after rapid freezing followed by rapid rewarming. In 1996, Chao and coworkers confirmed these results using ISP type I, II and III. Moreover, it was demonstrated (Tablin *et al.*, 1996) that platelets can be stored at 4°C for at least 21 days if preserved in the presence of ISGPs isolated from the serum of three Antarctic fish species (*Dissostichus mawsoni*, *Trematomus borchgreuinki*, and *Trematomus bernacchii*). These results shown a potential use of the ISPs as protective agents in platelets cold-preservation; however, other studies are required to identify the most appropriate ISP/storage temperature and medium conditions. For example, it would be of interest to evaluate the effects of plant derived ISPs in the preservation process.

In 2008 Hirano and collaborators shown that viability of human hepatoma cells (HepG2) stored at 4 °C to simulate clinical conditions of cold organ storage, can be improved by the addition of fish-derived type III ISPs. In the same year, Grondin and coworkers studied the protective activity of a wheat protein extract (WPE; it contains sugars, antioxidants, amino acids and proteins such as ISPs) on the cryopreservation of rat hepatocytes. They demonstrated that, instead of the standard DMSO cryoprotectant, WPE allows for the preservation of the hepatocytes viability, attachment efficiencies, and hepatospecific functions such as albumin secretion. They conclude that WPE is an excellent cryopreservant for long-term storage of primary hepatocytes; however, they still have to determine what is/are the compound/s present in the wheat extract responsible for the protective effect.

[12] Hemolysis refers to the destruction of erythrocytes (red blood cells) which leads to the release of their contents (hemoglobin) into surrounding fluid

Oocyte cryopreservation is considered a good alternative to the ethically problematic embryo cryopreservation (Bernard *et al.*, 1996). However, it was shown that the use of cryoprotective agents and low temperature disrupts the oocyte cytoskeleton rendering the oocyte impenetrable to sperm. Therefore, the use of ISPs to protect oocytes during the freezing process represents an interesting alternative. Rubinsky and coworkers (1992) demonstrate that the viability of pig oocytes is improved in presence of a fish ISGPs; they hypothesized that the protection effect was not related to the antifreeze proprieties of the glycoprotein, but that it probably resulted from the interaction with and the stabilization of the oocyte cell membrane. Similar results were observed for bovine and ovine embryos (Arav *et al.*, 1993), porcine oocytes (Chen *et al.*, 1995), mature mouse oocytes (O'Neil *et al.*, 1998), and chimpanzee (Younis *et al.*, 1998) and bovine (Prathalingam *et al.*, 2006) sperm. Moreover, in a recent work (Jo *et al.*, 2011) it was demonstrated that supplementation of ISP has a protective effect on mouse oocytes for chilling injury allowing the preservation of spindle/membrane integrity.

Cryopreservation of complex tissues and organs is obviously much more difficult than single cell preservation. Positive results in terms of ISPs protective activity were obtained with rat livers (Lee *et al.*, 1992) and hearts (Amir *et al.*, 2005). These findings suggests a possible role for the ISPs in lengthening the storage period of organs used in medical transplantation procedures; however, further research is needed before a clinical application of the ISPs can be envisaged.

The mechanism by which ISPs act as cryoprotectant in low-temperature storage of biological material is not yet fully understood. While it was initially proposed that the recrystallization inhibition activity was correlated to the efficacy in protecting the cells (Carpenter *et al.*, 1992; Chao *et al.*, 1996), it is now generally accepted that the main function of ISPs in cells protection is the membrane stabilization at low temperature (Tomczak *et al.*, 2002; Inglis *et al.*, 2006; Brockbank *et al.*, 2011). At physiological temperature membrane lipids are usually in the fluid phase while, during lowering of temperature lipids undergo a phase transition from the liquid phase to the more rigid gel phase. This phase transition is not completely cooperative and so liquid and gel phase co-exist during cooling. This intermediate phase are thought to be the cause of leakage across the bilayer, and so the

cause of cells damage and death due for example to ion gradients dissipation (Figure 1.27; Tomczack *et al.*, 2002I).

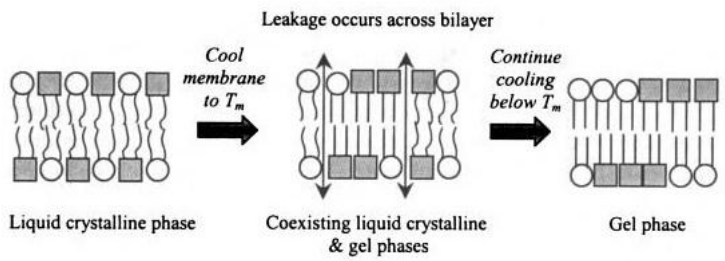

Figure 1.27 – Graphical representation of leakage that occurs during cooling caused by the transition from the liquid to the gel phase of a membrane bilayer; T_m refers to phase transition temperature (Tomczac *et al.*, 2002I)

Different studies suggested that ISPs and ISGPs are able to interact (possibly by hydrophobic interactions) and protect cells membrane during the cooling process (Hays *et al.*, 1996; Tomczak *et al.*, 2001; Wu *et al.*, 2001; Tomczak *et al.*, 2002; Beirao *et al.*, 2011), thus inhibiting the leakage across the membrane and so the cell damage and death. However, the interaction responsible for stabilization of membranes is not fully understood and represents an interesting field of study (Inglis *et al.*, 2006).

A more complete knowledge of this mechanism is required to attempt a use of ISPs in low-temperature preservation of biological materials. Moreover, it would be of interest to investigate the less studied insect and plant ISPs in order to evaluate their effect in comparison to the well-studied fish proteins. Since most of published works on this field were performed using a protein extract enriched in ISPs, another requisite for the medical application will be the obtainment of a large amount of a purified ISP; this goal will be reached by the recombinant expression of ISPs.

Chapter 2

MATERIALS AND METHODS

2.1. General molecular biology techniques

2.1.1. Bacterial and yeast strains

***E. coli* strain**	**Genotype**	**Application**
DH5α	endA1, recA1, hsdR17 (r^-_k, m^+_k), supE44, thi-1, gyrA96, relA1, lacZ ΔM15, Δ(lacZYA-argF), U169, deoR	Brazzein and ISP cloning procedures
BL21 (DE3)	F^-, ompT, hsdSB (r^-_b, m^+_b), gal dcm (DE3)	ISP expression
C41 (DE3)	F^-, ompT, hsdSB (r^-_b, m^+_b), gal dcm (DE3) (one uncharacterized mutation compared with BL21(DE3))	ISP expression
Origami2 (DE3)	Δ(ara-leu)7697, ΔlacX74, ΔphoA, PvuII, phoR, araD139, ahpC, galE, galK, rpsL, F'[lac+ lacIq pro] (DE3), gor522::Tn10 trxB (StrR, TetR)	ISP expression

***P. pastoris* strain**	**Genotype**	**Application**
X33	Wild type, Mut^+	Brazzein and ISP expression

2.1.2. Protein expression vectors

Vector type	**Antibiotic resistance**	**Promoter**	**Inductor**	**Fusion tag**
pET-28a	Kanamycin	T7	IPTG	His-tag
pPICZαA	Zeocin	AOX1	Methanol	C-myc and His-tag
PGAPZαA	Zeocin	GAP	/	C-myc and His-tag

2.1.3. Bacterial culture media

Type of media	Composition
LB (Luria-Bertani)	10 g Bacto tryptone; 5 g yeast extract; 5 g NaCl; 1 ml of 1 M NaOH; deionized water to 1 litre. Sterilize by autoclaving. For agar plating solution, add 15 g agar.
SOC	20 g Bacto tryptone; 5 g yeast extract; 0.5 g NaCl; 1.875 g KCl; deionized water to 1 litre. Sterilize by autoclaving. Add 20 ml of sterile 1 M glucose and 10 ml of sterile 1 M $MgCl_2$ before use.

2.1.4. Agarose gel electrophoresis buffers

Buffer	Composition
TAE Buffer 50 X (Tris-Acetate EDTA)	242 g Tris base salt; 57 ml Glacial acetic acid; 100 ml of 500 mM Na_2EDTA (pH 8.0); water to 1 litre (adjusted the pH to 8.0)
Loading Buffer 6X (Promega)	0.4% (w/v) Orange G ; 0.03% (w/v) Bromophenol Blue ; 0.03% (w/v) Xylene Cyanol FF; 15% (w/v) Ficoll 400; 100 mM Tris-HCl (pH 7.5); 50 mM EDTA (pH 8.0)

2.1.5. Restriction/Modifying enzymes and standard

Enzyme	Application
AvrII (New England BioLabs)	G↓CTAG G G GATC↑C
BamHI (Promega)	G↓GATC C C CTAG↑G
BglII (Promega)	A↓GATC T T CTAG↑A

BstBI (New England BioLabs)	TT↓CG AA AA GC↑TT
NdeI (Promega)	CA↓TA TG GT AT↑AC
NotI (Promega)	GC↓GGCC GC CG CCGG↑CG
SacI (Promega)	G AGCT↓C C↑TCGA G
XhoI (Promega)	C↓TCGA G G AGCT↑C
DpnI (New England BioLabs)	Digestion of template DNA vector in mutagenesis protocol
Pfu DNA Polymerase (Promega)	High fidelity PCR
Taq Polymerase (homemade)	Screening colony PCR
TSAP (Promega)	Catalyzes the removal of 5´ phosphate groups from DNA, thus preventing the recircularization and religation of linearized cloning vector DNA during ligation
1 Kb DNA ladder (Promega)	250 to 10000 bp reference
100 bp DNA ladder (Promega)	100 to 1500 bp reference

2.1.6. *Escherichia coli* competent cells

2.1.6.1. DH5α rubidium chloride competent cells

A single colony of DH5α *Escherichia coli* strain from a LB (Luria Bertani) plate was inoculated in 100 ml of LB broth. The flask was shaked at 37 °C until the optical density (OD_{600}) reached values between 0.22 to 0.50. After this step, pre-chilled supplies and solutions were used, and all operations were performed at 4°C. Cells at

OD_{600}=0.22-0.55 were chilled on ice for 20 minutes. The culture pellet, obtained after centrifugation at 7500 g for 10 minutes, was resuspended in 20 ml of TB I buffer (composition is reported in Table 2.1) and kept on ice for 5 minutes. Cells pellet was then resuspended in 2 ml of TB II buffer (composition is reported below) and incubated 15 minutes in we ice. Cells were dispensed 100 µl into pre-chilled microcentrifuge tubes, snap freezed in liquid nitrogen and stored at -80 °C.

Buffer	Composition
TBI	Rubidium chloride 100mM, Manganese chloride 50mM, Potassium acetate 30mM, Calcium chloride 10mM, Glycerol 15% v/v. Adjust to pH 5.8 using 0.2 M Acetic acid. Sterilize by membrane filtration.
TB II	MOPS 10 mM, Rubidium chloride 10 mM, Calcium chloride 75 mM, Glycerol 15% v/v. Adjust to pH 6.5 with 1M NaOH. Sterilize by membrane filtration.

Table 2.1 - Buffers for rubidium chloride competent cells

2.1.6.2. BL21, C41 and Origami2 calcium chloride competent cells

One colony from LB plate was inoculate into 5 ml LB and shacked overnight at 37 °C. 1 ml of the overnight cell culture was used to inoculate 100 ml fresh LB medium. Culture was grown shaking at 37 °C to an OD_{600} ~ 0.25-0.3. Culture was chilled on ice for 15 minutes and then centrifuged at 4 °C 4000 g for 5 minutes. After this step, pre-chilled supplies and solutions were used, and all operations were performed at 4 °C. Cell pellet was resuspended in 50 ml of cold 0.1 M $CaCl_2$ and incubated in ice for 30 minutes. Cells were centrifuge as above, and pellet was resuspended in 2 ml of 0.1M $CaCl_2$ plus 25% glycerol. Cells were dispensed 100 µl into pre-chilled microcentrifuge tube and kept on ice. Cells competence starts after one hour of ice incubation and reaches its maximum after 24 hours. Therefore, after 24 hours cells were snap freezed in liquid nitrogen and stored at -80 °C.

Cells competence was determined using 1 µg of DNA, and the efficiency obtained was between 10^7-10^9 cfu (colony forming unit)/µg of DNA.

2.1.7. Plasmid DNA extraction

Plasmid DNA was purified using the QIAprep Spin Miniprep Kit (Quiagen, Hilden) according to manufacturing instructions. Briefly, 10 ml of a single colony overnight culture were subjected to alkaline lysis and cellular RNA was digested by addition of RNase A; plasmid DNA was then bound to a silica-based membrane. Plasmid DNA was finally eluted in 50 µl of sterile Milli-Q water pH 8.4.

2.1.8. DNA quantification

UV-visible spectra was recorded on a Agilent 8453 UV-Visible spectrophotometer interfaced with a personal computer using the Chemstation Software for Windows® (Agilent technology). Absorbance at 260 nm was measured at room temperature with Suprasil® 70 µl quartz cell (Hellma), with 1 cm optical path-length. To avoid linear baseline artifacts, the absorption average over the range 700 to 900 nm was subtracted from the entire spectrum.

The concentration of pure double-stranded DNA with an A260 of 1.0 is 50 ng/µl. Thus, the following formula can be used to determine the DNA concentration of a solution:

ng/µl (unknown dsDNA) = 50 ng/µl x Measured A260 x Dilution factor

2.1.9. Agarose gel electrophoresis

Analytical and preparative separation of DNA fragments, according to their molecular weight, was obtained by agarose gel electrophoresis. Analysis of DNA plasmids of 1-10 kbp were performed using agarose 1% (w/v) gels; for smaller DNA fragments separation, a 2% (w/v) agarose gel was used. To prepare 1% (w/v) gels, 1 g of agarose was dissolved in 100 ml of TAE buffer by heating. 0.5 µg/ml ethidium bromide was added to the gel solution after cooling to about 60 °C.

Loading sample buffer 6X was added to DNA samples that were then separated by electrophoresis under constant voltage (50-100 V). DNA ladders (Promega) were loaded in each gel as reference. Following electrophoresis, DNA bands were identified by ethidium bromide fluorescence emission in the visible spectral region.

2.1.10. Polymerase chain reaction

Preparative PCR reactions were performed in 50 µl of a mixture containing 0.2 mM of mix dNTPs (Promega), 0.5 µM of each primer, 1.5 U of Pfu DNA polymerase, and Pfu buffer. 200-500 pg of template DNA were added to the mix. For Screening PCR, a Taq DNA Polymerase was used.

DNA was amplified with 25 cycles of denaturation (30 seconds at 95 ºC), annealing (30 seconds at 72 °C), extension (1 minute per kilobase at 72 ºC). The final extension was performed at 72 ºC for 10 min.

When required, a mutagenic phase was included before the amplification phase: DNA was amplified with 5 cycles of denaturation (1 minute at 95 ºC), annealing (30 seconds at temperature below the melting temperature of primers), extension (1 minute per kilobase at 72 ºC).

2.1.10.1. Site-directed mutagenesis

50 ng of template DNA were added to a mixture containing 0.2 mM dNTPs, 0.5 µM of each primer, 1.5 U of Pfu DNA polymerase, and Pfu buffer. DNA was amplified with 18 cycles of denaturing (30 seconds at 95 ºC), annealing (1 minutes at 55 °C), extension (1 minute per kilobase at 72 ºC). Mutagenic primers contain the desired mutation.

Parental (no mutated) DNA was digested wit 1 µl of DpnI that was directly added to the amplification reaction and incubated for 1 h at 37 °C.

An aliquot of DH5α competent cells were transformed (see 2.1.12) with 5 µl of digested reaction. Clones selection and stocks preparation were performed as described in 2.1.11.

2.1.11. Cloning procedures

Vectors and DNA inserts were digested with proper restriction enzymes. After separation by agarose gel electrophoresis the DNA band relative to the vector was extracted from gel (Agarose LMP, Preparative

grade for large fragment, Promega), using the Wizard® SV Gel and PCR Clean-Up System Kit (Promega). Purified vectors were de-phosphorilated, according to manufacture instructions, with the TSAP enzyme (ThermoSensitive Alkaline Phosphatase, Promega). Instead, PCR fragment inserts were purified with the GenElute™ PCR Clean-Up Kit (Sigma), digested with appropriate restriction enzymes, and further purified by gel purification or using the purification kit above mentioned.

Vectors and inserts were quantified and then ligated using 1 U of T4 DNA Ligase (Promega) using different vector:insert ratio (1:0, 1:3, 1:5). Ligation mixes were incubated for 3 hours at room temperature, and then they were used to transform a DH5α competent cells aliquot (see 2.1.12). Transformed cells were plated in LB plates additioned with specific antibiotics and incubated at 37 °C overnight.

Colonies in which the incorporation of the insert took place were selected by PCR analysis. Vectors extracted from positive clones were sequenced (BMR Genomics, Padova) to verify the accuracy of the sequence.

Clones containing the correct insert-vector were stored at -80°C in 30% glycerol diluted in LB medium.

2.1.12. Bacterial transformation

100 µl of competent *E. coli* cells were defrosted on ice. 200-400 ng of DNA from a ligation reaction or 10-100 ng of circular plasmid DNA were then added and cells were incubated for 20 min on ice. Cells were then heat shocked for 90 seconds at 42 °C in a water bath, and incubated on ice for another 2 min. 900 µl of SOC medium were added and cells were incubated for 1 h at 37 °C with shacking. Finally, cells were plated onto LB agar plates containing the corresponding antibiotics for selection of positive transformants.

2.2. Construction of brazzein expression plasmids

In this section will be described the procedures used for the construction of the brazzein expression plasmids for the *Pichia pastoris* expression system.

2.2.1. Construction of an expression vector for the inducible expression of brazzein

Brazzein cDNA was chemically synthesized (Sigma genosys) with codon optimization for the expression in *P. pastoris* and then cloned into the pPICZαA vector.

The pPICZαA vector for the inducible expression of brazzein was obtained from Invitrogen (San Diego, USA). This vector was digested with XhoI (Promega) and NotI (Promega). Brazzein cDNA was ligated with the treated pPICZαA vector, and then transformed into *E. coli* DH5α competent cells (see 2.1.6.1). Transformants (pPICZαA-BRA) were then selected on low salt LB plates (10g/l tryptone, 5g/l NaCl, 5g/l yeast extract, 15g/l agar) containing 25µg/ml Zeocin™ (Invivogen). The pPICZαA-BRA plasmid was sequenced to verify the accuracy of the sequence and then used for the expression of brazzein gene in *P. pastoris*. The pPICZαA vector comprises the pAOX inducible promoter, the secretion signal sequence from the *Saccharomyces cerevisiae* α factor prepro peptide, the brazzein reading frame sequence and the AOX1 terminator, and the dominant selectable shuttle marker Zeocin™, as reported in Figure 2.1.

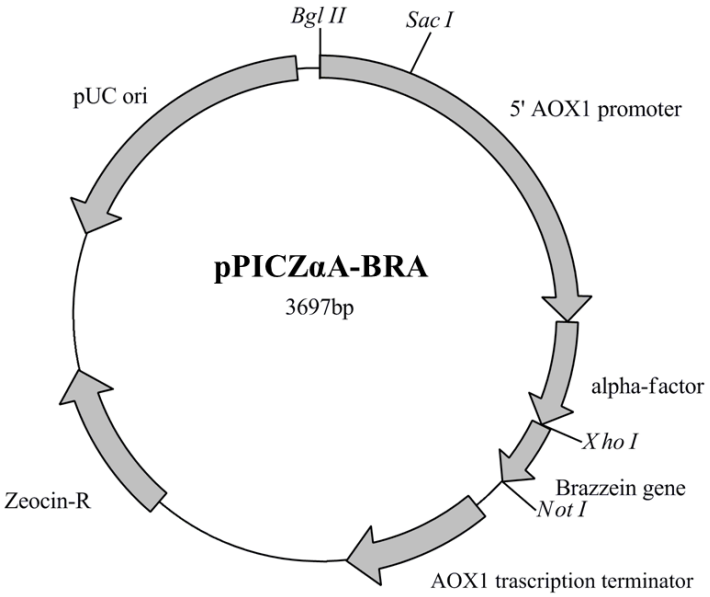

Figure 2.1 - Vector map of the plasmid for the inducible expression of brazzein in *P. pastoris* using the pAOX promoter

2.2.2. Construction of expression vectors for the constitutive expression of brazzein

The promoter pGAP was amplified by PCR from genomic of *P. pastoris* (chromosome 2). The forward primer and reverse primer used for amplification of GAP gene were 5'-CACTTGACAGGATCCTTTTTTGTAG-3' and 3'-CATCGTTTCGAAATAGTTGTTCAATTG-5'. The pPICZαA-BRA vector was digested with BglII (Promega) and BstBI (New England BioLabs), while the PCR product was digested with BamHI (Promega) and BstBI. The PCR product was then inserted into pPICZαA-BRA plasmid in place of the pAOX1 to generate plasmid pGAPZαA-BRA. The construction flow chart of integrative plasmid pGAPZαA-BRA is shown in Figure 2.2. As for the pPICZαA-BRA vector, the pGAPZαA-BRA vector was transformed into *E. coli* DH5α and then sequenced to verify that the correctness of the sequence.

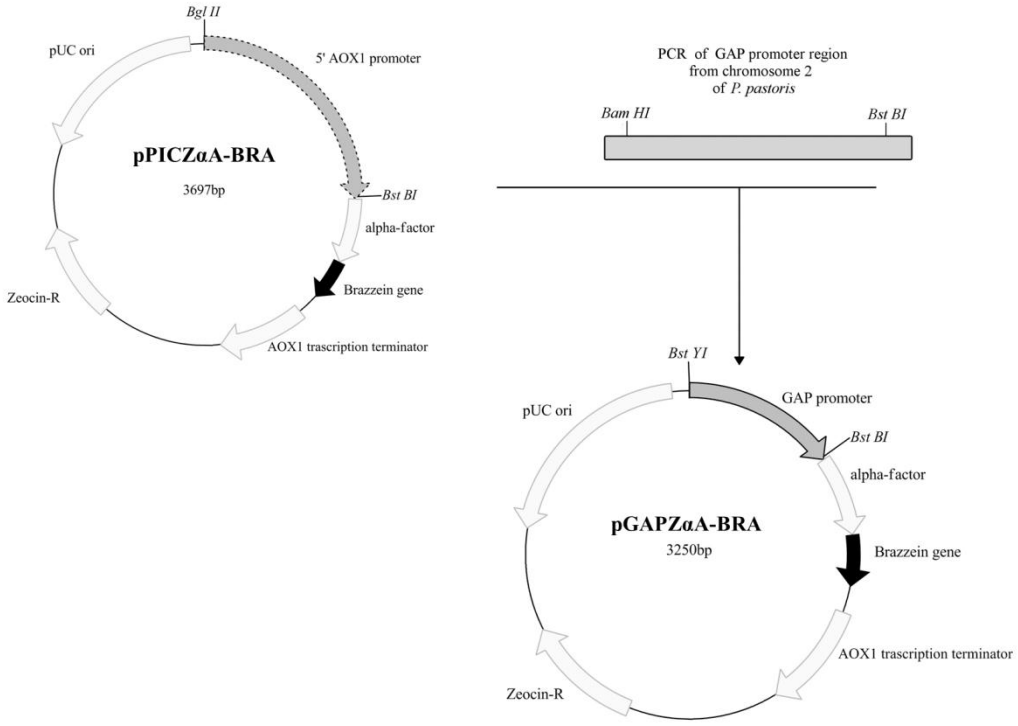

Figure 2.2 - Schematic diagram illustrating the construction of the pGAPZαA-BRA constitutive expression vector from the pPICZαA-BRA inducible expression vector

The pGAPZαA-BRAΔ1M vector was obtained directly modifying the pGAPZαA-BRA plasmid by site directed mutagenesis. The forward primer and reverse primer used to delete the first brazzein amino acid were 5'-GGGTATCTCTCGAGAAAAGAGATAAATGCAAGAAAG-3' and 5'-CTTTCTTGCATTTATCTCTTTTCTCGAGAGATACCC-3'.

2.3. Construction of ISP expression plasmids

In this section will be described the procedures used for the construction of the ISP expression plasmids for the expression both in *E. coli* and *P. pastoris* expression system.

2.3.1. Construction of the *E. coli* ISP expression vector

The ISP cDNA was obtained through chemical synthesis (GeneART, Regensburg - Germany) with codon optimization for the expression in both *E. coli* and *P. pastoris*. After digestion with NdeI and and NotI, ISP cDNA was cloned into the pET-28a vector for the expression in *E. coli* that carries a N-term His-tag sequence. As for the above mentioned vectors, the pET-28a-ISP vector was transformed into *E. coli* DH5α and then sequenced to verify that the correctness of the sequence.

2.3.2. Construction of the expression vectors for the constitutive ISP expression in *P. pastoris*

The pGAPZαA-ISP expression vector was obtained directly modifying the pGAPZαA-BRA plasmid. Both the vector and the ISP cDNA were digested with XhoI and NotI. After digestion ISP cDNA was inserted into pGAPZαA-BRA plasmid in place of the brazzein gene to generate plasmid pGAPZαA-ISP. The construction flow chart of integrative plasmid pGAPZαA-ISP is shown in Figure 2.3. The pGAPZαA-ISP vector was transformed into *E. coli* DH5α and then sequenced to verify that the correctness of the sequence.

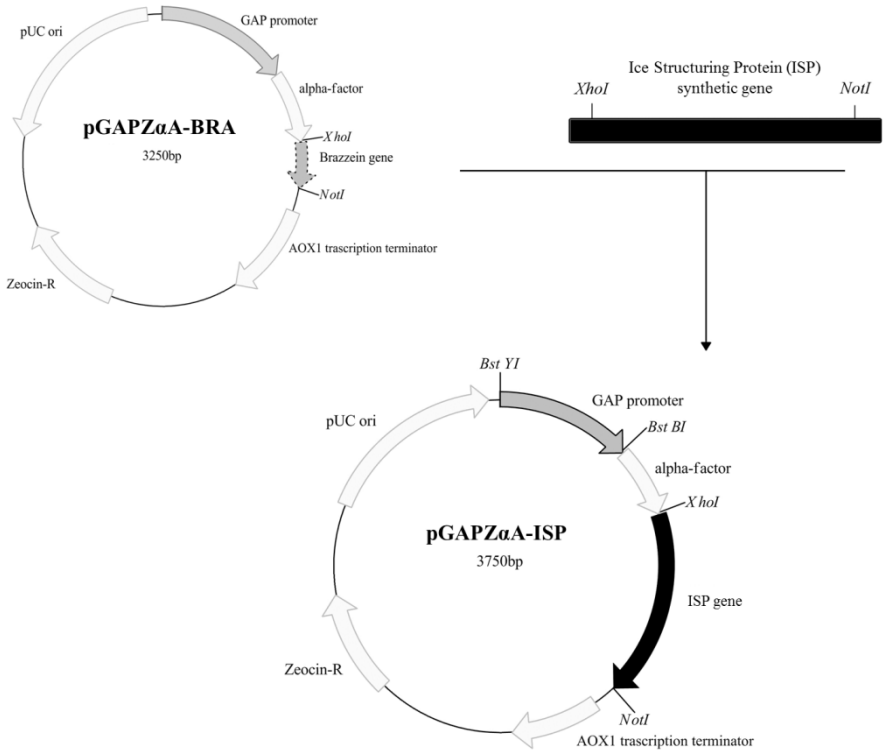

Figure 2.3 - Schematic diagram illustrating the construction of the pGAPZαA-ISP constitutive expression vector from the pGAPZαA-BRA expression vector

The pGAPZαA-ISP expression vector was modified by site-directed mutagenesis to obtain the pGAPZαA-ISPht vector. The forward primer and reverse primer used to eliminated the TAA stop codon allowing the transcription of the histidine-tag (ht) were 5'-CCAGATCGTTTTGTGTCCAGAACAAAAACTCATCTCAG-3' and 5'-CTGAGATGAGTTTTTGTTCTGGACACAAAACGATCTGG-3' (melting temperature 62.6 °C).

ISP was also expressed without the α-factor secretion signal sequence which was deleted from the pGAPZαA-ISP and the pGAPZαA-ISPht by PCR mediated deletion using the following forward and reverse primers: 5'-AACTATTTCATGGCTTCCACTAGAGTTTGC-3' and 5'-GGAAGCCATGAAATAGTTGTTCAATTGATG-3'. From these mutagenesis steps we obtain the pGAPZαA-ISP_cutα and pGAPZαA-ISPht_cutα expression vectors.

All the ISP vector was transformed into *E. coli* DH5α and then sequenced to verify that the correctness of the sequence.

2.4. Construction of pGAPZαA empty vector

The constitutive empty expression vector was obtained modifying the pGAPZαA-BRA vector. pGAPZαA-BRA was digested with XhoI and NotI in order to excise the brazzein gene. Digested vector was then purified by agarose gel electrophoresis and ligated with the MCS (Multiple Cloning Site) sequence to generate plasmid pGAPZαA. The MCS sequence was obtained by annealing (complementary primers were mixed in equal volume; the mix was placed in water at 95°C and allowed to cool to room temperature on the workbench) the following primers:

```
5′-TCGAGAAAAGAGAGGCTGAAGCTGAATTCACGTGGCCCAGCCGGCCGTCTCGGATCGGTACCTCGAGCCGCGGC-3′
       ||||||||||||||||||||||||||||||||||||||||||||||||||||||||||||||||||||||||
    3′-CTTTTCTCTCCGACTTCGACTTAAGTGCACCGGGTCGGCCGGCAGAGCCTAGCCATGGAGCTCGGCGCCGCCGG-5′
```

The pGAPZαA vector was transformed into *E. coli* DH5α and then the correctness of the sequence was verified by sequencing.

2.5. Transformation of *P. pastoris* cells with brazzein, ISP or empty expression vectors by electroporation

Electrocompetent *P. pastoris* X-33 cells were prepared using the protocol suggested in the Easyselect™ Pichia expression kit – Instruction manual (Invitrogen): an aliquot of competent *P. pastoris* cells resuspended in ice-cold 1M sorbitol (80 µl) was mixed with 10 µg of linearized DNA (in 10 µl sterilized water). The pPICZαA-BRA was linearized by SacI (Promega). Instead, pGAPZαA-BRA, pGAPZαA-ISP, and pGAPZαA recombinant plasmids were linearized by AvrII (New England BioLabs).

The mix was transferred to an ice-cold 0.2 cm electroporation cuvette and incubated in ice for 5 minutes. The cells were pulsed using a Biorad Gene Pulser II electroporator at 1500V, 25 µF, and 400 Ω.

The transformed cells were incubated with 1 ml of ice-cold 1M sorbitol at 30°C for 2 hours. Then cells were spread on YPDS (10 g/l yeast extract, 20 g/l peptone, 20g/l dextrose, 1M sorbitol) plates containing 100 µg/ml Zeocin™ as the selective markers. Plates were incubated for 3-5 days at 30 °C until colonies form.

2.6. Identification of transformed *P. pastoris* cells and small scale expression tests

High-level expression transformants were selected on YPDS agar plates (10 g/l yeast extract, 20 g/l peptone, 20g/l dextrose, 1M sorbitol, and 20 g/l agar) containing 100, 500, 1000 and 2000 µg/ml Zeocin™ and incubated at 30°C for 5 days. Clones which are able to grow on the 2000 µg/ml Zeocin™ plate are putative multi-copy recombinants.

Selected clones may be stored at -80°C in YPD medium (10 g/l yeast extract, 20 g/l peptone, 20 g/l dextrose) containing 15% glycerol.

2.7. Brazzein expression, purification and characterization

2.7.1. Small scale inducible and constitutive expression tests

Yeast transformed with the inducible expression plasmid were streaked onto 5 ml BMG medium (100 ml/l 1M potassium phosphate buffer pH 6.0, 100 ml/l 10X YNB, 2 ml/l 0.02% biotin, 100ml/l 10% glycerol) and incubated in 25 ml Erlenmeyer flask overnight. These cultures were used to inoculate 10 ml BMM medium (100 ml/l 1M potassium phosphate buffer pH 6.0, 100 ml/l 10X YNB, 2 ml/l 0.02% biotin, 100 ml/l 5% methanol) in 50 ml Erlenmeyer baffled flask to an initial OD of 1. These cultures were incubated at 30 °C for 3 days shaking at 230 rpm; every 24 hours 100% methanol was added to a final concentration of 0.5% in order to maintain induction.

Instead, single selected colonies of constitutive transformed yeast (with brazzein, ISP or empty vector) were streaked onto 5 ml YPD medium (10 g/l yeast extract, 20 g/l peptone, 20 g/l dextrose) and incubated in 25 ml Erlenmeyer flask overnight. These cultures were used to inoculate 10 ml YPD medium in 50 ml Erlenmeyer baffled flask to an initial OD of 1. These cultures were incubated at 30 °C for 3 days shaking at 230 rpm.

The supernatant of these cultures was obtained by centrifugation every 24 hours and use to analyze the protein expression by Tris-Tricine SDS-PAGE electrophoresis.

From this step the highest-level transformant was isolated and used for the successive scale-up of the process using a fermentor.

2.7.2. Expression of brazzein by recombinant *P. pastoris* using fermentor

The most efficient brazzein-inducible-expressing clone was selected and pre-cultured in 500 ml of a medium containing 100 ml/l phosphate buffer, 100 ml/l YNB 10X, 2.5 ml/l Biotin 500X, 5 ml/l 100% glycerol, and 792.5 ml/l of distilled water. This culture was further used to inoculate the fermentor yeast culture (1.5 l) to an initial OD of 1; the fermentation medium contains 18.2 g/l K_2SO_4, 14.9 g/l $MgSO_4 \cdot 7H_2O$, 26.7 ml/l H_3PO_4 (85%), 0.93 g/l $CaSO_4 \cdot 2H_2O$, 4.13 g/l KOH, 40 g/l glycerol, 4.35 ml/l PTM_1. The trace salts solution (PTM_1) consists of (per liter): 6.0g $CuSO_4 \cdot 5H_2O$, 0.08g NaI, 3.0 g $MnSO_4 \cdot H_2O$, 0.2 g $Na_2MoO_4 \cdot 2H_2O$, 0.02 g H_3BO_3, 0.5g $CoCl_2$, 20.0g $ZnCl_2$, 65.0 g $FeSO_4 \cdot 7H_2O$, 0.2g biotin and 5.0 ml H_2SO_4.

The culture was grown for 18-24 hours until the glycerol was completely consumed (this is indicated by an increase in the DO to 100%). Once all the glycerol was consumed a methanol-fed batch phase was initiated to induce the protein expression; the feeding medium consist of 100% methanol containing 12 ml/l PTM_1 trace salt. For the first 2-3 hours, while the culture adapts to methanol, the feed rate was set to 3.6 ml/hr per liter initial fermentation volume. When the culture was adapted to methanol utilization the feed rate was doubled at 7.3 ml/hr per liter initial fermentation volume. After 2 hours at the 7.3 ml/hr/liter feed rate, the methanol feed rate was increased to 10.9 ml/hr per liter initial fermentation volume. This feed rate is maintained until the end of the fermentation.

Constitutive fermentation was carried out in 1.5 liter of a medium containing 9.5 g/l K_2SO_4, 7.8 g/l $MgSO_4 \cdot 7H_2O$, 23.7 ml/l H_3PO_4 (85%), 0.6 g/l $CaSO_4 \cdot 2H_2O$, 2.6 g/l KOH, 40 g/l glycerol, 4.4 ml/l PTM_1. A single colony of the selected transformed yeast was inoculated into 500 ml of a medium containing 100 ml/l phosphate buffer, 100 ml/l YNB 10X, 2.5 ml/l Biotin 500X, 5 ml/l 100% glycerol, and 792.5 ml/l of distilled water, and used as seed culture to inoculate the fermentor to an initial OD of 1. The culture was grown for 24 hours and then a glycerol fed-batch phase (feeding solution: 550 g/l glucose, 12 ml/l PTM_1) was initiated at a feed rate of 3.6ml/hr per liter initial fermentation volume and maintained until the end of the fermentation.

At the end of both fermentation processes (72 hours of induction) the medium was harvested and centrifuged at 1500g in order to separate the cells from the supernatant. For larger fermentations other methods such as

membrane filtration can be used. Supernatant was then processed to purify brazzein.

2.7.3. Purification process

The first step of the purification process is the removal of the cells from the medium by centrifugation (10 minutes at 3000 g).

Supernatant can be directly processed in the successive purification steps, or it can be firstly concentrated until 300 ml of volume using a rotary evaporator (Büchi rotavapor R110). A rotary evaporator (or rotavap, Figure 2.4) is a device for the efficient and gentle removal of solvents from samples by evaporation without excessive heating (thanks to the reduction of the pressure, water evaporation can be conducted at 60-65 °C), thus reducing decomposition of heat-sensitive substances.

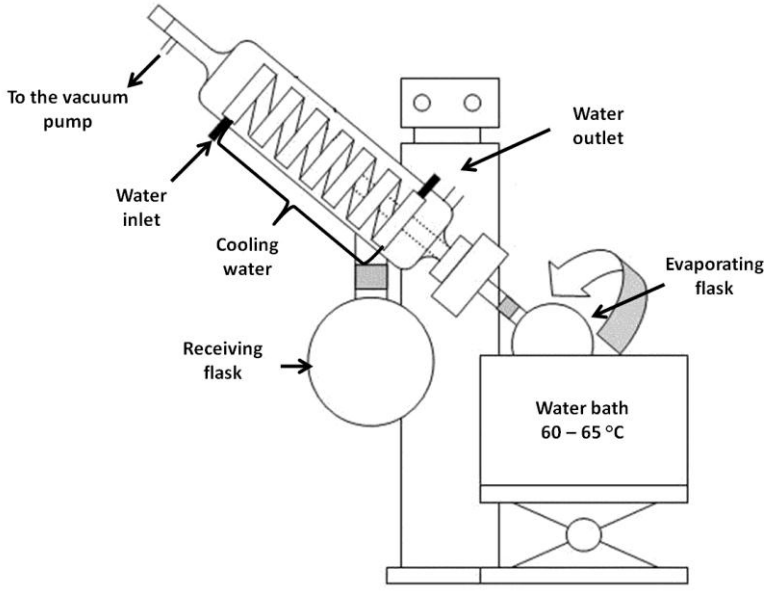

Figure 2.4 – Schematic rapresentation of a rotary evaporator

In order to achieve the desalting and the elimination of low molecular weight contaminants, the concentrated supernatant was dialyzed against water at 4 °C using a washed regenerated cellulose tubing with 3000 MWCO (Spectrum Laboratories). Then it was again concentrated by ultrafiltration using an Amicon device at 4°C with YM 3KDa nominal molecular weight cut-off (NMWCO) membrane: the protein is retained and salts and other low molecular weight contaminants pass through the membrane.

2.7.3.1. Ion exchange chromatography – test tube

The test tube pilot experiments to determine the better conditions for ion-exchange chromatography were performed using a Sepharose DEAE FF anionic resin (Amersham Biosciences) and a Sepharose CM FF cationic resin (Amersham Biosciences). 20 mg of lyophilized brazzein were diluted in 1 ml of 20 mM buffer at different pH; buffers for anionic and cationic resins are listed in Table 2.2.

	pH value	**Buffer 20 mM**
ANIONIC RESIN	5 - 6	Piperazine HCl
	7	Triethanolamine HCl
	8	TRIS HCl
CATIONIC RESIN	4 - 5	Na acetate
	6 - 7 - 8	Na phosphate

Table 2.2 – Buffers for anionic e cationic exchange chromatography

100 µl resin slurry were added to Eppendorf tubes: i.e. 4 tubes with Sepharose DEAE FF anionic resin and 5 tubes with Sepharose CM FF cationic resin. Each Sepharose DEAE and Sepharose CM tube was washed twice with the different buffers for anion and cation exchange respectively. 300 µl of brazzein solution (diluted in the corresponding buffer) were added to each tube and mixed for at least one minute by pipetting. Each tube was centrifuged for 3 minutes at 13000 rpm and the supernatant (proteins unbound to the resin) was collected. Tubes were washed with 1 ml of distilled water. Proteins bound to the resin were eluted adding 1ml NaCl 1M in each tube and mixing for at least one minute by pipetting. Each tube was centrifuged for 3 minutes at 13000 rpm and the supernatant (proteins bound to the resin) was collected.

Samples from each step were analyzed by SDS-PAGE analysis in order to determine the best chromatographic condition in terms of brazzein purity.

2.7.3.2. Ion exchange chromatography – column cation exchange process

After cells removal, supernatant was diluted to lower the conductivity from 65 mS/cm to approximately 14 mS/cm and the pH adjusted to 4. An aliquot of the sample was loaded into a SDS-PAGE gel (see Figure 3.21, Lane 2: S). The supernatant was then loaded into a Pharmacia Biotech XK 26 column, filled with 110 ml of Sepharose CM FF resin, pre equilibrated with Buffer A (Na-Acetate Buffer 20mM, pH 4). The flow through containing the unbound proteins was collected (see Figure 3.19, Fraction I) and an aliquot was loaded into gel (see Figure 3.21, Lane 3: I). After a washing step, the concentration of Buffer B (NaCl 1M in Na-Acetate 20mM pH 4) was increased with a linear gradient from 0% to 100% in 3.5 column volumes. Two fractions were collected (see Figure 3.20, Fraction II and III) and loaded into gel (see Figure 3.21, Lane 4 and 5: II and III). In order to wash out salts from the purified brazzein solution, subsequent steps of diafiltration were performed using filter membranes with cut offs ranging from 1 to 3.5 kDa.

Finally, the purified and desalted brazzein solution can be stored as a solution after sterilization by membrane filtration (0.22 µm filter), or as a powder directly freeze drying the purified protein.

2.7.4. Recombinant brazzein characterization

In this paragraph we will describe the techniques utilized for the characterization of the produced recombinant protein.

2.7.4.1. SDS-PAGE analysis

SDS-PAGE was done according to Laemmli (1970). 13% running gel was prepared mixing 3.25 ml 40% acrylamide solution (29:1=acrylamide:bisacrylamide), 2.5 ml 1.5 M Tris pH=8.9, 100 µl 10% SDS solution, 100 µl 10% ammonium persulphate (APS), 4 µl N,N,N',N'-Tetramethyl-ethylene-diamine (TEMED), diluting to a final volume of 10 ml with deionized water. 5% stacking gel was prepared mixing 0.62 ml 40% acrylamide solution (29:1=acrylamide:bisacrylamide), 2 ml 0.3 M Tris pH 6.7, 50 µl 10%

SDS solution, 50 µl 10% APS, 5 µl TEMED, diluting to a final volume of 5 ml with deionized water.

The method requires protein denaturation: samples were mixed with 4X loading buffer (0.225 M Tris, pH 6.8, 50% glycerol, 5% SDS, 0.05% bromophenol blue, 0.25 M dithiothreitol (DTT)) and boiled at 100°C for 10 minutes before loading. Electrophoretic run was carried out at room temperature. They started at 100 V; after about 30 minutes, when the sample had completely entered in the running gel, the potential was increased to 150 V. Low molecular weight-SDS markers (GE Healthcare or Bio-Rad) (Figure 2.5) was loaded in each gel as reference. Following electrophoresis, gels were stained with Coomassie Staining Solution (0.15% w/v Coomassie Brilliant Blue R-250, 40% v/v ethanol, 10% v/v acetic acid) and finally washed in Destain solution (10% v/v isopropanol, 10% v/v acetic acid).

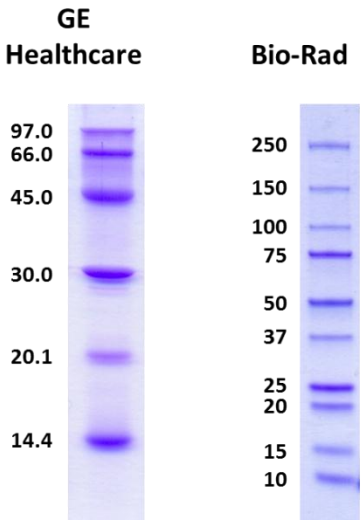

Figure 2.5 – Low molecular weight markers from GE Healthcare and Bio-Rad

2.7.4.2. Tris tricine SDS-PAGE analysis

Tricine-Sodium Dodecyl Sulfate-Polyacrilamide Gel was done according to Schagger and Von Jagow (1987). A 16.5% T-6% C (T denotes the total percentage concentration of acrylamide and bisacrylamide; C denotes the percentage concentration of the crosslinker relative to the total concentration T) separating gel was prepared mixing 2.5 ml 49.5% T-6% C acrylamide-bisacrylamide solution, 2.5 ml 3M Tris 0.3% SDS pH=8.45, 1g glycerol, 75 µl APS, 3 µl TEMED, diluting to a final volume of 7.5 ml with deionized water. A 4% T-3% C stacking gel was prepared mixing 400 µl 40% T-3% C

acrylamide-bisacrylamide solution, 0.992 µl 3M Tris 0.3% SDS pH=8.45, 40 µl APS, 4 µl TEMED, diluting to a final volule of 4 ml with deionized water.

Samples were mixed with 4X loading buffer (0.225 M Tris, pH 6.8, 50% glycerol, 5% SDS, 0.05% bromophenol blue, 0.25 M dithiothreitol (DTT)) and boiled at 100°C for 10 minutes before loading. Electrophoretic run was carried out at room temperature. They started at 50 V; after about 1 hour, when the sample had completely entered in the separating gel, the potential was increased to 100-120 V. Ultra-Low molecular weight markers (Sigma-Aldrich) (Figure 2.6) was loaded in each gel as reference. Following electrophoresis, gels were stained with Coomassie Staining Solution (0.15% w/v Coomassie Brilliant Blue R-250, 40% v/v ethanol, 10% v/v acetic acid) and finally washed in Destain solution (10% v/v isopropanol, 10% v/v acetic acid).

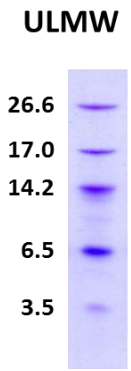

Figure 2.6 – Ultra-Low molecular weight marker (Sigma-Aldrich)

2.7.4.3. Absorbance

UV-visible spectra was recorded on a Agilent 8453 UV-Visible spectrophotometer interfaced with a personal computer using the Chemstation Software for Windows® (Agilent technology). Absorbance was measured at room temperature with Suprasil® 70 µl quartz cell (Hellma), with 1 cm optical path-length. To avoid linear baseline artifacts, the absorption average over the range 700 to 900 nm was subtracted from the entire spectrum. Extinction coefficient applied for brazzein sample was of 9440 $M^{-1} \cdot cm^{-1}$ at 280 nm.

2.7.4.4. Chromatography

Chromatography for analytical purpose was performed on a 1100 Series HPLC system (Agilent Technologies) equipped with a diode array absorbance detector. Protein-peptide elution was followed monitoring the absorbance at 280 nm and 226 nm. All chromatographies were performed at room temperature.

Reversed Phase Chromatography was performed on a C4 column connected to an HPLC system, to prepare highly purified proteins before mass spectrometry analysis. Moreover, it has been used as a general method to check the quality of the protein samples. The solvents used were water (A) and acetonitrile 95% (B), both supplemented with TFA 0.1% and 0.085% respectively. Elution was achieved with acetonitrile 0-95% gradient, optimized based on the sample features. The flow rate was 0.6 ml/min.

Brazzein purity

Protein purity was assessed monitoring the absorbance profile at 280 nm, of a reverse phase HPLC chromatographic run and reported as the relative percentage of the area of the brazzein peak. An aliquote of Fraction III (see Figure 3.20: Fraction II; Figure 3.21, Lane 5: III) was loaded into a Phenomenex Jupiter 5u C4 column, Eluant A was 0.1% TFA in milliQ H_20 and Eluant B was Acetonitrile additioned with 0.085% TFA. The chromatography is performed applying a non-linear increasing concentration of B to the column, with flow rate controlled at 0.6 ml/min. Protein purity was estimated at 280 nm using diode-array Agilent 8453 UV-visible spectrophotometer interfaced with Agilent Chemostation software.

2.7.4.5. Mass spectrometry

Molecules molecular weight measurements were carried out by Dr. Patrizia Polverino de Laureto (CRIBI, University of Padova). Electrospray ionization-mass spectrometry (ESI-MS) was performed on a ESI-Q-TOF Micro spectrometer (Micromass).

2.7.4.6. Calorimetric analysis

Calorimetric analysis were carried out by Dr. Rita Guzzi (Department of Physics, University of Calabria) on a VP-DSC MicroCalorimeter (MicroCal, Inc.).

Purified brazzein powder was diluted in water to a final concentration of 1mM. The reversibility of the transition was checked by performing a second scan with a previously heated sample. Finally, a 40-fold molar excess of DTT was added to verify if the four disulfide bonds typical of brazzein structure were responsible for the unfolding reversibility.

2.7.4.7. Nuclear Magnetic Resonance

NMR experiments were carried out by Dr. Ileana Menegazzo (Department of Chemical Sciences, University of Padova), accordingly with procedures reported in literature (Gao *et al.*, 1999). The experiments were acquired on a Bruker DMX 600 spectrometer equipped with a 5 mm x,y,z-gradient TXI probe. Data were processed with the Topspin 1.3 software.

Purified brazzein powder was diluted in 10% D_2O to a final concentration of 6.1 mg/ml; pH was adjusted to 3.5 using 0.02 mM HCl. To evaluate the protein heat-stability a brazzein water solution was heated at 98 °C for 2 hours; the solution was then diluted to a final concentration of 3.45 mg/ml in 10% D_2O; pH was adjusted to 3.5 using 0.02 mM HCl.

2.7.4.8. Brazzein relative sweetness – magnitude estimation method

A taste panel assay of four untrained volunteer subjects (two men and two women, staff members from the Department of Biology, University of Padova) was used to evaluate the brazzein sweetness compared to sucrose.

The method of magnitude estimation (Stevens, 1956; Stone *et al.*, 1969; Cardello *et al.*, 1999) was used to obtain the sucrose and brazzein power function.

Still water was used to prepare the solutions and was available to the 8 untrained subjects for rinsing purposes between each sample.

Solution were prepared using the 99.9% brazzein solution obtained after the purification protocol (see chapter 2.7.3.2) or pure sucrose (Sigma) as reference. All the solution were prepared at room temperature in volumetric flasks.

For the sucrose power function determination an initial 30% solution was prepared. This solution was then diluted with water to several dilution in order to obtain 5 different sucrose concentration: 1%, 2%, 4%, 8%, and 16%. The 4% sucrose solution was utilized as reference. The same procedure was followed for brazzein, starting form a 0.065% standard solution diluted to 5 different final concentration: 0.0020%, 0.0041%, 0.0081%, 0.0163%, and 0.0325%.

Brazzein and sucrose sample were randomly presented in 50 ml beakers coded with three digit random numbers.

The subjects were informed that they would be presented the reference sample (4% sucrose solution) with an arbitrary sweetness value of 100, followed by a random series of sucrose or brazzein solutions with intensities both less and greater than the reference intensity. Their task was to estimate the sweetness intensity of the unknowns relative to the reference; the reference was re-presented in the mid of the experiment to allow the subject to re-set the reference memory, and a second, random, time to allow us to evaluate the judge reliability. To give an example, a value of 200 should indicate a sample 2 fold sweeter than the reference, while a value of 50 should indicate a sample half as sweet as the reference.

Data were normalized and magnitude estimates were expressed using the geometric mean. The relationship between sweetness intensity and concentration for sucrose and brazzein was plotted on log/log coordinates and fitted by a linear regression defined by the function $\log S = \log a + n \log C$, where S is the intensity of the stimuli perceived, C is the concentration of the stimuli, n the slope and a the antilog of the value of the y intercept. From these results, it was possible to calculate the sweetness potency of brazzein; the sweet potency was defined as the number of times a brazzein solution is sweeter than a weight equivalent sucrose solution.

2.7.4.9. Pepsin digestion

1.28 mg/ml of pepsin from porcine stomach with an activity of 3.2 U/mg protein (Sigma) and 0.5 mg/ml of lyophilized brazzein, at a substrate:enzyme protein ratio of 1:2.56 (by weight), were incubated in 0.03 M NaCl pH 1.5 at 37°C in shaking water-bath. At different time points a mixture sample was collected and the pepsin activity was stopped by the addition of 0.8 M sodium carbonate (0.3 ml per 1 ml of incubation solution). The solution was then neutralized to pH 7 by adding HCl 3N (30 µl per 1 ml of incubation solution). The breakdown of brazzein was assessed by Tris-tricine SDS-PAGE.

2.8. ISP expression and characterization

2.8.1. ISP expression in *E. coli*

The three different *E. coli* strain (BL21, C41 and Origami 2) were transformed (see 2.1.12) with the pET28a vector carrying the ISP cDNA with His-tag. Some colonies were picked up and grown overnight in 20-50 ml of LB medium supplemented with proper antibiotics. Cultures were diluted to an initial OD_{600} of 0.15 in the final volume LB containing the relative antibiotics, and incubated with shaking at 37°C until an OD_{600} of 0.5-0.6.

ISP expression was induced with 0.2, 0.5, or 1 mM IPTG and cultures were incubated with shaking at 4 °C, 28 °C, room temperature (~23 °C), or 37 °C. At different time points (0', 30', 1h, 2h, 3h, 5h, ON) pellet of these cultures was obtained by centrifugation and use to analyze the protein expression by Western-dot-blot analysis.

At the end of the induction process cells was harvested by centrifugation at 5000 g for 10 minutes at 4 °C. Bacterial pellet was then washed with PBS 1X (sodium chloride 137 mM, potassium chloride 2.7 mM, sodium phosphate dibasic 10 mM, and potassium phosphate monobasic 2 mM) and centrifuge again; pellet can be stored at -20°C or processed to purify the protein.

2.8.1.1. Purification

After resuspension in cold PBS 1X and incubation in ice for 20 minutes, cells were disrupted by 1 cycle of French pressure (Constant Cell Disruption Systems, Costant System LTD, Northants, United Kingdom) using a P = 1.35 kBar. A cocktail of protease inhibitors (Protease Inhibitor Cocktail for use with bacterial cell extracts, Sigma) and phenylmethanesulfonylfuoride (PMSF, Sigma) 1mM were added to the solution. Cell debris were sedimented by centrifugation at 5000 g for 30 minutes at 4 °C. Pellet and supernatant obtained after centrifugation were analyzed for protein content by Western-dot-blot analysis.

2.8.1.2. Western dot-blot

1 µl of each sample was spotted onto a nitrocellulose membrane. When dry, membrane was incubated in blocking solution (Table 2.3) for 1 hour. After the blocking step, membrane was incubated with shacking with the antibody solution (Monoclonal Anti-polyhistidine peroxidase conjugate antibody, Sigma, diluted 1:5000 in blocking solution), for 1 hour at room temperature. Membrane was then washed in washing buffer (5 X 10 min, Table 2.3), incubated with ECL reagent (ECL™ Western Blotting Detection Reagents, GE Healthcare) for 1 min, and then covered with Saran-wrap. Finally, X-ray film was exposed in the dark room (several different lengths of exposure were tried).

Buffer	**Composition**
Blocking solution	0.1 g/ml milk powder in TTBS 1X
Washing buffer (TTBS 1X)	0.15 M NaCl, 10 mM TrisHCl pH 7.4, 1ml/l TWEEN 20

Table 2.3 - Buffers for western dot-blot

2.8.2. Small scale constitutive expression tests

The constitutive expression in *P. pastoris* was performed as above described for brazzein (see 2.7.1). Expression was carried out at 30 or 18 °C for a maximum of 7 days shaking at 230 rpm.

Culture supernatant was obtained by centrifugation every 24 hours and use to analyze the protein expression by SDS-PAGE electrophoresis. ISP expression was compared with the expression obtained with yeast transformed with the pGAPZαA empty vector, in the same culture conditions.

2.9. ISP activity characterization

2.9.1. Recrystallization inhibition activity in water solutions and in ice cream

To investigate the RI activity of different protein sources ice crystal sizes were analyzed by a cold-stage microscope and image analysis.

A 30% w/v aqueous sucrose solution was prepared as reference; the same solution was used to dissolve various ISP sources at different final concentrations: 2 or 0.2 mg/ml of two different batches of wheat extract (kindly provided by CHIMAB s.p.a.); 10 µg/ml of typeI or typeII fish ISP (kindly provided by Nichirei Foods Inc., Japan).

A drop of the aforementioned solutions was placed between a microscope slide and a cover slip and was loaded into a cold stage (Model LTS120, Linkam Scientific Instruments, Ltd., Surrey, UK); the cold stage was mounted on the Linkam Scientific Instruments Imaging Station connected with a QiCam Color camera. Ten images of different fields were collected at -5°C after a temperature cycling protocol (temperature [°C]/time [min]/cooling rate [°C/min]) (Figure 2.7): -32/0/30; -40/0/10, -10/10/10, -4/0/1, -6/0/1, and -5/60/1. The images were collected every 10 minutes of aging between 0 and 60 minutes at -5°C.

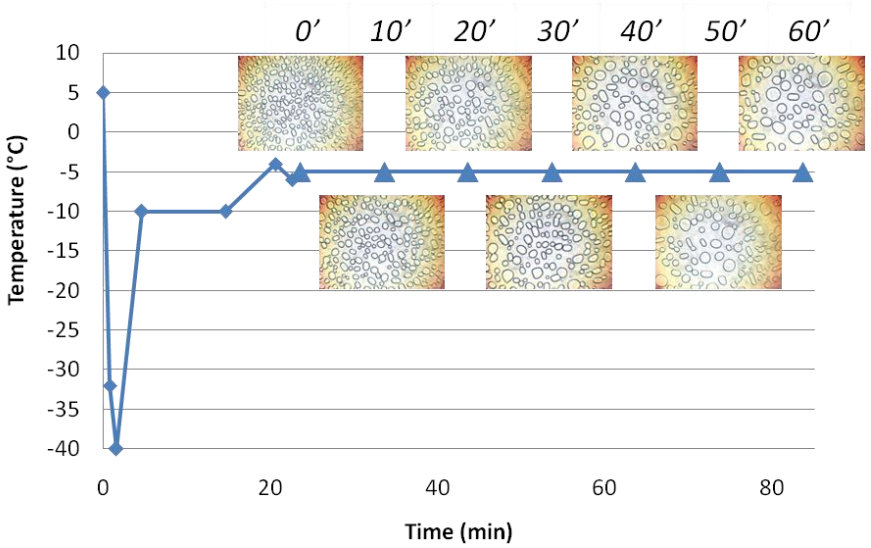

Figure 2.7 – Schematic representation of the temperature cycling protocol and of images capture

Images were analyzed for the ice crystal dimension using an image analysis software (ImageJ); 300 ice crystals were analyzed: mean ice crystals size (expressed as area in μm^2, and diameter in µm) and distribution statistics for ice crystals were calculated using a data analysis software (OriginPro8).

Also the aspect ratio of ice crystals were evaluated; aspect ratio of a shape refers to the ratio of its longer dimension to its shorter dimension. If we considered a circular ice crystal as a circle and a spicular ice crystal as an ellipse, aspect ratio would be 1 and greater than 1 respectively (Figure 2.8).

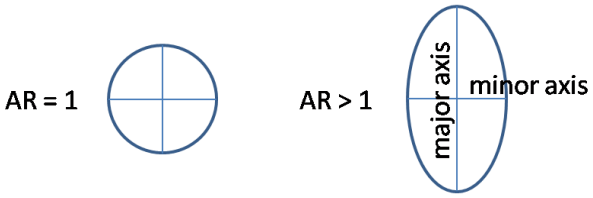

Figure 2.8 – Aspect Ratio (AR) graphical representation; an AR value of 1 corresponds to a circle, while an AR value greater than 1 corresponds to an ellipse

RI activity was also investigated in ice cream (kindly provided by CHIMAB s.p.a., Campodarsego, Padova, Italy) containing 0% (SE0305) or 0.3% (ICE PRO) propylene glycol monostearate (PGMS), a known anti-recrystallization agent. Moreover, the SE0305 sample was subjected to more freezing-thawing cycles than the ICE PRO one, causing an increase in the ice crystals dimensions. Approximately 5 mg of sample were placed in N-Butanol at -20°C in order to remove the air content from the ice cream. The

ice cream was then placed on a standard glass microscope slide. A cover slip was pressed on top of the ice cream and gently pressed back and forth with tweezers to disperse the sample into a layer thin enough to enhance separation of ice crystals (at about -15 °C); the microscope slide was then placed in a cold stage (Model LTS120, Linkam Scientific Instruments, Ltd., Surrey, UK) which was previously programmed to maintain a constant temperature of -17 °C. The cold stage was mounted on the Linkam Scientific Instruments Imaging Station connected with a QiCam Color camera. Several sample fields were photographed at -17°C to capture a total of 300 ice crystals.

Measurements of ice crystals size were performed using an image software (ImageJ); the perimeter of each ice crystal was manually traced using a pen tablet and the area of each crystal was automatically calculated by the software. The mean size and distribution statistics for ice crystals were determined using a data analysis software (OriginPro8).

2.9.2. Cells hypothermic preservation

HEK293T cells (cell line originally derived from human embryonic kidney cells, American Type Culture Collection) were grown in Dulbecco's modified Eagle's medium (Biological Industries, Beit Haemek, Israel) supplemented with 10% fetal bovine serum, 2 mM L-glutamine, 50 units/ml penicillin, and 50 µg/ml streptomycin (Invitrogen). Cells were cultured overnight in 6-well plates at density of $3 \cdot 10^5$ cells/well.

Cells were incubated in EuroCollins organ preservation solution (93.3 mM KCl, 15.1 mM KH_2PO_4, 9 mM K_2HPO_4, 10 mM $NaHCO_3$, and 194 mM glucose, pH 7.4) containing: 0 mg/ml protein; 10 mg/ml BSA (control); 10 mg/ml wheat extract; 10 and 20 mg/ml fish ISP type I.

Culture plate was sealed with tape and stored at 4°C to simulate clinical condition of cold organ storage for 24, 48 and 72 hours.

After hypothermic preservation the cells were transferred back to a 37°C incubator for 1 hour for rewarming.

Cell viability was determined with the trypan blue method (6 Burker fields/condition in triplicate).

Chapter 3

RESULTS

Expression, purification and characterization of the sweet protein brazzein

Until now, the sweet protein brazzein was produced using different expression systems (see 1.1.3.1, Developed expression methods), but none of the proposed methods yielded a sufficient quantity of protein for an industrial application. Moreover, the food industry requires the observation of strict rules in order to assure the safety of the food for the human consumption. For example, a protein for food cannot be expressed in bacteria such as *E. coli*, because of the existence of some strains capable of causing illness in humans (severe bloody diarrhea, abdominal cramps, and occasional vomiting); furthermore, due to the debate about genetically modified organisms, it is preferable to avoid the introduction of GMOs (Genetically Modified Organisms) for the production of food constituents.

For these reasons, brazzein produced using the *E. coli* expression system (Assadi Porter *et al.*, 2000) is suitable for a biochemical characterization but not for its introduction as sweetener in the market, while the maize expression system proposed by Lamphear *et al.* (2005) foresees the creation of a transgenic maize line that has to be introduced in the soil and then eaten by humans with the associated environmental and health risks.

On this ground, we proposed to develop an efficient and cost-effective method to produce brazzein in the GRAS (Generally Recognize As Safe) *Pichia pastoris* expression system.

3.1. Inducible expression in *Pichia pastoris*

We initially expressed brazzein using the pAOX1 strong inducible promoter. This system is suitable for the expression of protein toxic to the host because it foresees the generation of biomass in the absence of inductor, followed by induction of protein production in the presence of methanol as the only carbon source. Therefore, it is the first choice for the expression of a new protein in *P. pastoris*.

3.1.1. Construction of the pPICZαA-BRA expression plasmid

The expression plasmid containing the pAOX1 promoter (pPICZαA) for the inducible expression of the foreign protein was obtained from Invitrogen (version A; San Diego, USA). The plasmid harbor a dominant selectable shuttle marker, Zeocin™, which allows selection of both *E. coli* and *P. pastoris* transformant.

In order to improve the expression level of brazzein in *P. pastoris*, we synthesized (Sigma genosys) its cDNA based on the known aminoacidic sequence (with a Methionine in place of the Glutamine residue at the N-term position for optional expression in *E. Coli*) (Figure 3.1) selecting the optimized codon for protein expression in *P. pastoris*.

Codon bias is one of the most important parameter which influence heterologous gene expression; in general, more rare codons that a gene contains, less likely it is that a reasonable expression level of the heterologous protein will be obtained. Therefore, the optimization of the codon sequence, without modifying the amino acid sequence of the encoded protein, can improve expression level of heterologous gene.

Moreover, we eliminated all the possible restriction site from brazzein cDNA in order to facilitate subsequent gene manipulations such as swapping between vectors and adding or removing peptide tags or fusion partners.

```
        10         20         30         40         50
MDKCKKVYEN YPVSKCQLAN QCNYDCKLDK HARSGECFYD EKRNLQCICD YCEY
```

Figure 3.1 - Amino acids sequence of the sweet-tasting protein brazzein with methionine as first amino acid

The 162-bp brazzein cDNA was cloned into the XhoI/NotI site of the empty vector pPICZαA to generate pPICZαA-BRA (Figure 3.2).

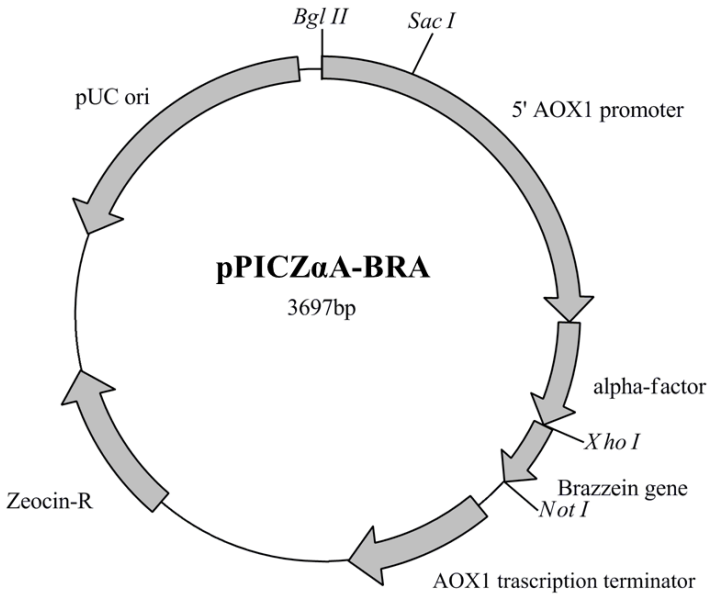

Figure 3.2 - Vector map of the plasmid for the inducible expression of brazzein in *P. pastoris* using the pAOX promoter

3.1.2. Yeast transformation and selection

After the linearization with *SacI* restriction enzyme, the pPICZαA-BRA plasmid was used to transform *P. pastoris* wild-type strain X33 by electroporation. High-level expression transformants were selected on YPDS plates with increasing concentration of Zeocin™: clones, which are able to grow on the highest concentration of Zeocin™ plate, are putative multi-copy recombinants (Figure 3.3). From this step eight recombinant clones were selected for the successive small expression test experiments.

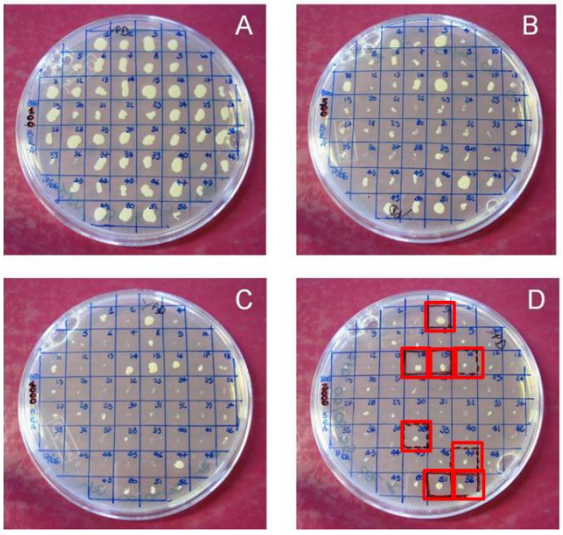

Figure 3.3 – Isolation of multi-copy recombinants in YPDS plates containing A) 100, B) 500, C) 1000 and D) 2000 µg/ml Zeocin™

3.1.3. Expression in shake flask cultures

The eight single selected colonies were then screened for their protein expression level. A 5ml BMG cultures were incubated at 30 °C for 24 hours shaking at 230 rpm; the cells was then harvested and used to inoculate 10 ml of BMM (medium with methanol) in order to induce protein expression. To maintain induction, methanol was added every 24 hours to a final concentration of 0.5 %. These 10 ml cultures were incubated at 30°C for 3 days shaking at 230rpm.

A time course analysis was performed with samples taken from the supernatant every 24 hours to examine protein expression by Tris-Tricine SDS-PAGE electrophoresis (Figure 3.4).

A band corresponding to an apparent molecular weight of 6.5 kDa was observed after 24 hours of induction and became more pronounced after 72 hours.

The most effective clone in terms of expressed protein appeared to be clone 3 (Figure 3.4, A); this clone will be utilized for the subsequent scale up of the process.

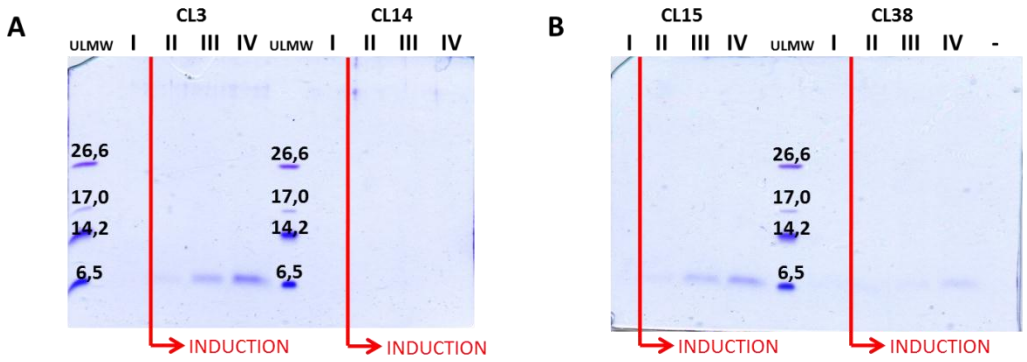

Figure 3.4 – Tris-Tricine SDS-PAGE analysis of small scale brazzein expression after 1, 2, 3 and 4 days of culture; A) clones 3 and 4; B) clones 15 and 38; ULMW= ultra low molecular weight

A first step for the scale up of the expression protocol was done using larger baffled flask.

A clone 3 pre-inoculum was prepared and then used to inoculate 100 ml or 500 ml of BMM culture medium in a 500 ml or 2000 ml baffled flask respectively, at an initial concentration corresponding to an OD_{600} value of 1. These cultures were incubated at 30 °C for 3 days shaking at 230 rpm. In order to maintain induction, 100 % methanol was added to a final concentration of 0.5% every 24 hours.

During incubation, samples were taken from the supernatant every 24 hours to monitor protein expression by Tris-Tricine SDS-PAGE electrophoresis (Figure 3.5).

Also in this case a band corresponding to an apparent molecular weight of 6.5 kDa was observed after 24 hours of induction and became more pronounced after 72 hours.

Moreover, the absence of high-level contaminants in the supernatant facilitate the successive purification protocol.

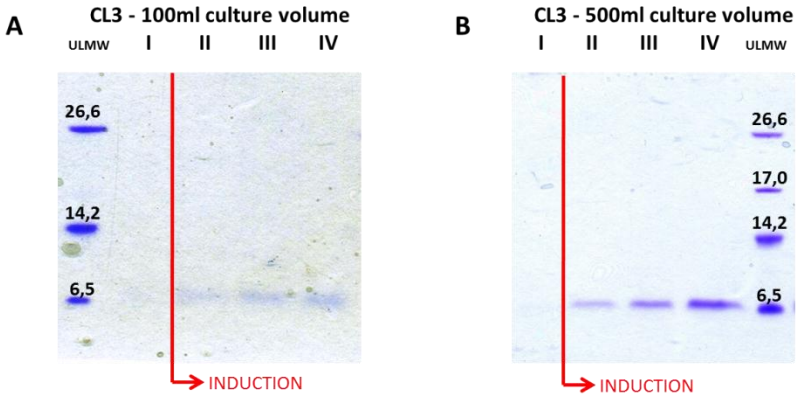

Figure 3.5 – Tris-Tricine SDS-PAGE analysis of CL3 medium scale brazzein expression after 1, 2, 3 and 4 days of culture; A) 100 ml culture volume; B) 500 ml culture volume; ULMW= ultra low molecular weight

3.1.4. Bioreactor fed-batch fermentation

The fermentation was carried out in a 3 l bioreactor (BioFlo 110, New Brunswick Scientific) with a 2 l working volume at 30 °C, DO (Dissolved Oxygen concentration; it is the relative percentage of oxygen in the medium where 100% is O_2-saturated medium, about 240 µM) 20% (about 48 µM; maintained by feedback controlled stirring and air bubbling) and pH 5.0. *Pichia* cells are grown in a feed-batch culture for 3 days: after 24 hours of growth the protein expression was induced by adding methanol to the culture, initially at a slow rate to allow the culture's acclimation to methanol and then at a progressively faster rate in order to maintain the required dissolved oxygen level. The medium was then harvested for protein purification by centrifugation and treated as described below.

Parameters that have to be optimized in a fermentation are: culture medium choice (we tested two different types of media: a) Yeast Nitrogen Base-based medium, b) optimized salts medium), temperature, pH value, aeration rate, agitation rate (300-1200 rpm on the basis of oxygen demand; in fact it is important to maintain the dissolved oxygen concentration above 20% to ensure *Pichia* growth on methanol), antifoam quantity, methanol concentration and induction time. From preliminary expression tests we determined that, in agreement with the *Pichia* Fermentation Process Guidelines manual (Invitrogen), the suitable temperature is 30 °C and the optimal pH value is 5; that the optimal aeration rate is 2-3 vvm (volume of air/unit of culture/unit of time; higher oxygen rates can become toxic and causes cells death; consequently cells would release in the supernatant nucleic acids that represent a problem for the following purification step); that the amount of antifoam sufficient to avoid foam formation during

fermentation is 70 µl/l; and that the quantity of methanol necessary for the induction changes with the utilized culture medium.

A time course analysis by Tris-Tricine SDS-PAGE of the level of protein expression was performed with samples taken from the supernatant after 24 hours of growth and then after 12, 24 and 46 hours of induction (Figure 3.6).

Yields obtained with the two different types of media tested were analyzed. In particular using the YNB medium (the same used in the small scale expression tests) we used 729 ml of methanol in 46 hours of induction obtaining a brazzein yield of about 45 mg/l. At variance, using the fermentation salts media we used 145 ml of methanol in 46 hours of induction obtaining a brazzein yield of about 100 mg/l. From this preliminary results it is possible to gather that brazzein inducible expression using fermentor can be optimized using the salts media.

Also the protein produced using fermenter in Tris-Tricine SDS-PAGE gel appears as a single band at an apparent molecular weight of 6.5 kDa.

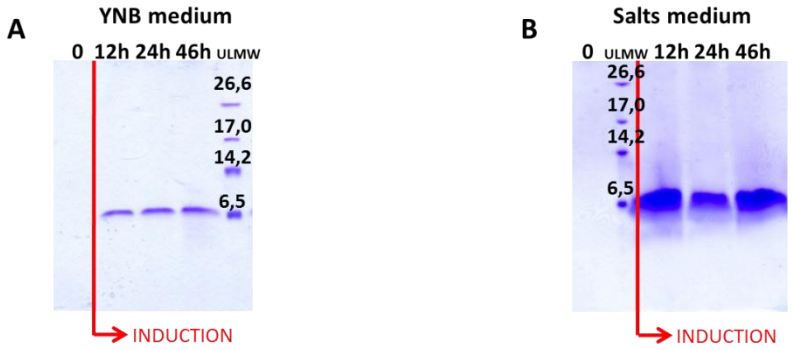

Figure 3.6 – Tris-Tricine SDS-PAGE analysis of brazzein expression in a fermenter after 12, 24, 46 hours of induction using A) YNB or B) Salts medium; ULMW= ultra low molecular weight

3.2. Constitutive expression in *Pichia pastoris*

The glyceraldehyde-3-phosphate dehydrogenase gene (GAP) has been shown to constitutively express recombinant proteins at a high level in *P. pastoris* without methanol induction. This system is also preferred because, at variance with methanol induction phase, does not require an accurate optimization of the culture conditions. Moreover, GAP promoter vectors allow for continuous production of the recombinant product making this system more suitable for large scale production of heterologous recombinant proteins.

3.2.1. pGAPZαA-BRA expression plasmid

The expression plasmid containing the pGAP strong constitutive promoter was instead obtained by modifying the pPICZαA-BRA vector: the promoter pGAP was amplified by PCR from genomic of *P. pastoris* (chr 2) and then it was inserted into pPICZαA-BRA plasmid in place of the pAOX1 to generate plasmid pGAPZαA-BRA. The construction flow chart of the new integrative plasmid pGAPZαA-BRA is described in Figure 3.7. The constitutive production of brazzein is preferred for an industrial application because it eliminates the health hazard and cost associated with the use (storage and delivery) of methanol. In the frame of the uses proposed for the protein produce by this expression system, i.e. human consumption, the exclusion of the methanol from the process is mandatory.

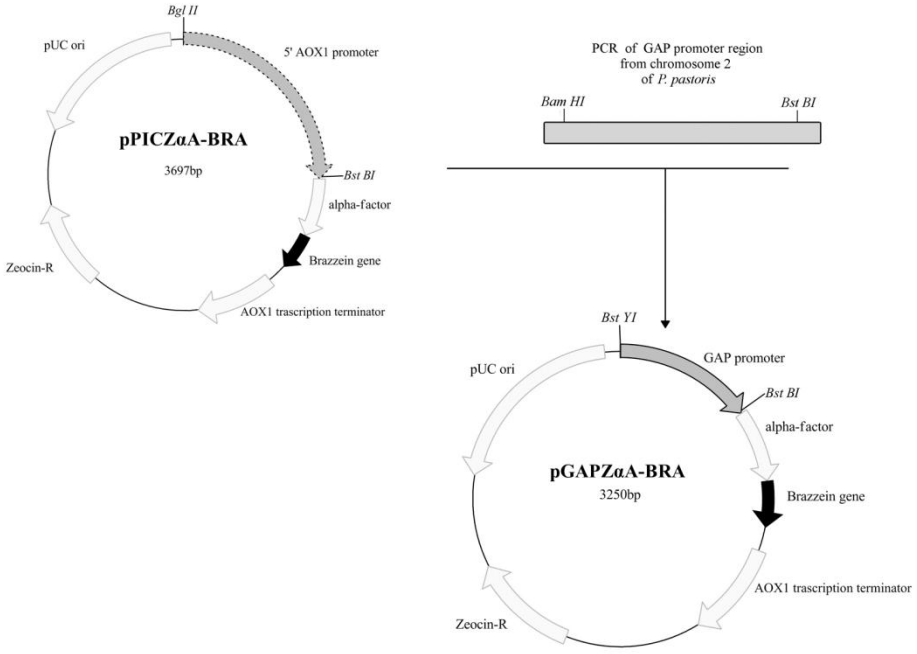

Figure 3.7 - Schematic diagram illustrating the construction of the pGAPZαA-BRA constitutive expression vector from the pPICZαA-BRA inducible expression vector

3.2.1.1. Construction of the pGAPZαA-BRAΔ1M expression plasmid

As reported in literature, the sweetness of brazzein without the first amino acid residue (Figure 3.8) is twice the one detected for the 54-wilt type amino acids form (Assadi-Porter *et al.*, 2000).

In order to produce this sweeter form, we modified the pGAPZαA-BRA expression plasmid by removing the codon encoding

for the first amino acid (Met) by PCR site-directed mutagenesis to generate plasmid pGAPZαA-BRAΔ1M.

```
        10         20         30         40         50
DKCKKVYENY PVSKCQLANQ CNYDCKLDKH ARSGECFYDE KRNLQCICDY CEY
```

Figure 3.8 – Amino acids sequence of the sweet-tasting protein brazzein without the first AA

3.2.2. Yeast transformation and selection

After the linearization with *AvrII* restriction enzyme, the pGAPZαA-BRA plasmid was use to transform *P. pastoris* by electroporation. High-level expression transformants were selected on YPDS plates with increasing concentration of Zeocin™: clones, which are able to grow on the highest concentration of Zeocin™ plate, are putative multi-copy recombinants (Figure 3.9). From this step six recombinant clones were selected for the successive small expression test experiments.

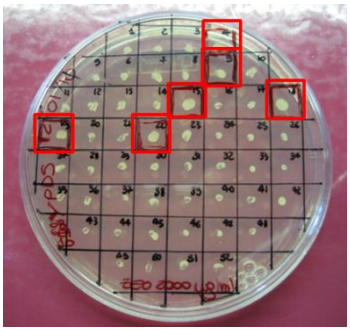

Figure 3.9 - Isolation of multi-copy recombinants clones transformed with the pGAPZαA-BRA plasmid in YPDS plate containing 2000 µg/ml Zeocin™

3.2.2.1. Mutant (pGAPZαA-BRAΔ1M)

As for the 54 amino acid form of brazzein *P. pastoris* cells were transformed with the *AvrII* linearized pGAPZαA-braΔ1M vector and then the positive multi-copy recombinants clones were selected on YPDS plates with increasing concentration of Zeocin™ (Figure 3.10). From this step we selected two recombinant clones for the following small scale expression experiments.

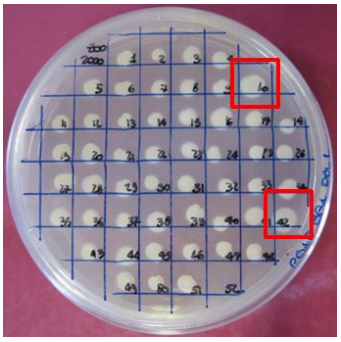

Figure 3.10 - Isolation of multi-copy recombinants clones transformed with the pGAPZαA-BRAΔ1M plasmid in YPDS plate containing 2000 µg/ml Zeocin™

3.2.3. Expression in shake flask cultures

Single selected colonies were screened for their ability to produce brazzein in order to identify the most performing ones. These 10 ml cultures were incubated at 30 °C for 3 days shaking at 230 rpm. The supernatant was obtained by centrifugation after 4, 24, 48 and 72 hours and use to analyze the protein expression by Tris-Tricine SDS-PAGE electrophoresis (Figure 3.11).

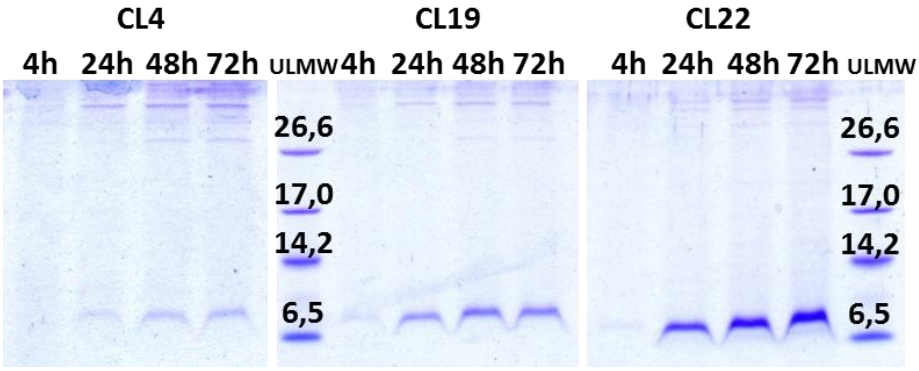

Figure 3.11 – Tris-Tricine SDS-PAGE analysis of small scale brazzein constitutive expression after 4, 24, 48 and 72 hours of culture by clones 4, 19 and 22; ULMW= ultra low molecular weight

Clone 22 appeared to be the most effective in terms of expressed protein (Figure 3.11); therefore, it was utilized for the subsequent scale-up of the process using a larger baffled flask.

A clone 22 pre-inoculum was prepared and then used to inoculate 100 ml of YPD culture medium in a 500 ml baffled flask, at an initial concentration corresponding to an OD_{600} of 1. These cultures were incubated at 30 °C for 3 days shaking at 230 rpm.

During incubation, samples were taken from the supernatant after 4, 24, 48 and 72 hours of culture to monitor protein expression by Tris-Tricine SDS-PAGE electrophoresis (Figure 3.12).

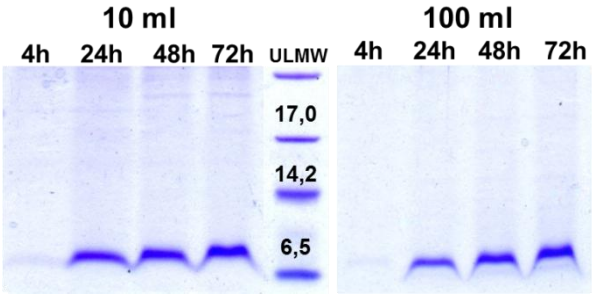

Figure 3.12 - Tris-tricine SDS-PAGE analysis of CL22 small and medium scale wild-type brazzein constitutive expression after 4, 24, 48 and 72 hours of culture; ULMW= ultra low molecular weight

Both in small (10 ml) and medium (100 ml) expression test we observed the production of the protein after 24 hours of culture; the amount of expressed protein increased after 48 and 72 hours.

The band representing the expressed protein had an apparent molecular weight higher than the expected one of 6.5 kDa; moreover, it was observed (Figure 3.11 and Figure 3.12) that the electrophoretic mobility of the protein changed during the time course.

We hypothesized that this can be due to the presence of nucleic acids in protein samples. This contamination was confirmed by the determination of the A_{260}/A_{280} ratio: typically a ratio of 0.57 correspond to a protein sample free of nucleic acid contamination, while a ratio of 2 indicate a 100% DNA presence (Glasel, 1995). The ratio relative to the sample of the medium scale expression experiment was in the range of 1.82-1.92, indicating a large nucleic acid contamination (61%-87% DNA presence).

An experiment based on a factorial design was performed in order to investigate if there is a correlation between protein purity and composition of the medium.

3.2.3.1. Factorial experiment

In order to determine the best medium composition to optimize the protein purity we performed a factorial experiment with clone 22 using a simple defined media based on 10% YNB 10X additioned with different combination of amino acid mix (M), phosphate buffer (B) and carbon source (C) as reported in Table 3.1. For the quantitative

variables (amino acid mix and phosphate buffer) the minus sign represents the low level while the plus sign represent the high one. For the qualitative variable 'carbon source' the two options 'dextrose (D) or glycerol (GY)' can also be conveniently coded by plus and minus sign respectively.

The response is the A260/A280 (y) ratio after 48 hours of culture at 30 °C at 230 rpm.

Condition A and B corresponded to 'intermediate' media composition (media composed by the mid-value concentration of each component) in order to evaluate the intrinsic uncertainty of the experiment: the standard deviation between y_A and y_B was considered as the intrinsic variability for all the experiments.

Test condition number *	Amino acid mix (M)	Phosphate buffer (P)	Carbon source (C)	A260/A280 (y)
1	-	-	+	2.16
2	+	-	+	2.10
3	-	+	+	1.40
4	+	+	+	1.29
5	-	-	-	2.10
6	+	-	-	2.03
7	-	+	-	1.75
8	+	+	-	1.47
ǂ A (1:2)	Intermediate concentration of each component			1.98
ǂ B (1:2)	Intermediate concentration of each component			1.92

Amino acid mix [%] #		Phosphate buffer [mM]		Carbon source [%]	
+	-	+	-	+	-
1% (w/v)	0	100mM	0	D (0.5% w/v)	GY (0.5% w/v)

* Each medium contains also *10% YNB 10X*

 # Aminoacid mix: 0.5% w/v solution of L-glutamic acid, L-methionine, L-Lysine, L-Leucine, L-isoleucine

ǂ Intermediate medium: 0.025% w/v solution of each amino acid, 50mM Phosphate buffer, 0.25% D and 0.25% GY

Table 3.1 – Design matrix and results for the 2^3 factorial experiment

Firstly, we evaluated the average effect of each condition over all the other variables. For instance, if we considered condition 1 and 2, the corresponding y_1 and y_2 (2.16 and 2.10) differ only because of amino acid mix. The phosphate buffer concentration (100 mM) and the carbon source (D) are the same for both of these conditions. In total there are four condition in which the only changing variable was M.

The average of these four measures is called the main effect of M (Table 3.2).

Individual measure of the effect of changing M from 1% to 0%	Condition at which comparison is made: P (mM)	C
$y_2 - y_1 = 2.10 - 2.16 = -0.06$	0	D
$y_4 - y_3 = 1.29 - 1.40 = -0.11$	100	D
$y_6 - y_5 = 2.03 - 2.10 = -0.07$	0	GY
$y_8 - y_7 = 1.47 - 1.75 = -0.28$	100	GY
main effect of M = -0.13		

Table 3.2 – Main effect of amino acid mix (M)

Obviously, there is a similar set of four measures for the effect of P (Table 3.3) and C (Table 3.4).

Individual measure of the effect of changing P from 100mM to 0mM	Condition at which comparison is made: A (%)	C
$y_3 - y_1 = 1.40 - 2.16 = -0.76$	0	D
$y_4 - y_2 = 1.29 - 2.10 = -0.81$	1	D
$y_7 - y_5 = 1.75 - 2.10 = -0.35$	0	GY
$y_8 - y_6 = 1.47 - 2.03 = -0.56$	1	GY
main effect of P = -0.62		

Table 3.3 – Main effect of Phosphate buffer (P)

Individual measure of the effect of changing C from D to GY	Condition at which comparison is made: A (%)	P (mM)
$y_1 - y_5 = 2.16 - 2.10 = +0.06$	0	0
$y_2 - y_6 = 2.10 - 2.03 = +0.07$	1	0
$y_3 - y_7 = 1.40 - 1.75 = -0.35$	0	100
$y_4 - y_8 = 1.29 - 1.47 = -0.18$	1	100
main effect of C = -0.10		

Table 3.4 – Main effect of carbon source (C)

A geometrical representation of the 3 variables and 2 levels design (defined as 2^3 factorial experiment) and the relative results is shown in Figure 3.13: each corner of the cube corresponds to one of the eight treatment combinations while, in the middle of every side of the

cube is reported the measure of the effect of each variable over all the conditions of the other variables.

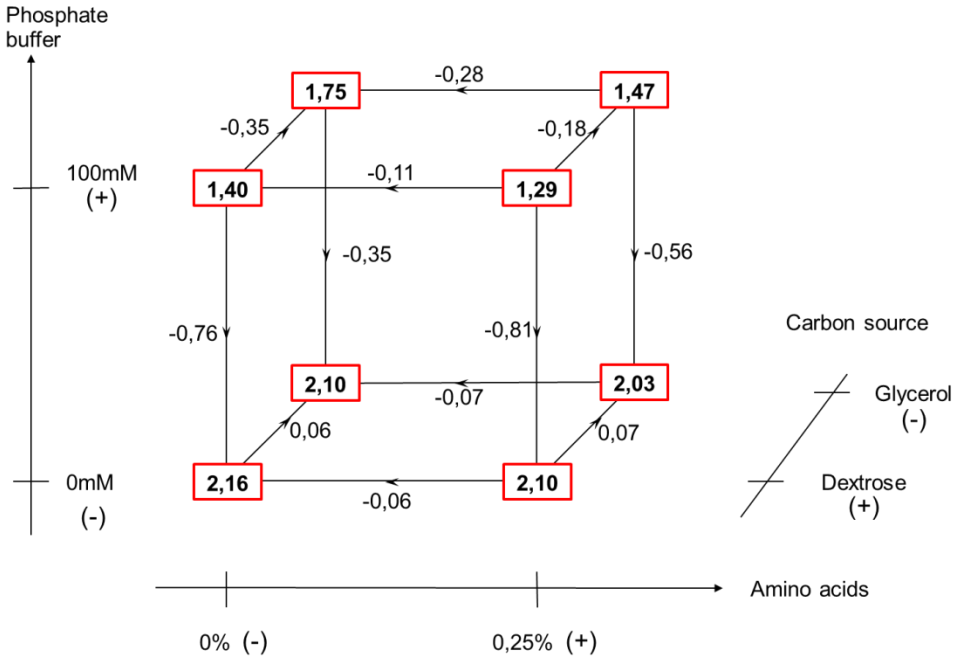

Figure 3.13 – Cube plot representation of factorial points

Also the two and three-factors interaction were evaluated in order to determine if there are changes in the A260/A280 ratio due to an interaction between two or more factors that are interacting with each other.

The two-factors interaction between M and P (M X P) is supplied by half the difference between the average M effect with P=100mM and the average M effect with P=0 mM (Table 3.5).

P		Average M effect
(+) 100 mM		-0.20
(–) 0mM		-0.07
	difference	-0.13

M X P interaction = -0.13/2 = -0.065

Table 3.5 – Evaluation of the M X P interaction

The P X C and the M X C interaction were obtained in a similar way (results reported in Table 3.7).

The three factor interaction between M, P and C (M X P X C) was calculated as half the difference between the M X P interaction with dextrose as carbon source, and the M X P interaction with glycerol (Table 3.6).

M X P interaction with dextrose (+):

$$\frac{(y_4 - y_3) - (y_2 - y_1)}{2} = -0.025$$

M X P interaction with glycerol (-):

$$\frac{(y_8 - y_7) - (y_6 - y_5)}{2} = -0.105$$

M X P X C interaction = (-0.025 – 0.105)/2 = 0.04

Table 3.6 – Evaluation of the M X P X C interaction

The results of the factorial analysis are collected in Table 3.7. The standard error for the experiment was calculated as the standard deviation between y_A and y_B and correspond to a value of ±0.04.

EFFECT	ESTIMATE
Average	1.79
Main effects	
Amino acid mix (M)	-0.13
Phosphate buffer (P)	-0.62
Carbon source [dextrose] (C)	-0.10
Two factor interaction	
M x P	-0.07
P x C	-0.17
M x C	0.05
Three factor interaction	
M x P x C	0.04
Average of A and B	1.95 ± 0.04

Table 3.7 – Calculated effects for the 2^3 factorial design; circled in red are the significant values

Comparison of the estimates with the error (see Table 3.7) suggests that the conditions that requires an interpretation are P and the interaction P X C, while the remaining effects could be generated by the intrinsic variability of the experiments.

In Table 3.7 is reported a large P effect, -0.62±0.4. But since P interact with the carbon source type (the P X C interaction is -0.17±0.4) the effect of P and C cannot be interpreted separately. As reported in Figure 3.14, with dextrose as carbon source the phosphate buffer effect is 0.79 units, while with glycerol is 0.46 units. Moreover, the protein purity obtained using 100 mM phosphate buffer and dextrose as carbon source was the highest, A260/A280=1.35, corresponding to a low DNA presence (about 10%).

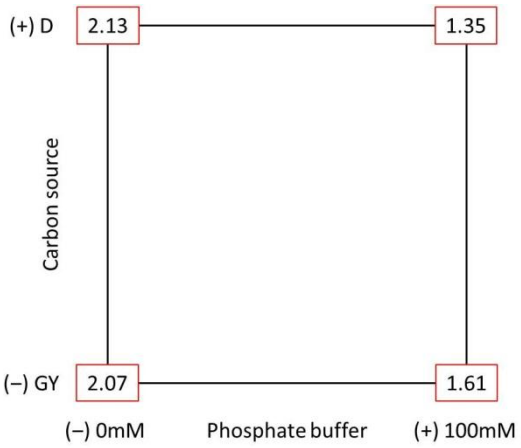

Figure 3.14 – The phosphate buffer-carbon source interaction

This finding established that for the small expression test and for the pre-inoculum culture for the successive scale-up of the process using a fermenter, the optimal medium composition consists of 100 mM phosphate buffer, 0.5% w/v dextrose and 10% YNB 10X.

3.2.3.2. Brazzein Δ1M expression

As for the 54 amino acids brazzein form, brazzein without the first amino acid was expressed in small scale experiments in order to select the most effective clone in terms of expressed protein. These 10 ml cultures were incubated at 30 °C for 3 days shaking at 230 rpm. The supernatant was obtained by centrifugation after 4, 24, 48 and 72 hours and use to analyze the protein expression by Tris-Tricine SDS-PAGE electrophoresis.

In Figure 3.15 is reported the time course relative to the clone showing the maximum brazzein expression level, clone 10, which was successively utilized for the scale-up of the process using a 500 ml

baffled flask with 100 ml YPD culture medium. Also this culture was incubated at 30 °C for 3 days shaking at 230 rpm, and the supernatant for the protein expression analysis was obtained at the same time point used for the small scale expression experiment (Figure 3.15).

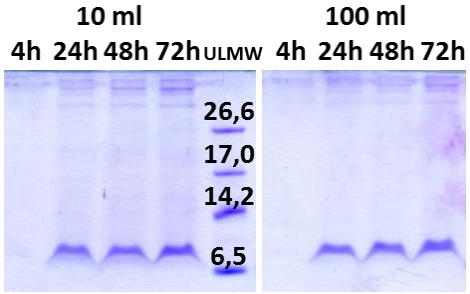

Figure 3.15 - Tris-tricine SDS-PAGE analisys of small scale brazzein Δ1M constitutive expression (clone 10) after 4, 24, 48 and 72 hours of culture; ULMW= ultra low molecular weight

3.2.4. Bioreactor fed-batch fermentation

Clone 22 and clone 10 were used for the expression of brazzein using a fermenter with a working volume of 1.5 liters. In agreement with the *Pichia* Fermentation Process Guidelines manual (Invitrogen) we performed the fermentation using a minimal salts medium, a temperature of 30 °C and a pH of 5. The agitation rate was adjusted from 300 to 1200 rpm on the basis of oxygen demand while the aeration rate was set to 2 vvm (volume of air/volume of culture/unit of time).

After 24 hours of growth a feeding phase was initiated using a dextrose feed solution (550 g/l dextrose, 12 ml/l PTM1) at a feed rate of 3.6 ml/hr per liter of initial fermentation volume and maintained until the end of the fermentation. In the supernatant, obtained after centrifugation of the culture, protein expression was tested every 24 hours by Tris-Tricine SDS-PAGE electrophoresis (Figure 3.16).

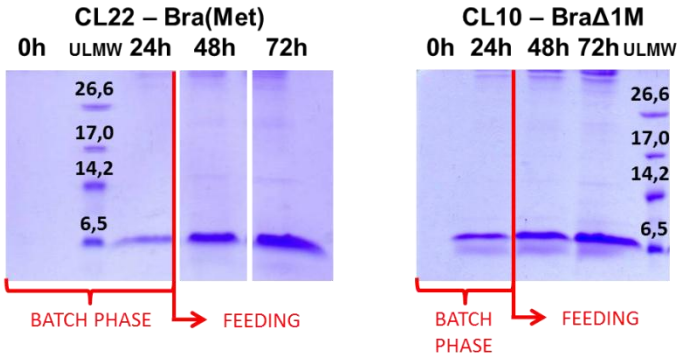

Figure 3.16 - Tris-Tricine SDS-PAGE analysis of brazzein constitutive expression in a fermenter after 0, 24, 48 and 72 hours using clone 22, expressing the 54 aa form, or clone 10, expressing the 53 aa form of brazzein; ULMW= ultra low molecular weight

The secretion of the recombinant protein was detected 24 hours after the culture was initiated, and a maximum level of protein expression was detected after 48 hours of feeding with dextrose.

For both the 54 and 53 amino acids form of brazzein the protein produced using fermenter appears as a single band at an apparent molecular weight of 6.5 kDa in Tris-Tricine SDS-PAGE gel.

3.3. Brazzein purification from yeast culture supernatant

As reported in the EasySelect *Pichia* Expression Kit Manual (Invitrogen) *Pichia pastoris* is able to grow to high biomass in a simple minimal defined medium and it secretes very low levels of native proteins into the medium. Therefore, the secreted heterologous protein represents the vast majority of the total proteins in the medium making the purification process relatively easy.

The first step of the purification process is the removal of the cells from the medium by centrifugation.

For the successive separation of brazzein from the other protein contaminants we decided to take advantage of ion exchange chromatography.

With the aim of determine the best chromatographic process in terms of brazzein purity we performed some preliminary tests by batch method using a CM-Sepharose FF cation exchange resin or a DEAE-Sepharose FF anion exchange resin.

The starting buffer pH for an ion chromatography has to be determine in order to allow the binding of the protein to the resin: for the anion exchanger it should be at least 1 pH unit above the protein isoelectric point (IP), while for cation exchanger it should be at least 1 pH unit below the IP.

The isoelectric point of wild type brazzein (54 amino acids form) is 5.4. Therefore, we analyzed the binding of brazzein to the two different resins at different pH values that range from 5 to 8 for the anionic exchanger, and from 4 to 8 for the cationic one.

As reported in Figure 3.17, the DEAE-Sepharose FF anionic resin bind the contaminants present in the supernatant, but didn't allowed the binding of brazzein in the tested pH range.

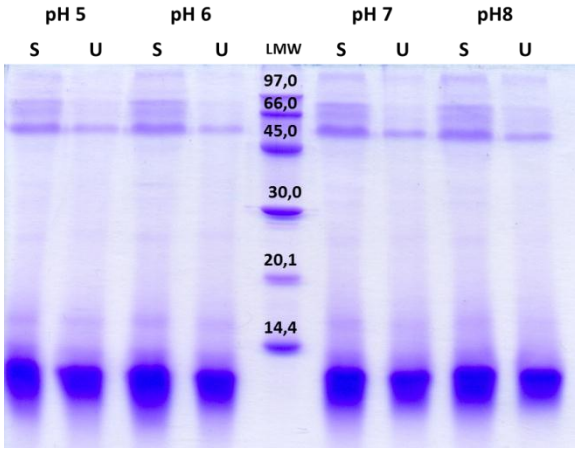

Figure 3.17 – SDS-PAGE analysis of the DEAE-Sepharose FF anionic batch process in the pH range 5-8; S=sample before the bindig, U=unbound sample, LMW=low molecular weight

Instead, the CM-Sepharose FF cation exchange resin allowed the total binding of brazzein at pH 4, a partial binding at pH 5 and almost no binding at pH 6, 7, and 8 (Figure 3.18). It is therefore possible to elute brazzein separately from the other proteins, by increasing the salts concentration applying to the resin a NaCl 1M buffer.

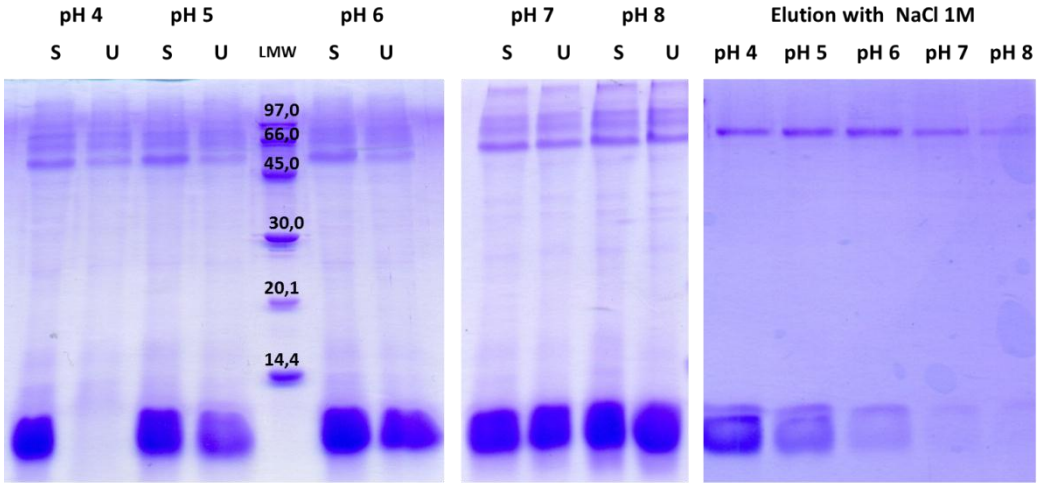

Figure 3.18 - SDS-PAGE analysis of the CM-Sepharose FF cationic batch process in the pH range of 4-8, and relative elution process; S=sample before the binding, U=unbound sample, LMW= low molecular weight

In Figure 3.18 – Elution with NaCl 1M – is possible to see that in addition to brazzein there is a contaminant bind to the resin. In order to separate the protein of interest from the other protein it was necessary to use a gradient of NaCl elution buffer.

We optimized the elution process by using a Pharmacia Biotech XK 26 column, filled with 110 ml of CM-Sepharose FF resin. To allow protein binding to the resin the supernatant was diluted 4.6 time to lower the conductivity value to approximately 14 mS/cm, and the final pH of the solution was adjusted to 4 by adding HCl.

The supernatant (Lane 2, Figure 3.21) was then loaded into the column pre-equilibrated with Buffer A (Na-Acetate Buffer 20mM pH4). The flow through, containing the unbound proteins, was collected (Fraction I, Figure 3.19) (Lane 3, Figure 3.22). After a washing stage, proteins bound to the resin were eluted by increasing the concentration of Buffer B (NaCl 1M in Na-Acetate 20mM pH 4) from 0% to 100% using a linear gradient.

Two fractions were collected: Fraction II (from 0 to about 40% B) corresponds to the contaminants (Fraction II, Figure 3.20) (Lane 4, Figure 3.21), while fraction III (from about 60 to 70% B) corresponds to brazzein (Fraction III, Figure 3.20) (Lane 5, Figure 3.21). A chromatographic baseline separation of the two fraction was achieved (R=2.2).

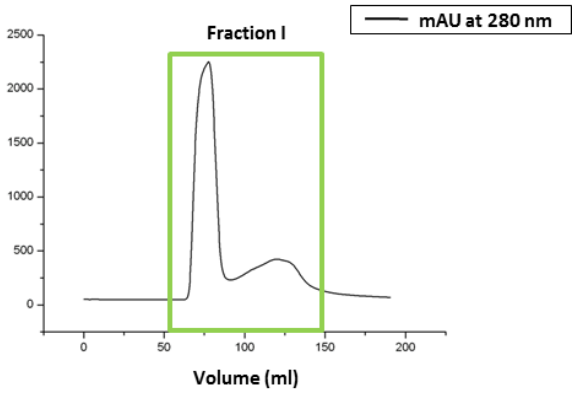

Figure 3.19 - Flow through of the cation exchange column after sample loading and column wash

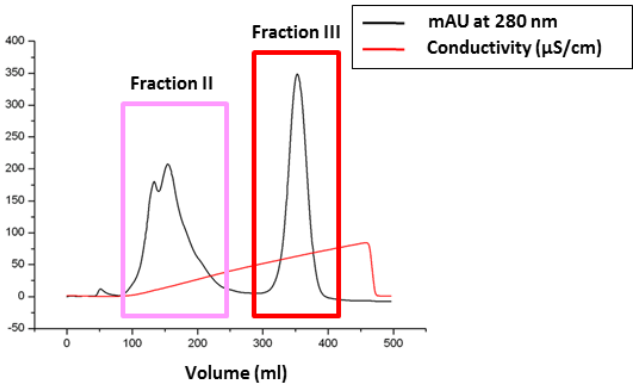

Figure 3.20 - Elution profile of proteins bound to the cationic resin, by a linear gradient of NaCl buffer

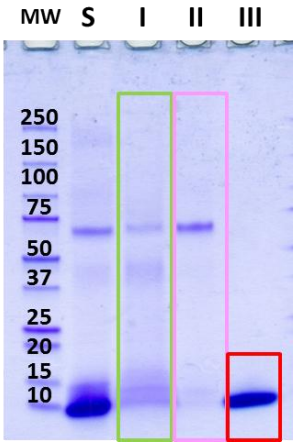

Figure 3.21 – SDS-PAGE analysis of the CM-Sepharose FF cationic process at pH 4, and the relative elution process; MW=molecular weight, S=starting sample, I=first collected fraction, corresponding to the column flow through, II=second collected fraction, corresponding to the contaminant eluted from the column at a B concentration between 0 and 40%, III=third collected fraction, corresponding to brazzein eluted form the column at a B concentration between 60 and 70%

In conclusion, brazzein can be successfully separated from other proteins present in the supernatant by a cation exchange chromatography because it bind to the resin and then elutes at a higher Buffer B concentration (approximately 0.6 M NaCl) by comparison with the contaminants. Moreover, brazzein eluted in a concentrated form and small volumes while, in the case of an anion exchange chromatography it will elute as flow through in a large volume and requires further concentration steps.

Subsequent steps of diafiltration were performed using filter membranes with cut offs ranging from 1 to 3.5 kDa, in order to washed out the NaCl from the final brazzein solution.

At the end of the purification protocol the concentrated brazzein solution can be stored as a solution after sterilization by membrane filtration (0.22 μm filter), or as a lyophilized powder directly freeze drying the purified protein.

The final yield of the process is about 100 mg of purified protein per liter of initial fermentation culture volume.

It is important to underline that this purification protocol doesn’t foresee costly or harsh chemical steps and so it is suitable for the food industry.

3.4. Brazzein characterization

The concentrated solution of brazzein was characterized by HPLC, NMR and mass spectrometry. In addition the thermal stability of the protein was investigated by calorimetric analysis. A taste panel assay for sweet taste control was performed in order to determine the sweetness potency of the produced recombinant protein. Finally, preliminary allergenicity studies were performed in order to evaluate the potential allergenicity of the protein.

3.4.1. HPLC and mass spectrometry analysis

Protein purity was assessed monitoring the absorbance profile at 280 nm of a reverse phase HPLC chromatographic run and reported as the relative percentage of the area of the brazzein peak. An aliquot of Fraction III (see Figure 3.20 and Figure 3.21) was loaded into a Phenomenex C4 column.

The chromatography was performed applying a non-linear acetronitrile gradient to the column.

HPLC runs showed that brazzein is eluted as a single peak (Figure 3.22). The protein purity, estimated at 280 nm using a diode-array UV-visible spectrophotometer interfaced with the Agilent Chemostation software, was estimated to be about 99.98%.

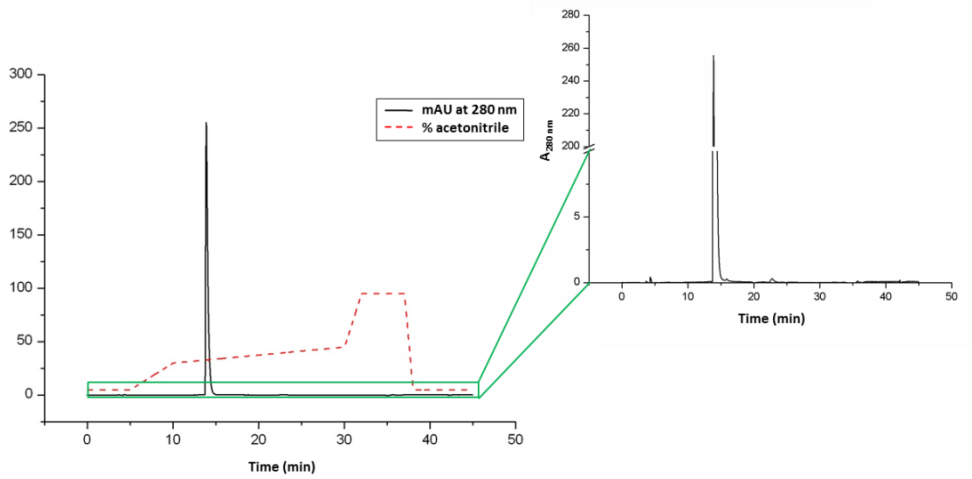

Figure 3.22 – Fraction III HPLC reverse chromatography profile on a C4 column relative to brazzein 54 amino acids form; similar results were obtained for the BraΔ1M form

The purified peak was then subjected to Mass Spectrometry analysis which provided a molecular weight of 6500.89±0.67 Da for brazzein with Met as first amino acid, and a molecular weight of 6369.93±0.03 for the BraΔ1M form (Figure 3.23). These results are very close to the expected

masses of 6501 Da and 6370 Da relative to the two brazzein forms. It can be therefore inferred that brazzein is not degraded by proteases in the supernatant and that the only post-translational modification present is the four disulfide bonds typical of the brazzein structure; other modifications, such as glycosylation, are not present.

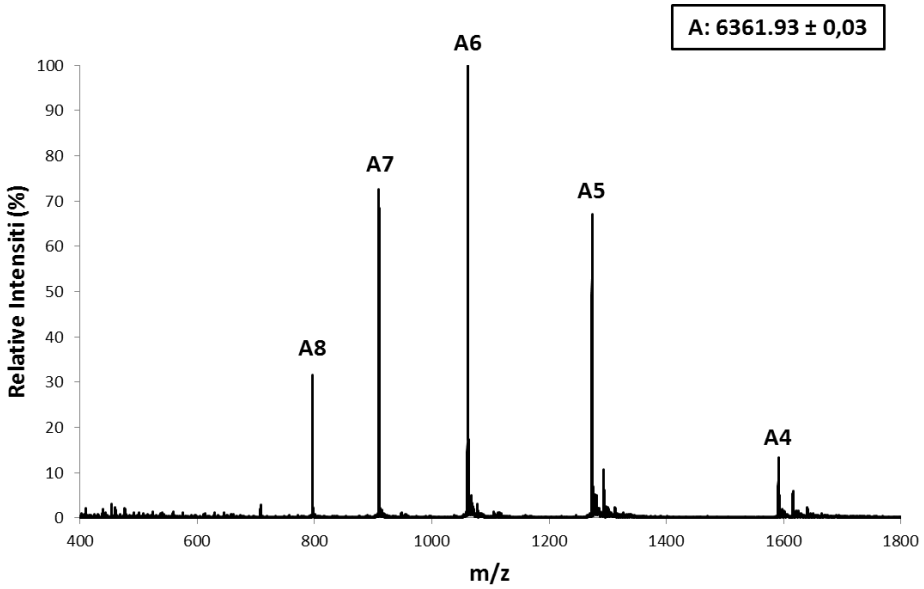

Figure 3.23 – Mass spectrometry analysis of the purified recombinant brazzein without Met as first amino acid (Δ1M form)

3.4.2. NMR

The structural similarity of the recombinant protein with Met as first amino acid expressed by *P. pastoris* (Figure 3.24, B) with the wild-type brazzein extracted from the natural plant (Figure 3.24, A) was confirmed by TOCSY NMR experiment, performed as described in "Studies on solution NMR structure of brazzein" (Gao *et al.*, 1999).

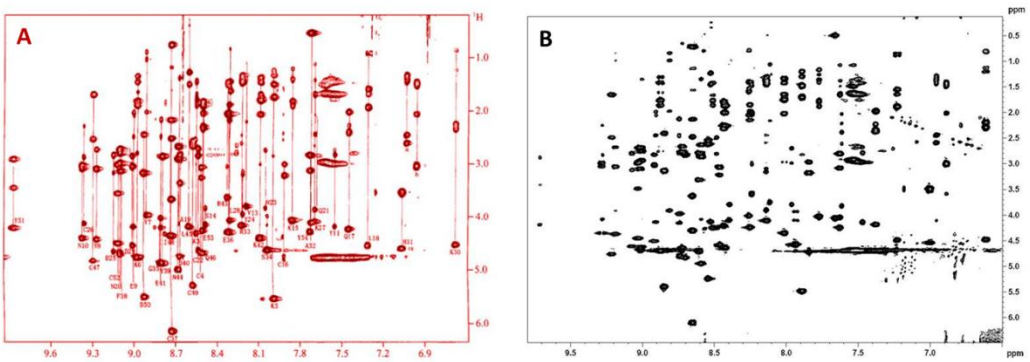

Figure 3.24 – TOCSY NMR comparison between wild type brazzein extracted from its natural source (A, in red; Gao *et al*, 1999) and the recombinant one (B, in black)

Furthermore, as shown in Figure 3.25, the protein maintains the correct folding (and therefore its sweet taste) even after heat treatment at 98°C for 2 hours.

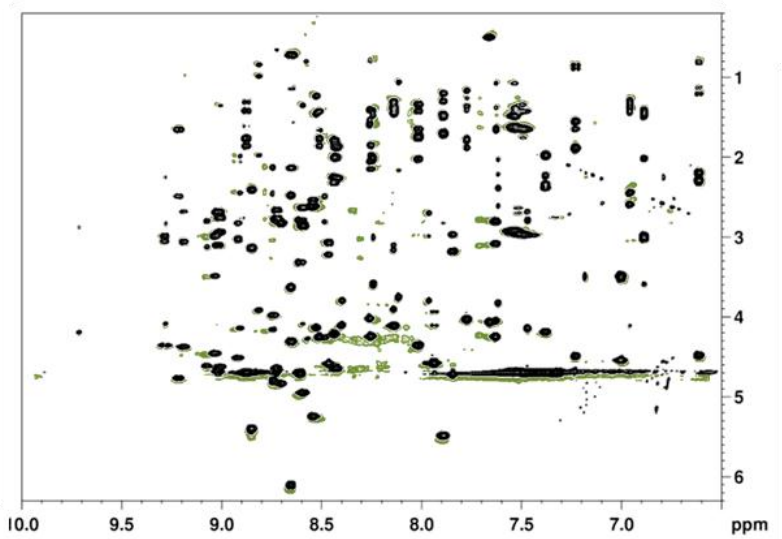

Figure 3.25 - TOCSY NMR comparison between recombinant brazzein after 2 hours at 98 °C (in green) and the no heat-treated one (in black)

3.4.3. Calorimetric analysis

Some Differential Scanning Calorimetric (DSC) analysis were done (in collaboration with Dr. Rita Guzzi, Physics Department - University of Calabria) to investigate the thermal stability of the 54 amino acids brazzein. As shown in Figure 3.26 brazzein denatures at 65.8 °C, while in literature is reported that brazzein is stable for two hours at 98 °C (Ming *et al.*, 1994). An explanation of such apparent discrepancy could be found in a correct re-folding of the protein due to the presence of the four disulfide bonds when the temperature returns to room temperature. To verify this hypothesis we did a taste panel assay after incubating the protein for two hours at 98 °C. For both testers the protein was sweet even after two hour at 98 °C, suggesting that the protein retained its correct folding.

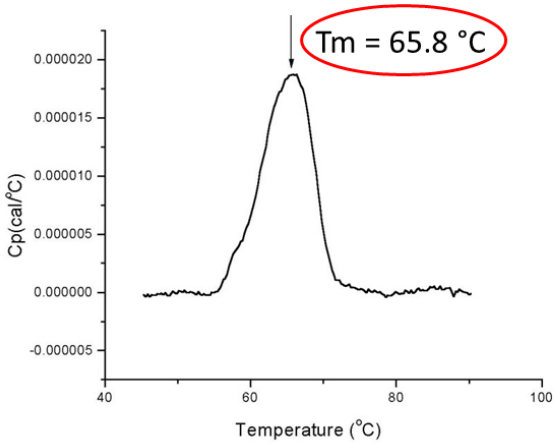

Figure 3.26 – DSC scan of brazzein

Moreover, we investigated the reversibility of the thermal unfolding. As reported in Figure 3.27, in successive DSC heating scans brazzein denatured at about the same temperature (condition verified for 5 successive scans; in Figure 3.27 is shown only the first re-scan); this is indicative of the correct re-folding of the protein when temperature returns to room temperature.

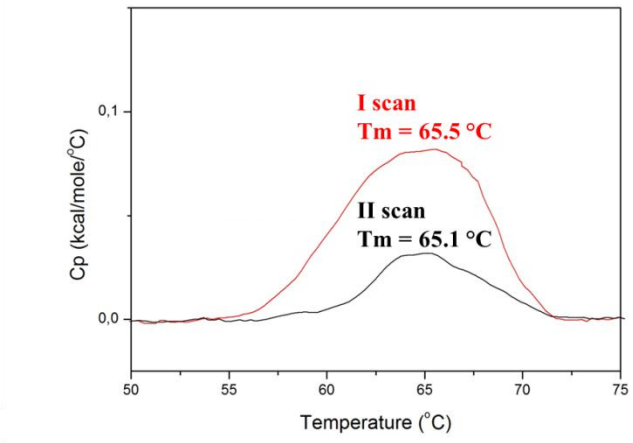

Figure 3.27 – Reversible DSC scans of brazzein

To verify the importance of the 4 disulfide bonds in the correct re-folding mechanism we studied the reversibility of the thermal unfolding in presence of DTT. As indicated in Figure 3.28 the melting temperature of brazzein lowers by approximately 5 °C; moreover, there is no heat absorption in the first re-scan, indicating that the unfolding process is completely irreversible in presence of DTT.

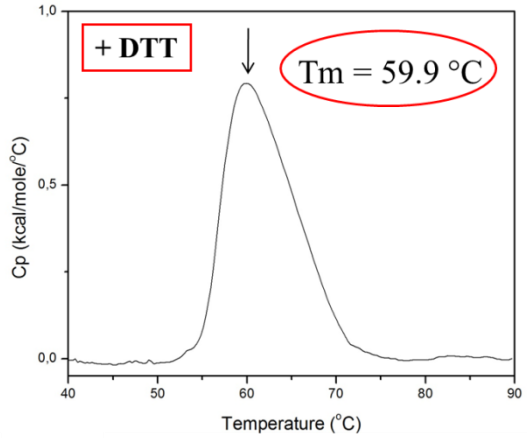

Figure 3.28 – Irreversible DSC scans of brazzein in presence of DTT

3.4.4. Sensory analysis in humans

According to the literature (Ming *et al.*, 1994), brazzein is estimated to be 500 to 2000 times sweeter then sucrose on a weight basis. However, sweetness values reported in these articles were obtained from preliminary tests, lacking a common evaluation methodology or a rigorous data analysis.

In order to determine the variation on the sucrose equivalent sweetness of recombinant brazzein (with Met as first amino acid) with the increase in its concentration, we applied the magnitude estimation method (Stevens, 1956; Stone *et al.*, 1969; Cardello *et al.*, 1999), which yields a quantitative measure of the subjective intensity of sweetness.

Four untrained volunteers subjects (two women and two men, staff members from Department of Biology - University of Padova – Italy), who were between 25 and 58 years of age, participated in the experiment.

Sucrose and 54 aa-brazzein concentrations utilized in the test are listed in

Table 3.8; this concentrations range was chosen on the basis of preliminary experiments to avoid the use of samples with sweetness out of the linearity range between stimulus (C) and intensity of the stimulus (S).

Sucrose concentration	1%	2%	4%*	8%	16%
Brazzein concentration for equivalency	0.002%	0.004%	0.008%	0.016%	0.032%

Table 3.8 - Samples concentration (w/v %) used in the magnitude estimation test
***Sample used as reference with arbitrary sweet intensity value of 100**

When the geometric mean intensity of the stimulus converted to logarithmic value was plotted against the logarithm of the stimulus concentration (C), the data could be fitted by a linear regression defined by the function logS=loga+nlogC (where *S* is the intensity of the stimulus, *C* is the concentration of the stimulus, *n* is the slope and *a* is the antilog of the value of the y intercept) (Figure 3.29). The adjusted coefficient of determination, R^2, is 0.94 for brazzein linear regression, and 0.97 for sucrose; these results indicated a good fit of the regression line for both sweeteners.

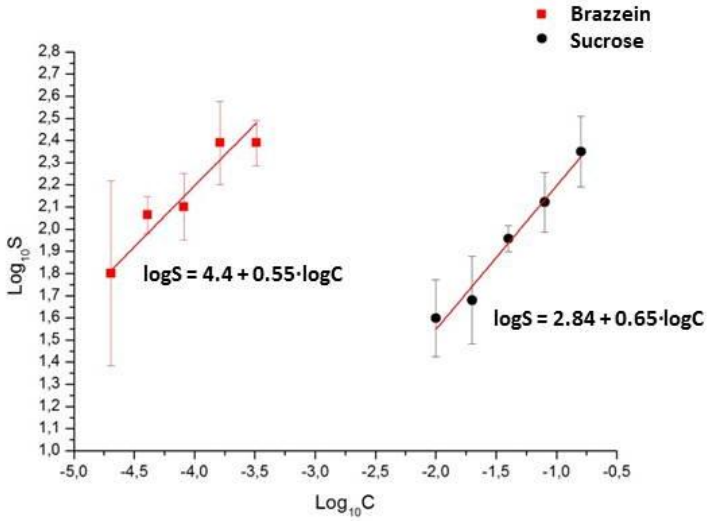

Figure 3.29 – Sweetness power funtion for 54 aa-brazzein (in red) and sucrose (in black) in aqueous solution (n = 4)

From these results, it was possible to calculate the sweetness potency of brazzein; the sweet potency was defined as the number of times a brazzein solution is sweeter than a weight equivalent sucrose solution. The sweet potency values at different concentrations of brazzein are presented in Table 3.9.

Sucrose concentration	1%	2%	4%	8%	16%
Brazzein sweet potency (X sucrose)	1492	1323	1172	1039	921

Table 3.9 – 54 aa-brazzein sweet potency (X sucrose)

As reported in Table 3.9, brazzein sweet potency ranges from 920 folds to about 1500 folds in the considered concentrations interval. As

shown in Figure 3.30, brazzein curve exhibited a decrease in sweetness potency as its concentration increased, in agreement with previous studies on other high intensity sweeteners (Cardello *et al.*, 1999).

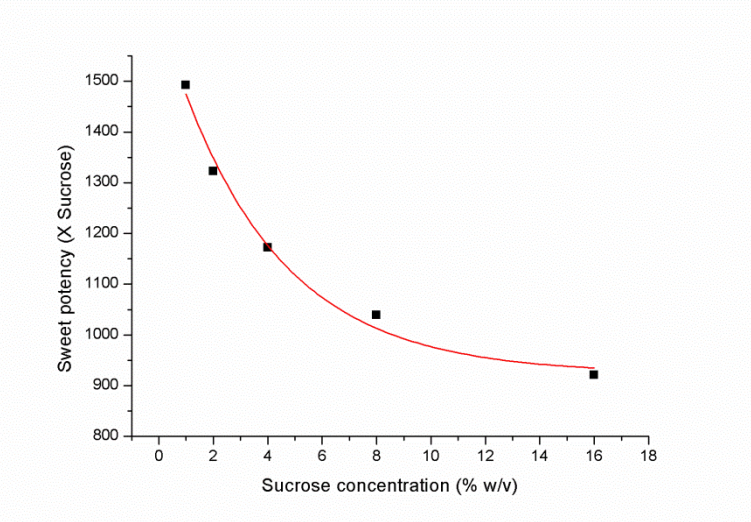

Figure 3.30 – Sweet potency of brazzein over a range of sucrose sweetness equivalencies

As shown Figure 3.30, brazzein works most efficiently as sucrose replacer when used to achieve a sucrose equivalence lower than 8%. Moreover, it seems that the maximum sweetness achievable with brazzein can't exceed the stimulus intensity obtained with a 16% sucrose solution.

Future development will be the evaluation of brazzein sweetness temporal profile. As previously described for other high intensity sweeteners (see Chapter 1.1.2 and 1.1.3), from our preliminary results (comments reported by the four judges) brazzein sweetness dies out slower than that of sucrose.

3.4.5. Brazzein allergenic potential

3.4.5.1. Sequence analysis

In the FAO/WHO report (2001) is indicated that cross-reactivity between the query protein and a known allergen has to be considered if there is 1) more than 35% identity in the amino acid sequence of the expressed protein, using a window of 80 amino acids and a suitable gap penalty, or 2) identity of at least 6 contiguous amino acids.

Lamphear and coworkers (2005) reported that brazzein presents no substantial homology to known allergens (not ≥ 35% identity over the 53-amino acid length of brazzein). Taking advantage of the

Allergenicity Prediction Tool available at the ADFS (Allergen Database for Food Safety) web site (http://allergen.nihs.go.jp/ADFS/index.jsp) we confirmed there was no homology with any type of allergen, both for the 54 and 53-amino acids form of brazzein.

However, for both brazzein forms, the identity search for contiguous of 6 amino acids produced 2 hits (Table 3.10), both corresponding to the following sequence: ANQCNY (residues 18-24 of wild type brazzein).

Match description (from UniProt)	Match source	N° of exact word matches
RecName: Full=Venom allergen 5.01; AltName: Full=Antigen 5-1; Short=Ag5-1; AltName: Full=Allergen Vesp c V.01; AltName: Allergen=Vesp c 5.01	Vesp	1
RecName: Full=Venom allergen 5.02; AltName: Full=Antigen 5-2; Short=Ag5-2; AltName: Full=Allergen Vesp c V.02; AltName: Allergen=Vesp c 5.02	*Vesp*	*1*

Table 3.10 - Sequence matches with brazzein in agreement with the second FAO/WHO criteria

Nevertheless, a comparison of the full sequence of brazzein with both forms of venom allergen showed no significant similarity (3% of query coverage). Moreover, in order to reduce the number of unspecific candidates as suggested by Poulsen (2004), we reduced the stringency by evaluating 7 or 8 contiguous residues and we obtained no matches.

Therefore, we concluded that no health risks related to an allergenic potential could be demonstrated with the sequence analysis approach.

However, due to the high stability of brazzein in a broad range of pH and temperature, the regulatory approval of brazzein for human consumption will probably require other tests for the evaluation of its allergenic potential.

3.4.5.2. Pepsin resistance

A first step towards the evaluation of possible recombinant protein allergenicity, was achieved by an *in vitro* test of Pepsin sensitivity according to the general guidelines published by FAO/WHO (2001). The breakdown of brazzein was assessed by Tris-Tricine SDS-PAGE electrophoresis (Figure 3.31) that allowed us to verify that after

five minutes at 37 °C in Simulated Gastric Flow conditions brazzein was degraded by pepsin in smaller peptides, indicating that there is a low probability that the protein can elicit any allergic reaction.

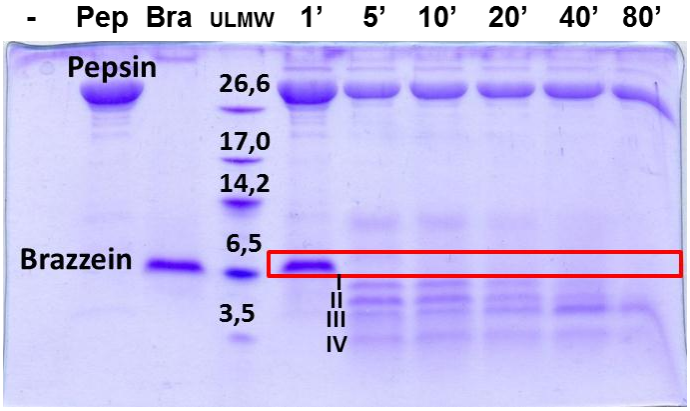

Figure 3.31 – Tris-Tricine SDS-PAGE analysis illustrating pepsin hydrolysis of brazzein at pH 1.5. Pep) Pepsin control 1.28 mg/ml, Bra) Brazzein control 0.5 mg/ml, ULMW) Ultra Low Molecular Weight, 1') Brazzein incubated with Pepsin in NaCl 30mM, pH 1.5, 37°C after 1 minutes, 5') 5 min, 10') 10 min 20') 20 min, 40') 40 min, 80') 80 min. Peptides derived from digestion are indicated as I) 5.7-6 kDa, II) 4.8-5.3 kDa, III) 4.3-4.6 kDa, IV) 3.3-3.6 kDa

To predict the potential pepsin cleavage sites of brazzein we used the PeptideCutter tool (http://www.expasy.org/tools/peptidecutter) (Figure 3.32).

Most of the peptides predicted to be formed are very small, with the largest having a mass of 1418 Da. Since fragments greater than 3.5 kDa suggest a potential allergic protein (FAO/WHO, 2001), brazzein shows a low probability to be allergenic. However, this evidence has to be confirmed with other tests, such as the *in vitro* investigations on possible reactivity of IgE antibodies in sera of patients with known allergies to source material and the investigations *in vivo* in patients allergic to the source food (FAO/WHO, 2001).

In Figure 3.32 are represented the specific cleavage sites and all the possible fragments resulting from 1 or 2 pepsin cuts (fragments detectable in the Tris-Tricine SDS-PAGE gel). In the Tris-Tricine SDS-PAGE gel (Figure 3.31) we verified the formation of all the predicted fragments: band I (estimated molecular weight 5.7-6 kDa) should correspond to the peptide 1-50 (5.9 kDa); band II (estimated molecular weight 4.8-5.3 kDa) should correspond to the peptide 11-54 (5.0 kDa); band III (estimated molecular weight 4.3-4.6 kDa) should correspond to fragments 1-39, 11-50, and 18-54 (4.6, 4.5, 4.3 kDa respectively); band IV (estimated molecular weight 3.3-3.6 kDa) should correspond to

peptides 1-28, 11-39, 18-50, 24-54 (3.3, 3.2, 3.8, and 3.6 kDa respectively).

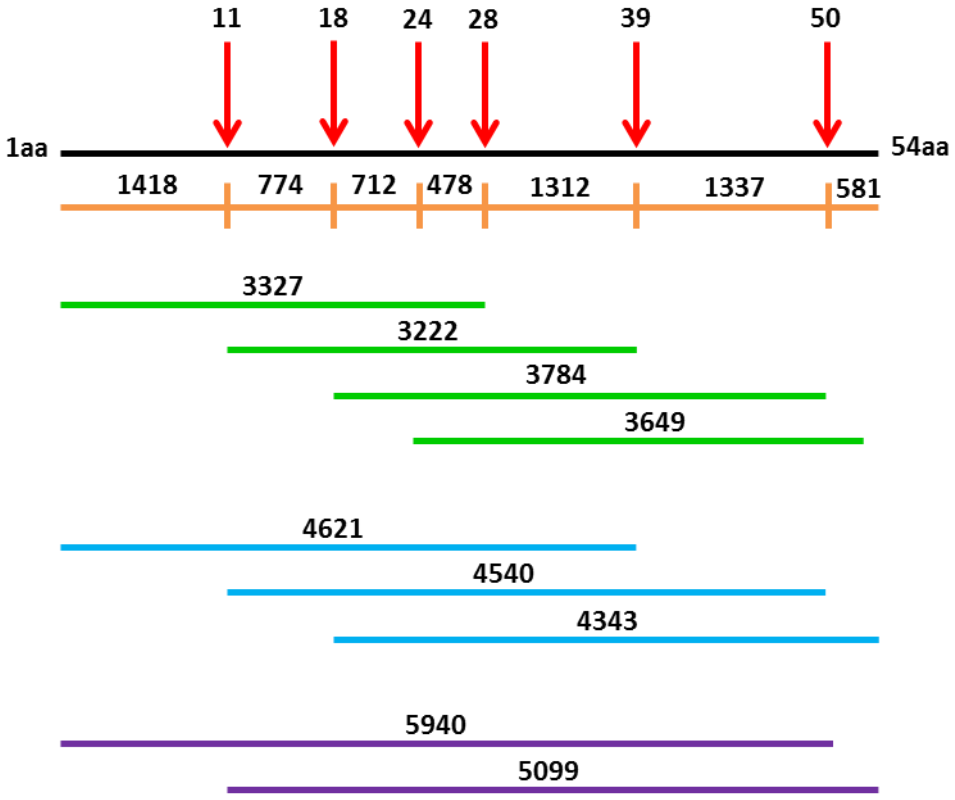

Figure 3.32 – Cleavage sites of brazzein for pepsin (at pH = 1.3), predicted by PeptideCutter; represented are the possible fragments resulting from 1 or 2 pepsin cuts

To quantify pepsin hydrolysis of brazzein we also performed a densitometric analysis of Tris-Tricine SDS-PAGE gel. As shown in Figure 3.33 brazzein was broken down with a half-life lower than 2 minutes 30 seconds under these conditions.

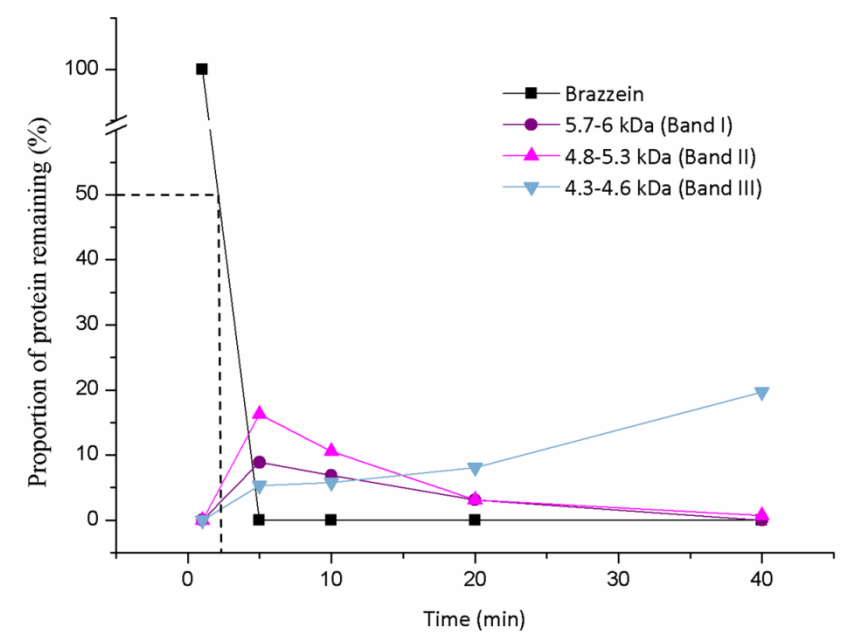

Figure 3.33 – Proteolytic degradation of brazzein by pepsin estimated by densitometric analysis of Tris-Tricine SDS-PAGE gel

With the PeptideCutter tool we also predict that brazzein would be hydrolyzed by trypsin (Figure 3.34) and chymotrypsin (Figure 3.35), providing other evidences of the extensive protein degradation in the gastrointestinal tract.

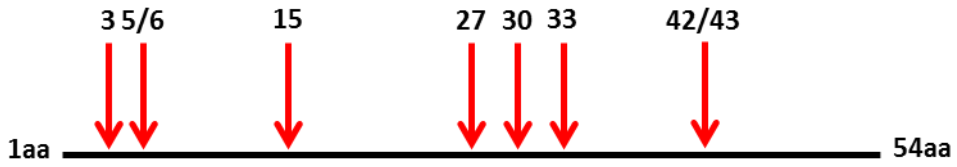

Figure 3.34 - Cleavage sites of brazzein for trypsin (cleavage probability > 70%), predicted by PeptideCutter

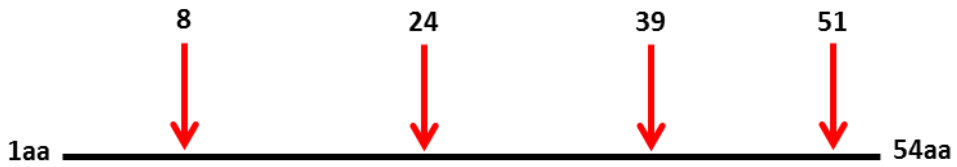

Figure 3.35 - Cleavage sites of brazzein for chymotrypsin (cleavage probability > 80%), predicted by PeptideCutter

Chapter 4

RESULTS

Expression and characterization of a wheat Ice Structuring Protein

The ability of ISPs to retard ice recrystallization[1] makes them particularly suitable in food industry as natural ice modulators for cold storage of frozen products such as ice cream.

Griffith and collaborators (2004) shown that plant ISPs are good inhibitors of the ice-recrystallization process compare to other ISPs (e.g. fish ISPs). Therefore, the goal of this work was to identify a plant ISP and to develop an efficient expression and purification method for its industrial production. We preferentially selected an ISP with stability at high temperatures since this property is fundamental for the industrial application of the protein. In fact, many industrial processes require heat-treatment before freezing, such as ice-cream (pasteurization), ready meals (pre-cooking), or frozen vegetables (blanching[2]).

We identified, after a bibliographical documentation, a promising ice structuring protein from the winter wheat grass *Triticum aestivum* (Figure 4.1). Kontogiorgos and collaborators (2007) showed that this protein, isolated from a wheat extract, has a re-crystallization inhibition (RI) activity. Moreover, the wheat ISP is heat stable.

```
        10         20         30         40         50
MASTRVLHLI ALVLAVATAA DAATITVVNR CSYTVWPGAL PGGGVRLDPG
        60         70         80         90        100
QSWALNMPAG TAGARVWPRT GCTFDGSGRG RCITGDCGGT LACRVSGQQP
       110        120        130        140        150
TTLAEYTLGQ GGNKDFFDLS VIDGFNVPMN FEPVGGSCRA ARCATDITKE
       160        170        180        190        200
CLKELQVPGG CASACGKFGG DTYCCRGQFE HNCPPTNYSK FFKGKCPDAY
       210        220
SYAKDDQTST FTCPAGTNYQ IVLCP
```

Figure 4.1 – Amino acids sequence of the wheat Ice Structuring Protein (GenBank: AAM15877.1)

Consequently, the first step of this study was to obtain ISP cDNA through chemical synthesis (GeneART, Regensburg - Germany) with codon optimization for the expression in both *E. coli* and *P. pastoris*.

In order to perform preliminary studies ISP cDNA was cloned into a specific expression vector, pET-28a, for the expression in *E. coli* that carries a N-term His-tag sequence. Then, with the aim of obtaining the necessary amount

[1] Ice recrystallization is the growth of large ice crystals at the expense of smaller ones in partially frozen solutions

[2] Blanching is a cooking term that describes a process of food preparation wherein the food substance, usually a vegetable or fruit, is plunged into boiling water, removed after a brief, timed interval and finally plunged into iced water or placed under cold running water (shocked) to stop the cooking process

and purity required for the ISP industrial application, we moved to the *P. pastoris* constitutive expression system.

4.1. Expression in *Escherichia coli*

4.1.1. Construction of the pET28a-ISP expression vector

The ISP cDNA was obtained through chemical synthesis (GeneART, Regensburg - Germany) with codon optimization for the expression in both *E. coli* and *P. pastoris*. Then, the ISP cDNA was cloned into a pET-28a *E. coli* expression vector that carries a N-term His-tag sequence (Figure 4.2).

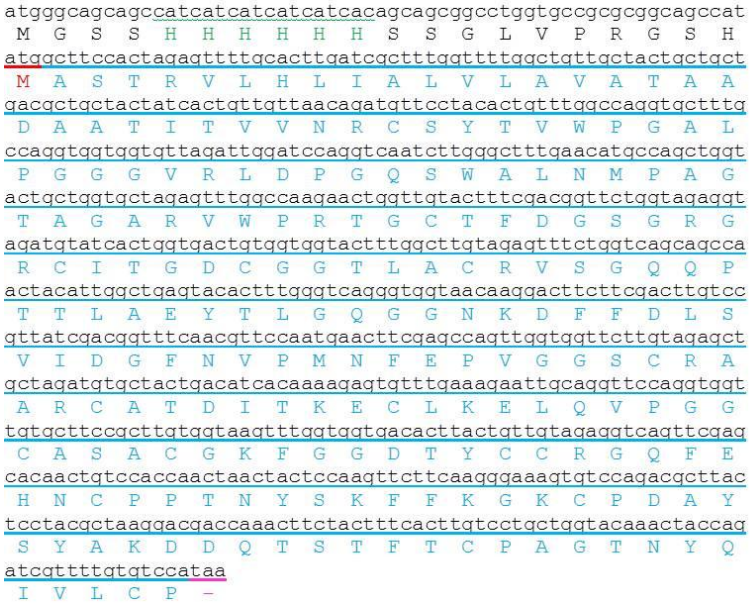

Figure 4.2 – Plasmid sequence for the ISP expression in *E. coli* with N-term His-tag (in green). Underline in red is the first ISP amino acid, in pink the stop codon sequence

4.1.2. Expression in shake flask cultures

ISP expression was initially tested in 50 ml culture volume in the BL21 strain under three different inductor concentration (0.2, 0.5, 1 mM IPTG) at 37 °C. In terms of expressed protein and absence of impurities, 0.5 mM IPTG and 3 hours induction time turned out to be the optimal expression conditions (Figure 4.3).

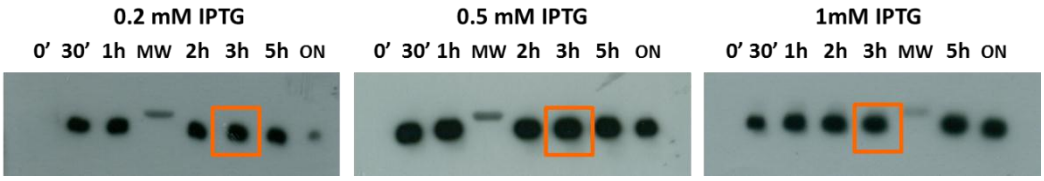

Figure 4.3–Anti-His dot-blot analysis of ISP expressed in the BL21 *E. coli* strain under three different inductor concentration at 37°C

We later did some experiments using the BL21 and the C41 *E. coli* strains at three different temperatures (4°C, RT, 37°C) and 0.5 mM IPTG. The C41 strain was derived from the BL21 one (Miroux *et al.*, 1996): it presents one uncharacterized mutation, which prevents the cell death associated with the expression of toxic recombinant proteins. We verified that 37 °C is the only temperature that allows protein expression for both strains (Figure 4.4).

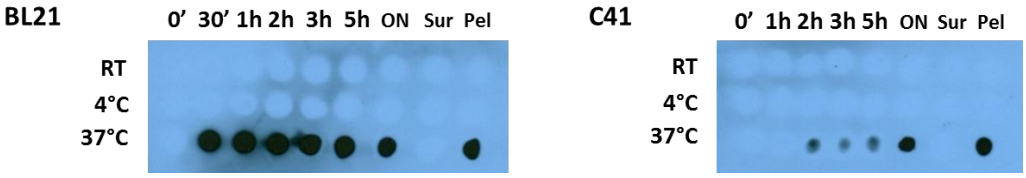

Figure 4.4 – Anti-His dot-blot detection of ISP expressed in the BL21 and C41 *E. coli* strains at 3 different temperatures (RT, 4°C, 37°C)

Unfortunately, both BL21 and C41 *E. coli* strains expressed a very low quantity of the recombinant protein, detectable only by western-blot analysis. Moreover, after sonication and centrifugation of the culture, the protein precipitated in the pellet hindering the successive purification process (Figure 4.4).

We hypothesized that the low expression level and the protein precipitation in the inclusion body could be due to the low ability of *E. coli* to form disulfide bonds because of its reducing cytoplasmic environment. Consequently, in *E. coli*, a protein with many disulfide bonds generally accumulates into insoluble aggregates in a misfolded and biologically inactive form. Therefore, it is very likely that the eight disulfide bonds distinctive of the ISP structure would not be correctly formed in the *E. coli* expression system.

To improve the disulfide bonds formation we expressed the wheat ISP in the *E. coli* Origami2 strain. In fact, because of mutations in both the

thioredoxin reductase (*trxB*) and glutathione reductase (*gor*) genes, this strain greatly enhances disulfide bond formation in the cytoplasm.

We performed the expression tests at different temperatures (37°C, 28°C, RT and 4°C) using 0.5 mM IPTG.

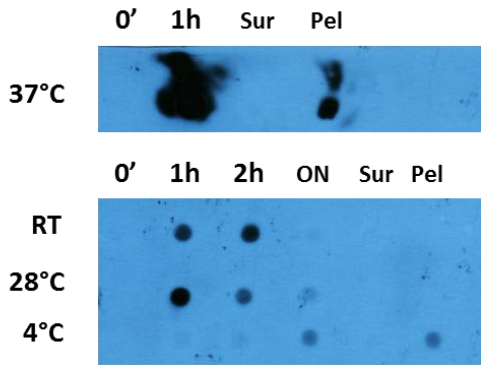

Figure 4.5 - Anti-His dot-blot detection of ISP expressed in the Origami2 *E. coli* strain at 4 different temperatures

As reported in Figure 4.5, the Origami2 strain expressed the wheat ISP at all temperatures tested. However, as for the BL21 and C41 strains, it produced a low quantity of the recombinant protein which precipitate in the pellet during the purification protocol.

Therefore, in order to obtain high levels of soluble recombinant ISP, we decided to move to the *P. pastoris* expression system.

4.2. Constitutive expression in *Pichia pastoris*

4.2.1. Construction of the constitutive expression plasmids

As a first step towards our goal of obtaining high-levels of recombinant ISP, we obtained the constitutive pGAPZαA-ISP expression vector through the modification of the pGAPZαA-BRA vector: ISP gene was inserted into pGAPZαA-BRA plasmid in place of the brazzein gene. The construction flow chart of the new integrative plasmid pGAPZαA-ISP is described in Figure 4.6.

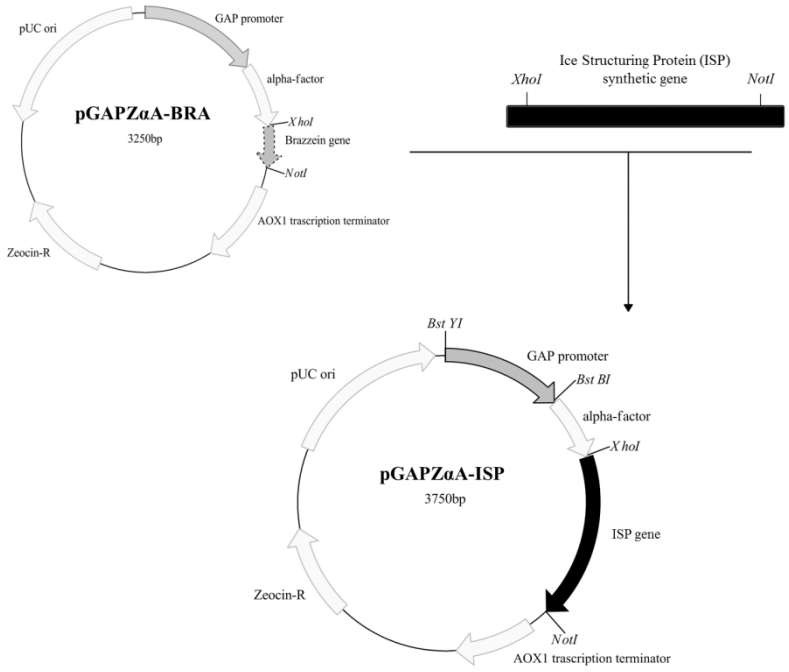

Figure 4.6 – Schematic diagram illustrating the construction of the pGAPZαA-ISP constitutive expression vector from the pGAPZαA-BRA vector

In order to simplify the detection and purification protocol we decided to express the protein also with an histidine tag (ht) at the C-terminus (Figure 4.7).

```
        10         20         30         40         50         60
MASTRVLHLI ALVLAVATAA DAATITVVNR CSYTVWPGAL PGGGVRLDPG QSWALNMPAG

        70         80         90        100        110        120
TAGARVWPRT GCTFDGSGRG RCITGDCGGT LACRVSGQQP TTLAEYTLGQ GGNKDFFDLS

       130        140        150        160        170        180
VIDGFNVPMN FEPVGGSCRA ARCATDITKE CLKELQVPGG CASACGKFGG DTYCCRGQFE

       190        200        210        220        230        240
HNCPPTNYSK FFKGKCPDAY SYAKDDQTST FTCPAGTNYQ IVLCPEQKLI SEEDLNSAVD

HHHHHH
```

Figure 4.7 - Amino acids sequence of the wheat Ice Structuring Protein with an His-tag at the C-term

We modified the pGAPZαA-ISP expression vector to obtain the pGAPZαA-ISPht vector (Figure 4.8): by site directed mutagenesis we eliminated the TAA stop codon allowing the transcription of the histidine-tag.

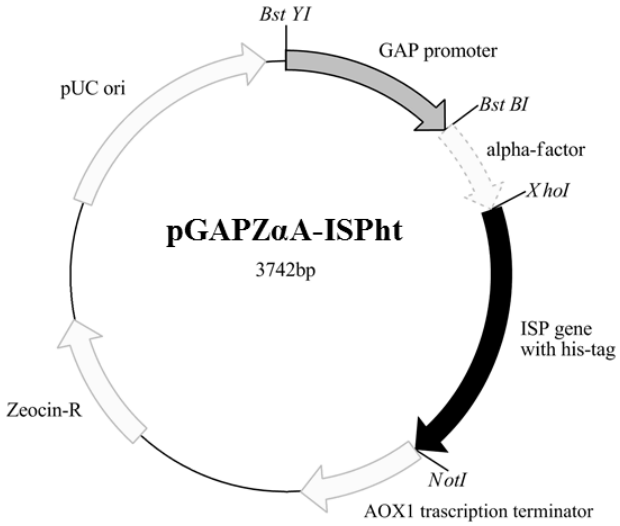

Figure 4.8 – Vector map of the plasmid for the constitutive expression of ISP with His-tag in *P. pastoris*

As for the pGAPZαA-BRA vector, the pGAPZαA-ISP and the pGAPZαA-ISPht plasmids harbor a dominant selectable shuttle marker, Zeocin™, which allows selection of both *E. coli* and *P. pastoris* transformant. They also contain the native *Saccharomyces cerevisiae* α-factor secretion signal, which allows for efficient protein secretion in *P. pastoris*.

However, in literature is reported that some proteins have been expressed and secreted by *P. pastoris* using the native signal sequence of the protein itself. For instance, *P. pastoris* correctly process the native signal sequence of the sweet protein thaumatin while, when the α-factor sequence was used the protein was incompletely processed at the N-terminus. Therefore, the use of the native signal sequence allowed for an high yield of secreted thaumatin correctly folded and correctly processed at the N-term (Ide *et al*., 2007).

The wheat ISP sequence analysis, performed by TargetP 1.1 Tool (http://www.cbs.dtu.dk/services/TargetP), suggested that the protein contains a 22-amino acid N-terminal signal peptide that targets the protein to the secretory pathway (Table 4.1).

Sequence length	225
Score of predicted localization for chloroplast	0.024
Score of predicted localization for mitochondrion	0.025
Score of predicted localization for secretory pathway	0.965
Score of predicted localization for any other localization	0.018
Prediction of localization	Secretory pathway
Reliability class	1
Predicted pre-sequence length	22

Table 4.1 - TargetP 1.1 output prediction. The predicted location with the highest score is the most likely according to TargetP, and the relationship between the scores (the reliability class, see below) may be an indication of how certain the prediction is. Reliability class (RC), from 1 to 5, is a measure of the size of the difference between the highest (winning) and the second highest output scores: the lower the value of RC the safer the prediction

Hence, we modified by the α-factor PCR mediated-deletion the pGAPZαA-ISP and the pGAPZαA-ISPht plasmids in order to obtain the pGAPZA-ISP cutα (Figure 9) and the pGAPZA-ISPht cutα (Figure 10) plasmids.

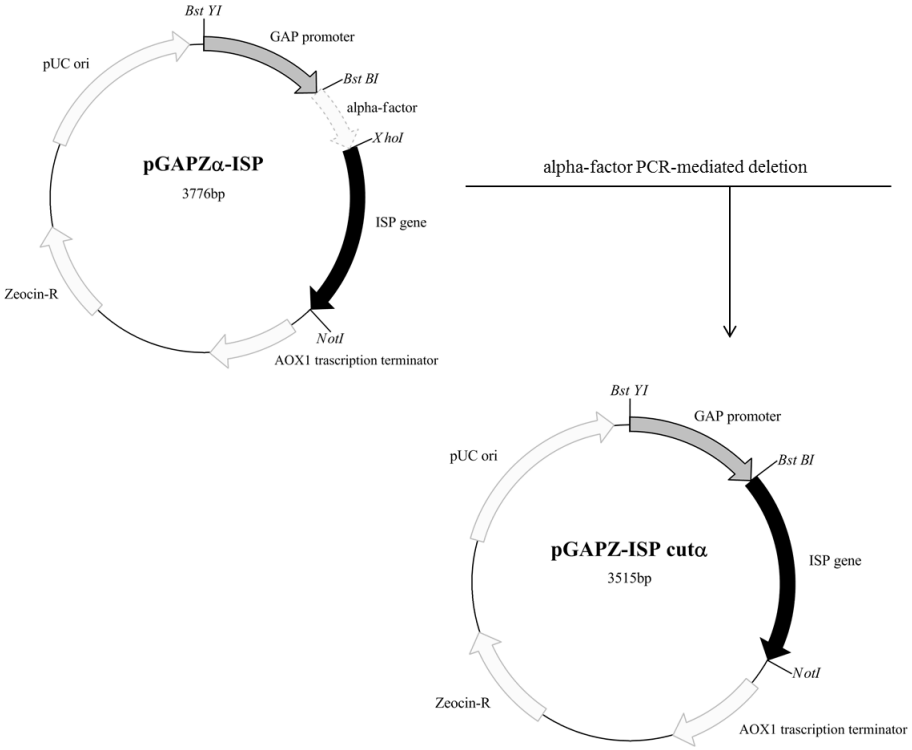

Figure 9 - Schematic diagram illustrating the construction of the pGAPZA-ISP cut*α* constitutive expression vector from the pGAPZ*α*A-ISP vector

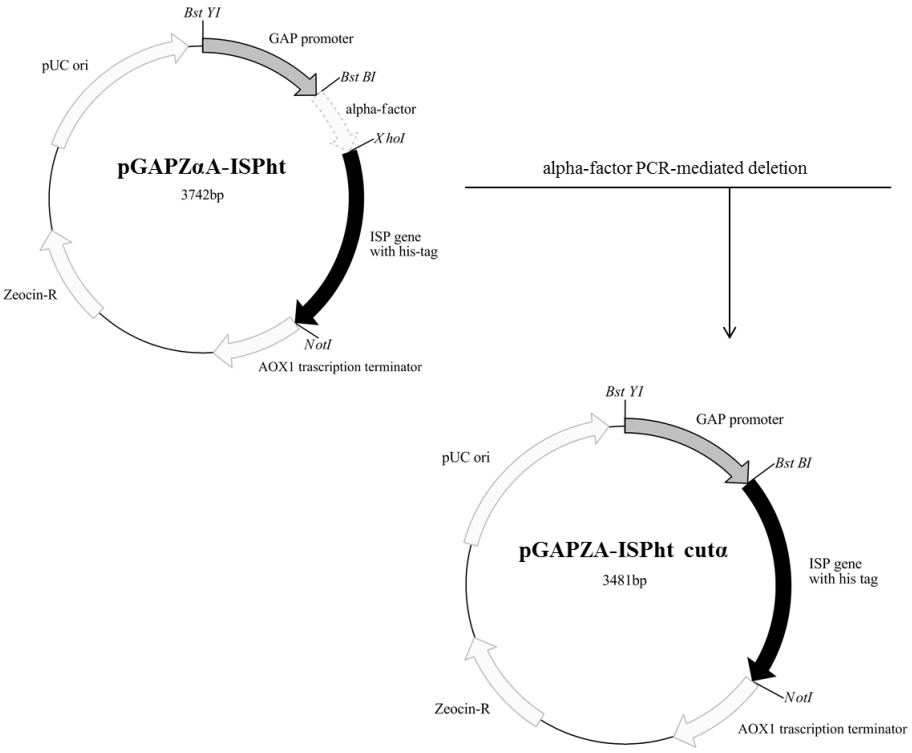

Figure 10 - Schematic diagram illustrating the construction of the pGAPZA-ISPht cut*α* constitutive expression vector from the pGAPZ*α*A-ISPht vector

4.2.2. Yeast transformation and selection

After the linearization with AvrII restriction enzyme, all the plasmids were used to transform *P. pastoris* wild-type strain X33 by electroporation. High-level expression transformants were selected on YPDS plates with increasing concentration of Zeocin™: clones which are able to grow on the highest concentration of Zeocin™ plate (2000 µg/ml), are putative multi-copy recombinants (Figure 4.11).

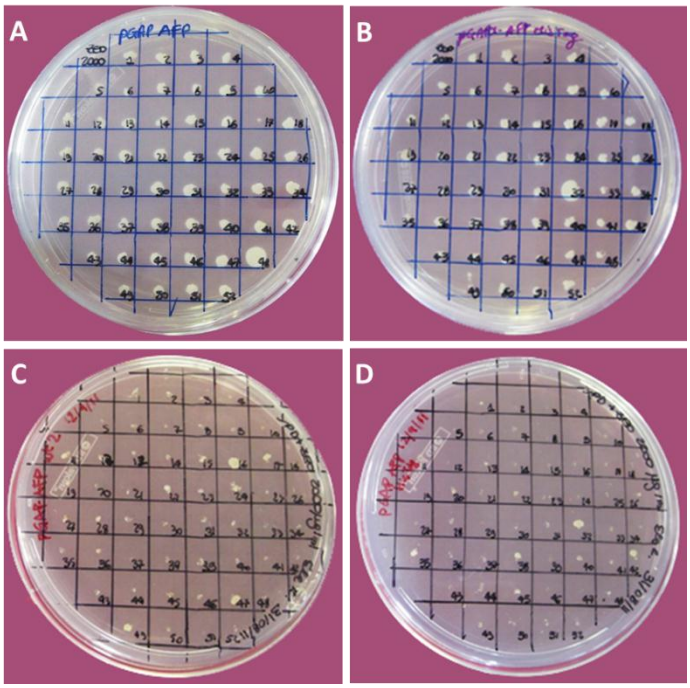

Figure 4.11 - Isolation of multi-copy recombinants in YPDS plates containing 2000 µg/ml Zeocin™; *P. pastoris* X33 strain transformed with: A) pGAPZαA-ISP, B) pGAPZαA-ISPht, C) pGAPZA-ISP cutα and D) pGAPZA-ISPht cutα

From this step we selected the recombinant clones for the successive small scale expression tests.

4.2.3. Expression in shake flask cultures

4.2.3.1. α-factor mediated ISP and ISPht secretion

Single selected colonies from each transformation were screened for their ability to produce wheat ISP in order to identify the most effective in terms of expressed protein. These 10 ml cultures were incubated at 30 °C for 3 days shaking at 230 rpm. The supernatant was obtained by centrifugation after 24, 48 and 72 hours and use to analyze the protein expression by SDS-PAGE electrophoresis.

All the 52 clones transformed with the pGAPZαA-ISP plasmid were tested for the ISP expression: 2 bands corresponding to an apparent molecular weight of about 47 kDa and 33 kDa were observed respectively after 24 hours and 48 hours of culture (Figure 4.12).

The same result was observed for the expression experiments performed with 5 clones transformed with the pGAPZαA-ISPht expression vector (Figure 4.12).

To verify if one of the two bands could represent the ISP, or if they correspond to some *P. pastoris* products, we performed an expression experiment with a clone transformed with the empty pGAPZαA vector. As shown in Figure 4.12 the 47 kDa and 33 kDa bands appeared also in the negative control (NC) test; therefore, they weren't representative of the wheat ISP expression.

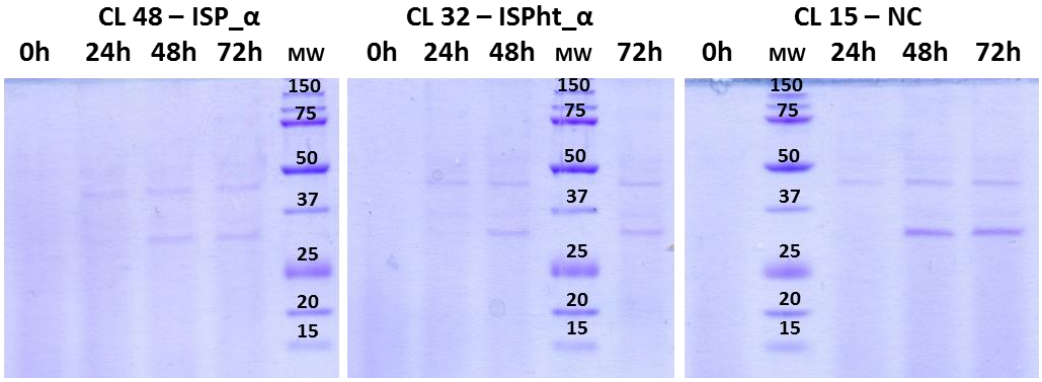

Figure 4.12 - SDS-PAGE of small scale what ISP expression after 0, 24, 48 and 72 hours of culture at 30 °C; expression experiments performed with yeast transformed with pGAPZαA-ISP (CL 48 – ISP_α), pGAPZαA-ISPht (CL 32 – ISPht_α) and empty vector (CL 15 – NC); MW=molecular weight

The expression of the ISP with the α-factor secretion signal (ISP_α) was also tested in 10 ml culture volume at 30 °C for 7 days shaking at 230 rpm, and compared to the NC in the same conditions (Figure 4.13).

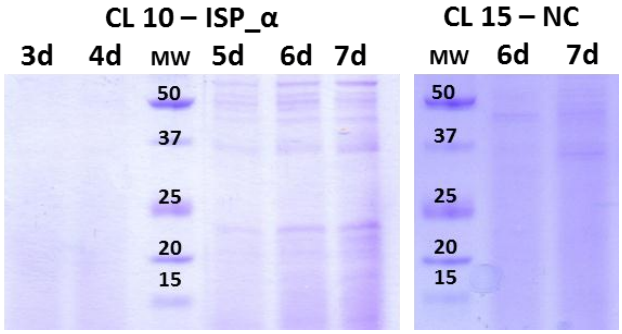

Figure 4.13 - SDS-PAGE of small scale what ISP_α expression after 3, 4, 5, 6 and 7 days of culture at 30 °C compared to the NC (negative control) at 6 and 7 days in the same culture conditions; MW= molecular weight

As represented in Figure 4.13 a band corresponding to an apparent molecular weight of about 23 kDa was observed after 5 days of culture and became more pronounced after 7 days. The observed molecular weight of 23.5 kDa is comparable with the expected one of 23.6 kDa. Unfortunately, we could notice the presence of high-level contaminants in the supernatant that represent a problem for the successive purification protocol.

Li and coworkers (Li *et al*., 2001) shown that *P. pastoris* expressed an herring ice structuring protein at higher level at low temperature (23 °C) than at 30 °C. Therefore, we expressed the wheat ISP_α in 10 ml culture volume at 18 °C for 3 days shaking at 230 rpm; we compared the results at 18°C with that obtained in the NC in the same culture conditions and with the 7 days sample obtained at 30°C (Figure 4.14).

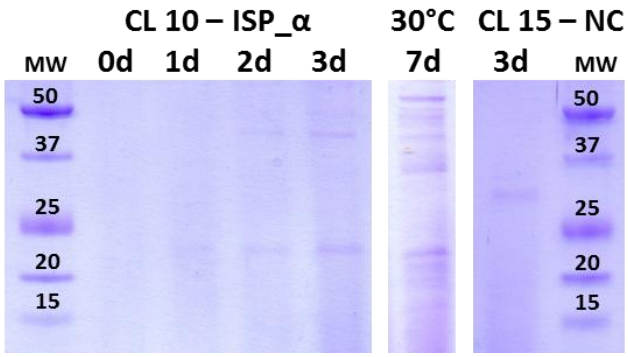

Figure 4.14 - SDS-PAGE of small scale what ISP_α expression after 0, 1, 2 and 3 days of culture at 18°C compared to the NC (negative control) at 3 days in the same culture conditions and to the ISP_α expression after 7 days of culture at 30 °C; MW= molecular weight

In the SDS-PAGE analysis shown in Figure 4.14 we could notice after 2 days of culture the presence of a band at an apparent molecular weight of about 23 kDa corresponding to the one observed after 7 days at 30 °C. Moreover, the presence of lower contaminants in the supernatant would facilitate the successive purification protocol.

4.2.3.2. Native signal sequence mediated ISP and ISPht secretion

As for the α factor ISP mediated secretion, the ISP_cutα and ISPht_cutα were expressed in 10 ml culture volume at 30 °C and 230 rpm for 3 and 7 days.

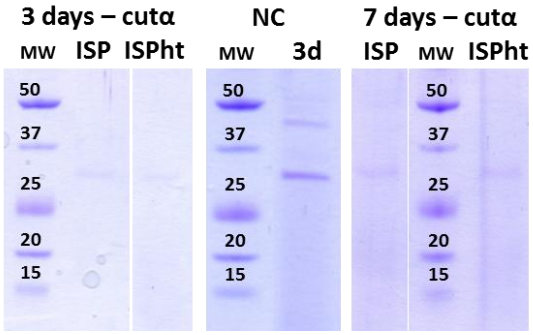

Figure 4.15 - SDS-PAGE of small scale wheat ISP_cutα and ISPht_cutα expression after 3 and 7 days of culture at 30 °C compared to the NC (negative control) at 3 days in the same culture conditions; MW= molecular weight

As reported in Figure 4.15 there was no detectable ISP expression in all the tested condition.

Also for the ISP_cutα expression at 18 °C for 3 days we couldn't detect any band corresponding to the protein of interest (Figure 4.16).

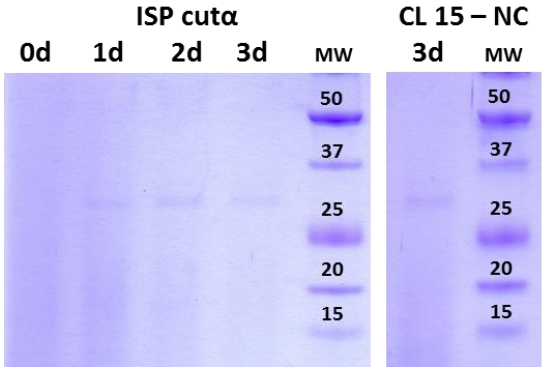

Figure 4.16 - SDS-PAGE of small scale wheat ISP_cutα expression after 0, 1, 2 and 3 days of culture at 18°C compared to the NC (negative control) at 3 days in the same culture conditions; MW=molecular weight

4.3. Wheat ISP allergenic potential

4.3.1. Sequence analysis

To assess the wheat ISP potential allergenicity we analyzed its primary amino acid sequence to determine if there is a sequence homology with known allergens. This step represents the start point of the FAO/WHO Decision Tree for the assessment of the likelihood that a novel protein is or not likely to be allergenic.

In the FAO/WHO report (2001) is indicated that cross-reactivity between the query protein and a known allergen has to be considered if there is 1) more than 35 % identity in the amino acid sequence of the expressed protein, using a window of 80 amino acids and a suitable gap penalty, or 2) identity of at least 6 contiguous amino acids.

Therefore, the amino acid sequence of the ISP was compared *in silico* with the sequence of known allergens using the Allergenicity Prediction Tool available at the ADFS (Allergen Database for Food Safety) web site (http://allergen.nihs.go.jp/ADFS/index.jsp). This tool allows for the analysis of the potential allergenicity of the query protein according to the two above mentioned FAO/WHO criteria.

The search for sequence similarity in agreement with the first criteria produced 13 hits corresponding to allergens from 5 different plant sources (kiwifruit, juniper, cypress, cherry and apple) (Table 4.2).

Match description (from Swissprot)	Match source	Identity (%)
RecName: Full=Thaumatin-like protein; AltName: Allergen=Act d 2; Flags: Precursor	Kiwifruit	57.5
SubName: Full=PR5 allergen Jun r 3.2	Juniper	57.3
SubName: Full=PR5 allergen Jun r 3.1	Juniper	57.3
RecName: Full=Pathogenesis-related protein; AltName: Full=Pollen allergen Jun a 3; AltName: Allergen=Jun a 3; Flags: Precursor	Juniper	54.5
SubName: Full=PR5 allergen Cup s 3.2;	Cypress	56.3
SubName: Full=PR5 allergen Cup s 3.1; SubName: Full=PR5 allergen Cup s 3.3	Cypress	55.8
SubName: Full=Cup a 3 protein; Flags: Fragment	Cypress	55.8
SubName: Full=Thaumatin-like protein	Cypress	53.4
RecName: Full=Pathogenesis-related protein; AltName: Full=Putative major pollen allergen Jun v 3; AltName: Allergen=Jun v 3; Flags: Precursor; Fragment	Juniper	62.5
RecName: Full=Glucan endo-1,3-beta-glucosidase; EC=3.2.1.39; AltName: Full=(1->3)-beta-glucanendohydrolase; Short=(1->3)-beta-glucanase; AltName: Full=Beta-1,3-endoglucanase	Cherry	42.4
RecName: Full=Thaumatin-like protein 1a; AltName: Full=Mdtl1; AltName: Full=Pathogenesis-related protein 5a; Short=PR-5a; AltName: Allergen=Mal d 2; Flags: Precursor	Apple	40.9
SubName: Full=Thaumatin-like protein; Flags: Precursor	Apple	40.5
SubName: Full=Thaumatin-like protein; Flags: Precursor	Apple	40.1

Table 4.2 – Sequence matches showing more than 35% amino acid sequence similaritywith the wheat ISP

The identity search for contiguous of 6 amino acids produced 12 hits (Table 4.3): ten hits are redundant with results shown in Table 4.2, while two correspond to allergens from different sources (pea and acari).

Match description (from UniProt)	Match source	N° of exact word matches
SubName: Full=Thaumatin-like protein	Cypress	2
SubName: Full=Vicilin; Flags: Fragment	*Pea*	*1*
RecName: Full=Glucan endo-1,3-beta-glucosidase; EC=3.2.1.39; AltName: Full=(1->3)-beta-glucanendohydrolase; Short=(1->3)-beta-glucanase; AltName: Full=Beta-1,3-endoglucanase; AltName: Full=Thaumatin-likeprotein; Short=TLP; AltName: Full=AllergenPru a 2; AltName: Allergen=Pruav 2; Flags: Precursor	Cherry	2
RecName: Full=Pathogenesis-related protein; AltName: Full=Pollen allergen Jun a 3; AltName: Allergen=Jun a 3; Flags: Precursor	Juniper	4
RecName: Full=Thaumatin-like protein; AltName: Allergen=Act d 2; Flags: Precursor	Kiwifruit	3
SubName: Full=Group 2 allergen Sui m 2	*Acari*	*1*
SubName: Full=PR5 allergen Cup s 3.1; SubName: Full=PR5 allergen Cup s 3.3	Cypress	3
SubName: Full=PR5 allergen Cup s 3.2	Cypress	3
SubName: Full=PR5 allergen Jun r 3.2	Juniper	4
SubName: Full=PR5 allergen Jun r 3.1	Juniper	4
SubName: Full=Cup a 3 protein; Flags: Fragment	Cypress	3
RecName: Full=Pathogenesis-related protein; AltName: Full=Putative major pollen allergen Jun v 3; AltName: Allergen=Jun v 3; Flags: Precursor; Fragment	Juniper	2

Table 4.3 – Sequence matches with wheat ISP in agreement with the second FAO/WHO criteria

Moreover, using a new methodological approach, Sotkovsky and coworkers (2011) identified 27 wheat proteins showing positive IgE reaction with sera from 22 patients with a suspect history of wheat allergy. Among these 27 IgE-binding proteins they isolated a 23.6 kDa protein (Accession no. Q8S4P7_WHEAT) that shows a 100 % sequence identity with our recombinant ISP protein.

4.4. ISPs activity characterization

In order to study the possible applications of an ISP as ingredient in the food industry or as cryoprotectant in medicine, we set up an experimental approach to evaluate the ice recrystallization inhibition activity and the cryopreservation ability of different ISP sources.

4.4.1. Ice recrystallization inhibition activity: ice crystals dimension analysis

As described in Chapter 1.2.2, ISPs have two related effects on aqueous solutions, thermal hysteresis (TH) and ice recrystallization inhibition (RI). The ability of ISPs to retard ice recrystallization makes ISPs particularly suitable in food industry as natural ice structure modulators for cold storage of frozen products such as ice cream. Indeed, ice crystals size and rate of re-crystallization need to be minimized throughout the whole process of ice cream production from product formulation, storage and distribution conditions. In this context, ISPs hold the great potential to act as re-crystallization control agents, thus providing smoother ice creams and higher quality products compared to the current available products (Regand *et al*., 2006).

4.4.1.1. Recrystallization inhibition activity in water solutions

To investigate the RI activity of different protein sources, ice crystal sizes were analyzed by a cold-stage microscope and image analysis.

The detailed description of the protocol is described in Chapter 2.9.1. In brief, after a temperature cycling protocol, the images depicting the crystal size were collected at -5 °C every 20 minutes (Figure 4.17).

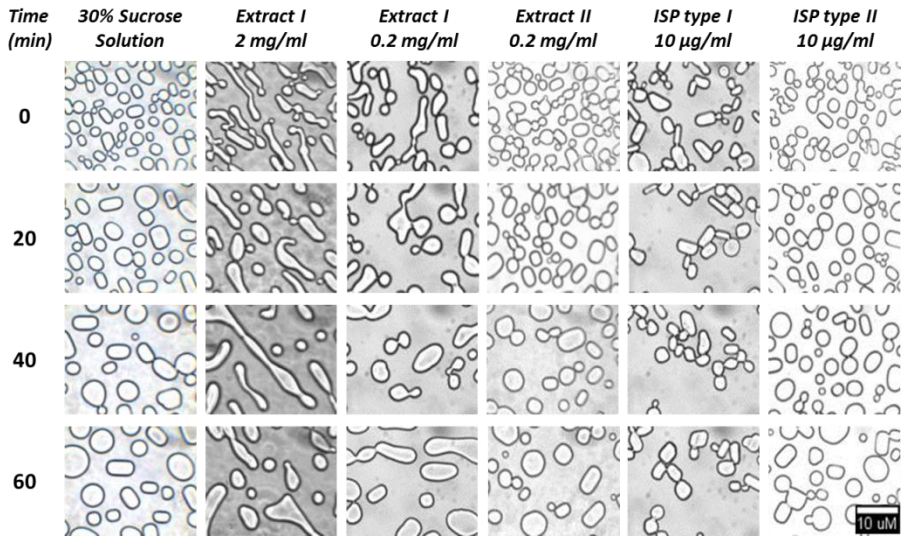

Figure 4.17 – Bright field images acquired every 20 minutes at -5 °C from sucrose 30 %, 2 different batch of wheat extract (I and II), and fish ISP type I and II

The images collected at t=60 min were then analyzed for particles area: frequency count of particles was performed setting a bin size of 100 µm^2 and the results were plotted in a histogram. Gaussian fit was then applied to the data (Figure 4.18) in order to determine the mean particle area. Gaussian fit for all the tested conditions are represented in Figure 4.19, and the relative mean particle area are shown in Figure 4.20 and reported in Table 4.4.

The mean ice crystal diameter in µm for each tested condition was calculated (Table 4.4).

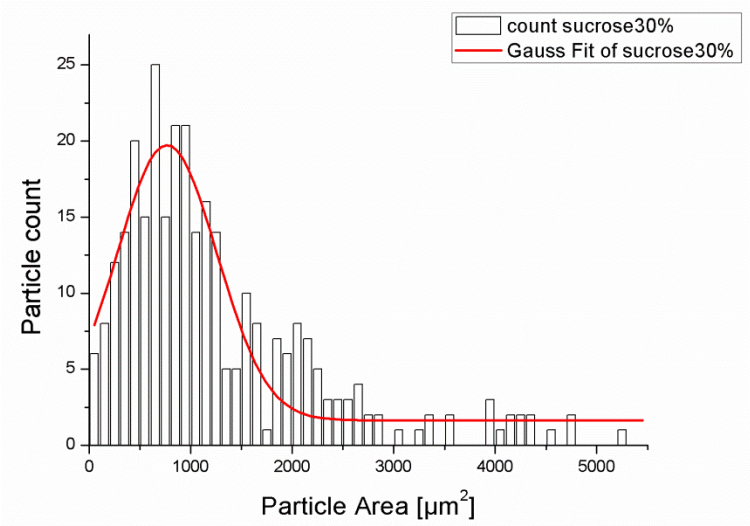

Figure 4.18 – Image analysis for sucrose solution 30 %; 60 min; -5 °C; bin size of the frequency count = 100 µm^2. Gaussian fit applied to the data (in red).

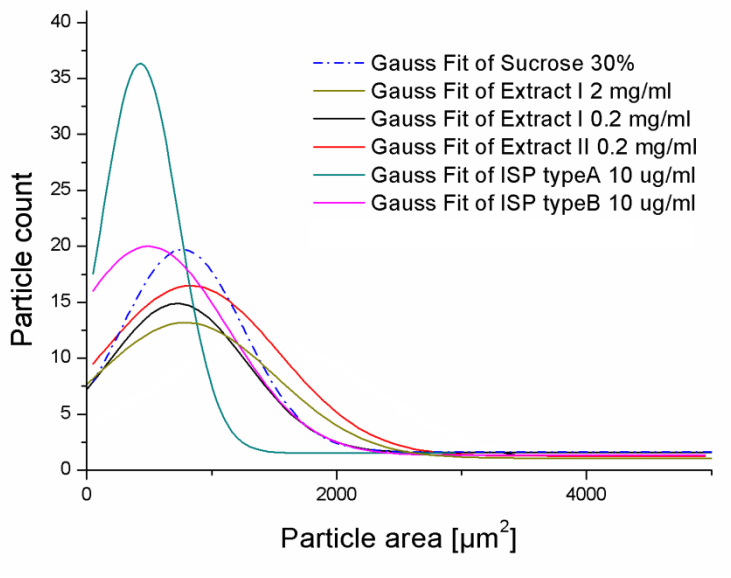

Figure 4.19 – Image analysis (Gaussian fit) relative to all the tested conditions

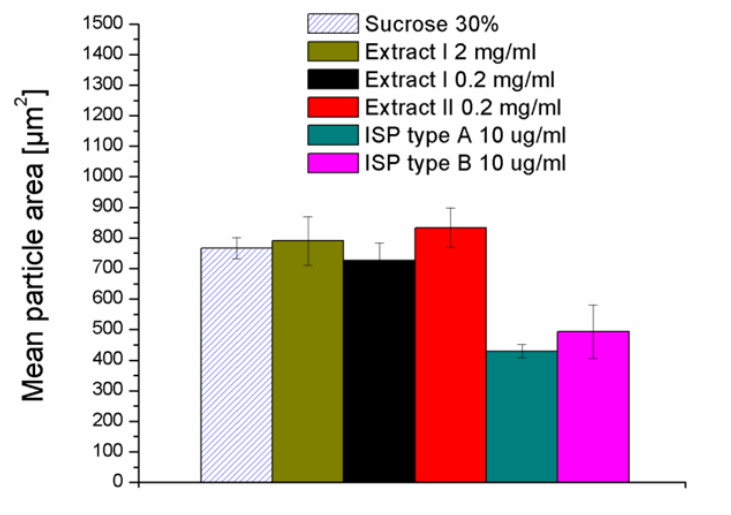

Figure 4.20 – Mean particle area for all the tested conditions

Sample	*Mean area [µm²]*	*Peak width [µm]*	*Mean diameter [µm]*
Sucrose 30%	766 ± 35	982 ± 81	31.23±0.81
Extract I 2mg/ml	791 ± 80	1436 ± 186	31.72±1.81
Extract I 0.2 mg/ml	727 ± 58	1106 ± 126	30.41±1.37
Extract II 0.2 mg/ml	834 ± 64	1414 ± 157	32.58±1.41
ISP type I 10 µg/ml	430 ± 22	609 ± 52	23.39±0.68
ISP type II 10 µg/ml	493 ± 87	1278 ± 186	25.06±2.50

Table 4.4 – Mean particle area, peak width and mean diameter relative to all the tested conditions

Only the addition of fish ISPs type I and II resulted in a significant reduction in ice crystal size. Compared to the control (sucrose 30%), ISP type I-containing sample presents a 44 % reduction of the mean area value, instead of the 36 % shown by the ISP type II-containing sample.

We also considered the peak width at half the peak height to evaluate the ice crystal size distribution. Fish ISP type I sample presents the narrowest peak, index of an homogeneous, small, population of ice crystals. For the fish ISP type II-containing sample we notice a larger peak width than the type I sample. Obviously, the application of the ISPs requires the optimization of both the dimension and the size distribution of the ice crystals, in order to obtain an uniform population of small ice crystals. As a matter of fact, in ice cream a uniform size distribution of small crystals produces smooth texture and enhance storage stability and shelf life of the products (Hagiwara *et al.*, 1996).

In Figure 4.17 we can note the different shape conformation of ice crystals: for samples containing extract I at both concentrations a lengthened conformation was observed instead of the circular one of the other samples. We compare the different ice crystals shape determining the Aspect Ratio (AR) at 60 minutes for the 30 % sucrose solution and for the extract I and II containing samples (Figure 4.21): AR corresponds to the ratio of the longer dimension of a shape to its shorter dimension. As for the dimension, we performed a frequency count of particles AR, setting a bin size of 0.1 and the results were plotted in a

histogram. Gaussian fit was then applied to the data in order to determine the mean AR value (Figure 4.22). An AR value of 1 is representative of a circular shape, while an AR value greater than 1 represents an elliptical shape.

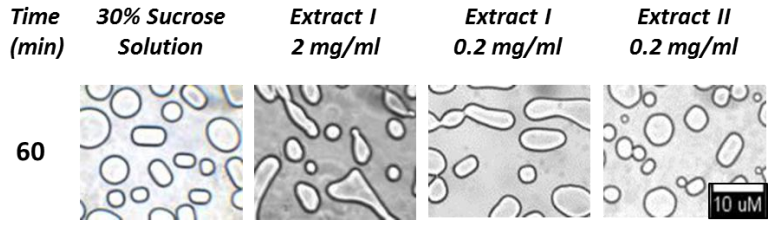

Figure 4.21 – Bright field images acquired at 60 minutes at -5 °C from sucrose 30 % and 2 different batch of wheat extract (I and II)

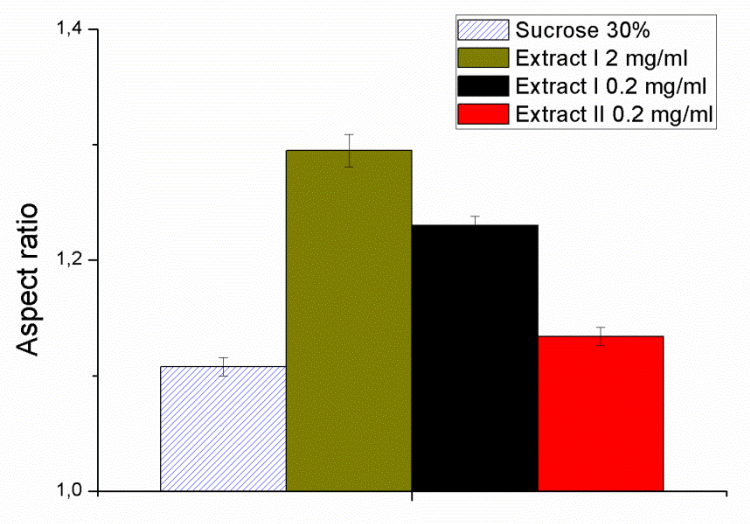

Figure 4.22 – Aspect ratio relative to 30% sucrose solution and to 2 different batch of wheat extract (I and II) containing sample

As represented in Figure 4.21 and Figure 4.22 the addition of extract I to the solution lead to the formation of lengthened ice crystals with an AR value of 1.30±0.01 and 1.23±0.01 for the 2 mg/ml and 0.2 mg/ml concentration respectively. Instead, the 0.2 mg/ml extract II-containing sample shows an AR value (1.13±0.01) similar to the one relative to the 30% sucrose solution (1.11±0.01).

To evaluate the possible effects of the ice crystal shape on the texture and mouthfeel of a product (e.g. ice cream) we plan to prepare samples with the ISP source under consideration and to perform a sensory evaluation experiment.

4.4.1.2. Ice cream analysis

We investigate the ice crystals size in ice cream containing 0% (SE0305) and 0.3% (ICE PRO) of propylene glycol monostearate (PGMS), an ice recrystallization inhibition agents (Danisco A/S). Moreover, the SE0305 sample was subjected to more freezing-thawing cycles than the ICE PRO one, causing an increase in the ice crystals dimensions. The details of the image analysis protocol is described in Chapter 2.9.1. In brief, an ice cream sample was placed on a standard glass microscope slide. A cover slip was pressed on top of the ice cream in order to generate a sample layer thin enough to enhance separation of ice crystals (at about -15 °C); the microscope slide was then placed in the cold stage (Linkam Scientific Instrument) which was previously programmed to maintain a constant temperature of -17 °C. Several different fields on the slides were photographed at -17 °C to obtain a total of 300 ice crystals (Figure 4.23).

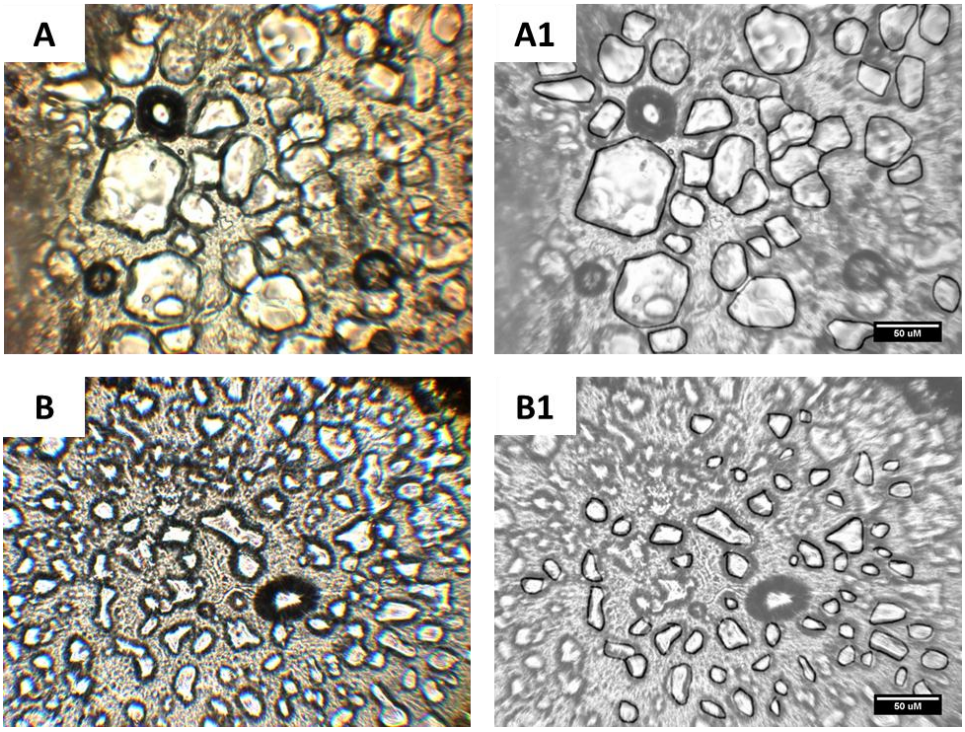

Figure 4.23 - Bright field images acquired at -17 °C from SE0305 (A) and ICE PRO (B) ice cream samples. A1 and B1 pictures represent the image processing made by manually tracing the perimeter of each crystal with a computer graphic tablet

As for the water solution samples, images were analyzed for particles area: frequency count of particles was performed setting a bin size of 100 μm^2 and the results were plotted in a histogram. The mean

particle area was determined applying a Gaussian fit to the data and shown in Figure 4.24 and reported in Table 4.5.

The mean ice crystal diameter in µm for each tested condition was calculated (Table 4.5).

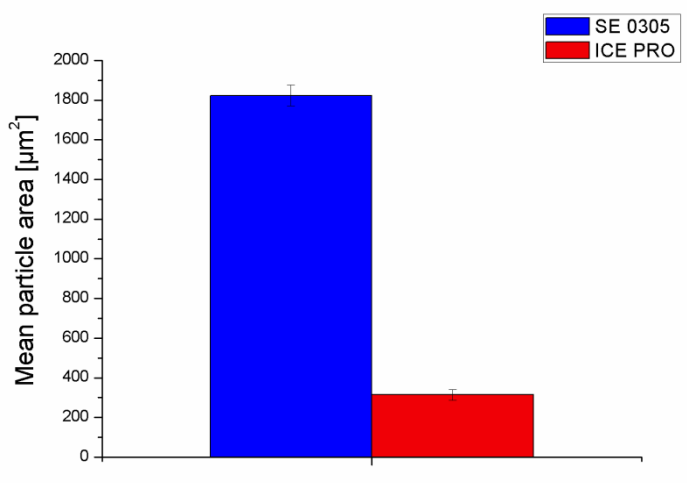

Figure 4.24 - Mean particle area for SE0305 and ICE PRO ice cream samples

Sample	*Mean area [µm²]*	*Peak width [µm]*	*Mean diameter [µm]*
SE0305	1823 ± 53	2035 ± 117	48.18 ± 0.79
ICE PRO	325 ± 27	534± 63	20.01 ± 0.94

Table 4.5 - Mean particle area, peak width and mean diameter relative to SE0305 and ICE PRO ice cream sample

Compared to the SE0305, ICE PRO sample presents a 82 % reduction of the mean area value. Ice crystals in the ICE PRO sample has a mean diameter value of 20.01 µm, bestowing a smooth texture to the ice cream. Instead, SE0305 ice crystals has a mean diameter value of 48.18 µm which produce a coarse, grainy and icy texture (Hagiwara *et al.* 1996).

Moreover, the two samples present a different peak width at half the peak height: with a value of 2035 µm the SE0305 sample has a larger peak width compared to the ICE PRO one (534 µm), index of an heterogeneous ice crystals population.

4.5. Cells hypothermic preservation

It is well known that cryopreservation or low-temperature storage of cells, tissues, and organs are fundamental for their long-term storage. However, the different cold-preservation techniques developed as yet, often cause cell injury which lead to morphological and biochemical alteration raising to cells death.

As reported in previous studies (see 1.2.5.2) ice structuring proteins are potential cryoprotectant.

We evaluated the preservation ability of two different ISP sources (wheat extract and TypeI ISP form fish), compared with that of BSA (Bovine Serum Albumin, a known cryoprotective agent), at different time points. HEK293T (cell line originally derived from human embryonic kidney cells) survival was determined with the trypan blue method.

In some preliminary experiments we determined that no one of the tested substances are able to protect cells during cryopreservation at -180 °C.

Therefore, we evaluated their preservation ability at 4 °C; Figure 4.25 shows cells viability after 24, 48 and 72 hours of cold-preservation at 4 °C.

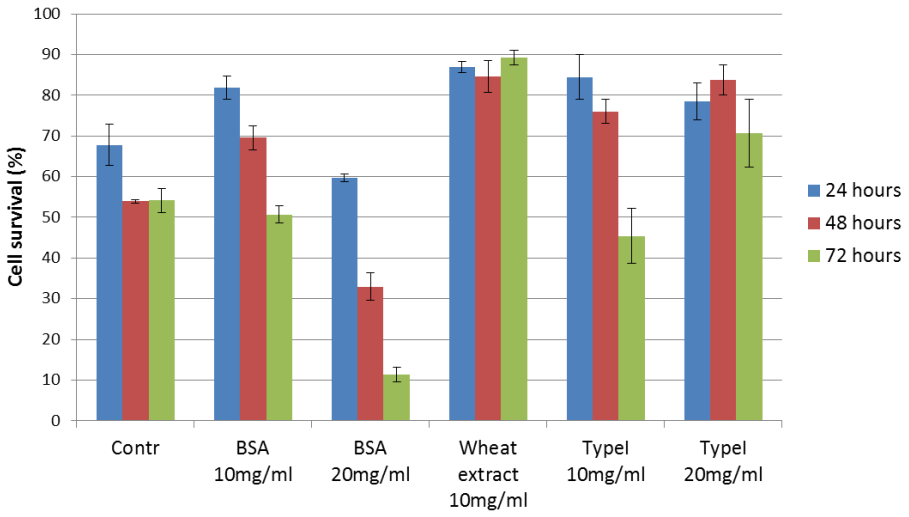

Figure 4.25 – Viability of HEK293T cells cold-preserved at 4 °C for 24, 48 and 72 hours

In the control sample, cells grown in EC solution (Euro Collins preservation solution) without the addition of any protein, the viability decrease from 68 % to about 54 % after 72 hours of incubation at 4 °C.

The viability of cells that were grown in EC solution + BSA 10 mg/ml was 82 % after 24 hours at 4 °C and decrease to 50 % after 72 hours. Instead, very low viability was obtained with 20 mg/ml BSA (only 11 % at 72 hours).

Significant results were obtained with 10 mg/ml of wheat extract: about 89 % of cells was vital even after 72 hours of cold-preservation.

When EC solution + TypeI fish ISP 10 mg/ml or 20 mg/ml were used, the HEK293T viability was about 80 % for the first 48 hours of growth, and decrease to 45 % and 70 %, respectively, after 72 hours.

From these preliminary results we can see that, instead of BSA, the wheat extract and the TypeI ISP exhibit a cells protective activity in the 4 °C preservation process.

Hamel and collaborators (2006) reported that wheat extract from *Triticum aestivum* was an efficient cryopreservation agent, comparable with, but without the toxic effect of, the most used DMSO (Dimethyl Sulfoxide). The wheat extract is composed of various components with a possible protective function: sugars, antioxidants and proteins such as ISPs. Therefore, further studies will be performed to better evaluate this feature, in order to determine what is/are the compound/s present in the extract responsible for the protective effect.

Chapter 5

DISCUSSION

Agribusiness, one of the most important field of bioindustries, refers to the various business involved in food production, including farming, seed supply, food processing, distribution, marketing and sales.

In the modern food production, food biotechnology has the great potential to bring about technological innovation by improving the production, conservation, nutritional and physical characteristics, safety, and taste of foods.

My research project was focused on the design, production and characterization of recombinant proteins to improve food quality. In particular, my work concerns two different aspects of food quality: the first one refers to the production of food suitable for people with specific diseases (e.g. obesity, caries and diabetes) without altering the pleasure of the sweet taste sensation; the second one concerns the improvement of the shelf life and of the physical characteristics (e.g. texture and palatability) of frozen food, especially ice cream.

To address the first question, we developed an efficient method to express and purify the non-calorigenic sweet protein brazzein in the GRAS (Generally Recognize As Safe) yeast *Pichia pastoris*; several techniques were applied in order to characterize the produced protein: HPLC and mass spectrometry analysis were performed to evaluate respectively the purity and the mass/post-translational modifications present in the final product; the thermal stability of the protein was investigated by calorimetry and NMR analysis; NMR experiments were also performed to confirm the structural similarity of the recombinant brazzein with the wild-type brazzein extracted from the natural plant; the sweetness potency of the produced recombinant protein was determined by a taste panel assay for sweet taste control; finally, preliminary allergenicity studies were performed in order to evaluate the allergenic potential of the protein before its possible introduction in the market.

With regard to the improvement of the shelf-life and of the physical properties of frozen food we are interested on the inhibition of ice recrystallization by plant Ice Structuring Proteins (ISPs). In particular, we focused our attention on a wheat ISP. To perform preliminary studies we initially expressed this protein in *Escherichia coli*; then, we moved to the *P. pastoris* expression system in order to obtain high levels of soluble recombinant ISP for its possible application in the food industry. Finally, with the aim to examine the possible applications of an ISP as ingredient in the food industry or as cryoprotectant in medicine (another scope for ISPs application), we developed an experimental approach to evaluate the ice recrystallization inhibition activity and the cryopreservation ability of different ISP sources (wheat extract, and type I and II fish ISPs).

5.1. Brazzein

Lifestyle-related diseases such as obesity, diabetes, cardiovascular disease, and caries have reached epidemic proportions not only in high-income countries, but also in low- and middle-income ones.

The thrifty gene hypothesis proposed by the geneticist James V. Neel (see 1.1.1) gives an explanation of the possible mechanism responsible for the epidemic increase of obesity and related diseases. This hypothesis attributes to the inheritance of traits, that allowed to our ancestors to maximize absorption of ingested calories, the risk to grow obese in the contemporary industrial civilization. These genes conferred survival advantage in ancient times characterized by seasonal availability of food.

However, it is important to bear in mind that overweight, obesity and related diseases are correlated with an excessive intake of sucrose and high calorie foods. Therefore, there is an intense and ongoing search for alternative low-calorie sweeteners that can be used in foods, beverages, and medicines.

We normally associate sweetness with carbohydrate sweeteners (in particular sucrose), but sweetness is a taste imparted by many structurally different compounds that can be perceived as sweet: sugars, amino acids, peptides, proteins and synthetic sweeteners. Among natural compounds, sweet-tasting proteins show a great potential as sugar substitutes: they contain no carbohydrates and they are several hundred or thousand times sweeter than sucrose on a weight basis; in other words, they provide no calories and a small quantity of them is sufficient to impart a sweet taste. Moreover, they don’t present particular concerns from a toxicological point of view since they come from edible plants and fruits that have a long history of human consumption.

Thanks to its high thermal and pH stability, and to its sweet taste that is very similar to sucrose, brazzein is the most promising sweet protein isolated until now. Since the large scale production of brazzein from its natural source (the fruit of the West African plant *Pentadiplandra brazzeana* Bailon) is not feasible, several research groups have tried to produce it taking advantage of recombinant DNA technology. Brazzein has been already produced using different synthetic and expression systems. However, while some of them (chemical synthesis, *Escherichia coli*, *Lactococcus lactis*) didn’t yielded a sufficient quantity of protein for an industrial application, others are not considered safe for the production of protein for human consumption because of their ability to cause illness in humans (*Escherichia coli*), or because of the environmental and health risks associated with the creation of a transgenic organism (*Zea mays* seed).

Therefore, the first objective of this research line was to develop an high yield method for brazzein expression in the GRAS yeast *P. Pastoris*.

P. pastoris is a methylotrophic yeast that can be genetically engineered to express proteins for both basic research and industrial use. We choose *P. pastoris* for four important reasons: I) it can be easily manipulated at a molecular genetic level; II) it can express proteins at high levels, intracellularly or extracellularly; III) it possesses the ability to perform post-translational protein modifications similar to those found in higher eukaryotic organisms (e.g. glycosylation, disulfide-bond formation, and proteolytic processing); IV) it can be considered safe as a source of food ingredients since it has the GRAS status.

P. pastoris can express recombinant proteins either via inducible (with the use of the highly toxic solvent methanol) or constitutive (using glycerol or glucose as the sole carbon source) method.

The first choice for the expression of a new protein in *P. pastoris* is the inducible system, because it allows for the expression of protein toxic to the host. On the other hand, the constitutive expression system is obviously preferred for an industrial application because it prevents problems due to the toxicity, the hazard and cost associated with methanol storage and delivery. The constitutive system is also preferred because, at variance with methanol induction phase, does not require an accurate optimization of the culture conditions. Moreover, it allows for continuous production of the recombinant product, making this system more suitable for large scale production of heterologous recombinant proteins.

We successfully cloned a synthetic codon-optimized DNA fragment coding for brazzein in the inducible expression plasmid pPICZαA vector to generate pPICZαA-BRA. The pGAPZαA-BRA expression plasmid containing the pGAP strong constitutive promoter was instead obtained by modifying the pPICZαA-BRA vector. We also obtained the constitutive expression vector for the production of brazzein without its first amino acid, pGAPZαA-BRAΔ1M; the sweetness of this 53-amino acids form of brazzein is reported to be double that of the 54-wild type amino acids form (Assadi-Porter *et al.*, 2000). Both inducible and constitutive expression plasmids were transformed into the host cell yeast *P. pastoris* by electroporation. Single selected colonies were then screened in order to identify the best clone in terms of high-level expression; the most performing one was then exploited to produce brazzein in 1.5 liter fermentation volume.

The two different expression methods were optimized and in both cases a 1.5 liter fermentation yielded about 200 mg of brazzein.

A simply and low cost purification method was developed: with the cation CM-Sepharose FF resin at pH 4, only brazzein and few other contaminants bind to the resin; therefore, it is possible to elute brazzein separately from the other proteins, by increasing the salts concentration. A chromatographic baseline separation of the two collected fractions (the first one corresponding to contaminants, while the second one corresponding to brazzein) was achieved. Finally, a step of diafiltration was performed in order to washed out the NaCl from the final brazzein preparation. At the end of the purification protocol the concentrated brazzein solution can be stored as a solution after sterilization by membrane filtration (0.22 µm filter), or as a lyophilized powder directly freeze drying the purified protein.

On the contrary, with the anion exchange DEAE-Sepharose FF resin only the contaminants present in the medium bind to the resin, allowing pure brazzein recovery in the column flow through after sample loading. Compared with the cationic exchange process, the anionic one allows for brazzein recovery without using high concentration of salts. However, in order to lower the conductivity, and so to allow the binding of the proteins to the resin, the starting sample (i.e. supernatant of the culture) has to be diluted about two folds in the anionic process (10 folds dilution) than in the cationic one (4.6 folds). Therefore, the anionic process is more time consuming and more difficult to manage because of the limitations posed by the handling of a large volume of sample. Moreover, the protein elutes as flow through in a large volume and requires further concentration steps.

In conclusion, in our view, while anionic chromatography is a viable alternative for purification of small batch size, the cationic exchange process represents the best method for processing a large batch of culture supernatant in both the laboratory and industry. It is also important to underline that this purification protocol doesn’t foresee costly or harsh chemical steps and so it is suitable for the food industry.

The final yield of the expression and purification process was determined and the purity of the expressed protein was assessed by HPLC. As reported above, for both the inducible and the constitutive expression system, a 1.5 liter fermentation yielded about 100 mg of brazzein per liter of initial fermentation volume. HPLC runs showed that the purified brazzein is eluted as a single peak; the protein purity, assessed monitoring the absorbance profile at 280 nm, was estimated to be about 99.98 %. The high degree of purity achieved, is suitable for the use of brazzein as sweetener in the food industry.

The HPLC brazzein peak was then subjected to mass spectrometry analysis which provided a molecular weight close to the expected value, both for

the 53 and 54 brazzein amino acids forms. This means that the produced protein corresponds to brazzein and that it isn't degraded by proteases in the supernatant. Moreover, this result underline that recombinant brazzein presents as post-translational modification only the four disulfide bonds of its own structure, and doesn't present other modification such as glycosylation that would be a problem in terms of allergenicity for human consumption.

We also analyzed the brazzein heat stability by calorimetry and NMR analysis. The stability at high temperatures is a physical property of the recombinant protein fundamental for its application within food industry where high temperature treatments (e.g. pasteurization) are routinely used to inhibit microbial proliferation. Moreover, as sweetening agent, brazzein would be added for example to hot beverage (e.g. tea and coffee) and baked goods. In this latter context, brazzein shown a great potential because to date when too much sugar (more than 10 % by weight) is added to the dough it fails to leaven since it absorbs water causing the dehydration of yeast cells (Vaclavik *et al.*, 2007).

Differential Scanning Calorimetric (DSC) analysis shown us that brazzein denatures at 65.8 °C; however, we verified that the unfolding process is reversible upon cooling, thanks to the presence of the four disulfide bonds typical of brazzein structure. Through NMR analysis we confirmed the high thermostability of brazzein: it maintains the correct folding (and therefore its sweet taste) even after 2 hours incubation at boiling point; in other words, its sweetening power is not reduced by heating cycles. Importance of disulfide bonds for protein thermal stability was also reported for other sweet tasting proteins (e.g. mabinlin, Li *et al.*, 2008; thaumatin, Kim *et al.*, 1988) and for a variety of heat-resistant proteins (Wetzel *et al.*, 1988; Betz, 1993; Tigerström, 2005; Sakaguchi *et al.*, 2008; Jorda *et al.*, 2011).

In addition, NMR analysis allowed us to confirm the structural similarity of the recombinant brazzein with the wild-type brazzein extracted from the pulp of the fruit. This is an important result for two reasons: our recombinant brazzein has the same functional-structural form of the wild-type one, i.e., a form providing sweet taste and that doesn't cause allergic reaction in local consumers.

The sweet potency (number of times a brazzein solution is sweeter than a weight equivalent sucrose solution) of the produced recombinant protein was determined by a taste panel assay. In agreement with literature data (Ming *et al.*, 1994), brazzein sweet potency ranges from 920 folds (in comparison with a 16% sucrose solution) to about 1500 folds (when compared to a 1% sucrose solution). So, in agreement with previous studies on other high intensity sweeteners (Cardello *et al.*, 1999), we demonstrated that brazzein exhibited a decrease in sweetness potency as its concentration increased: in particular, we found that

brazzein works most efficiently as sucrose replacer when used to achieve a sucrose equivalence lower than 8 %. This represents an important result for the upcoming formulation/reformulation of recipes containing brazzein as sweetener for food and beverage. Future work will be the evaluation of the sweet potency of the 53-amino acids form; since Yoon and coworkers (2011) reported that this form of brazzein has a sweetness double that of brazzein having a methionine instead of pyroglutamate at its N-terminus, we expect to observe a similar result. Moreover, we will evaluate the brazzein sweetness temporal profile, i.e. its sweetness intensity over time, with particular attention to the appearance time and extinction time of sweetness in the mouth. Many studies shown that the known sweet proteins share not only their intense sweetness, but also a slower rate of sweet taste appearance than sugar, and a lingering aftertaste (Faus, 2000; Pfeiffer *et al.*, 2000). The delay on sweetness onset is mainly due to their lower diffusion coefficient (e.g. $18{,}17 \cdot 10^{-11}$ m^2/sec for brazzein) in comparison to that of sucrose ($60{,}64 \cdot 10^{-11}$ m^2/sec). Instead, it was proposed (Xue *et al.*, 2009) that the lengthened aftertaste may be due to a prolonged protein-receptor bound state caused by the charge complementary between sweet proteins and their taste receptor binding domain: this electrostatic attraction may increase the protein local concentration near the receptor and/or favor orientation of the interaction surfaces. Analysis of salt concentration dependence of protein binding to taste receptor, and so of lingering aftertaste perception, may support the 'electrostatic-hypothesis'. Concerning brazzein, it was reported in literature that its sweet perception is more similar to sucrose than that of the other sweet proteins (Pfeiffer *et al.*, 2000): its taste is purely sweet with no sourness, saltiness or bitterness, and its sweetness grows and dies out at a slightly slower rate than that of sucrose (Hellekant *et al.*, 2005). For these reasons brazzein could be used in combination with other sweeteners to reduce their side aftertaste and complement their sweetness profile. For example, it was reported that brazzein combines well with most high intensity sweeteners such as acesulfame-K and aspartame, providing both quantitative and qualitative synergy[1] (Hellekant *et al.*, 2005).

To conclude, sensory analysis is a fundamental and crucial assay for evaluating consumer sweet taste perception and to study (by mutagenesis experiments) the relationship between sweetness and amino acidic/conformational requirements in a sweet protein. A taste panel assay requires a large amount of protein material. The biotechnological production of brazzein developed in this study may provide a sufficient amount of protein to

[1] Quantitative synergy can be defined as increased potency of a blend of sweeteners compared to that achieved by individual sweeteners. Qualitative synergy means that the taste profile of a blend matches that of sugar more closely than that achieved by a single sweetener.

perform this kind of experiments. These studies may not only be useful to do a step towards a better comprehension of the interaction between sweet proteins and their receptor, but also help in designing new sweeteners molecules.

Finally, we performed some preliminary experiments in order to assess the potential allergenicity of brazzein: first of all we analyzed its amino acidic sequence to identify similarity to known allergens, and then we evaluated the resistance of the protein to pepsin digestion. As reported in previous published data (Lamphear *et al.*, 2005) we confirmed that there was no homology with any type of allergen, both for the 54 and 53-amino acids form of brazzein. However, we identified a short sequence of 6 amino acids in common with two known forms of *Vespa crabro* venom allergen. Nevertheless, a comparison of the full sequence of brazzein with both venom allergen forms showed no significant similarity (3% of query coverage). Therefore, it is possible to state that the primary sequence analysis doesn't indicate health risks related to an allergenic potential of brazzein. In order to totally exclude the possibility of an allergic reaction due to the hypothetical 6-amino acids epitope, we will modify just one of its residues; since the epitope is not in a key region for brazzein sweetness, we could hypothetically change any one of them. However, the correct brazzein structure is fundamental for its sweetness; therefore, we will not modify the cysteine residue and its neighbors amino acids. In conclusion, the best candidate might be the alanine residue in position 18 of the wild type brazzein sequence.

We also verify that brazzein was readily hydrolyzed by pepsin, indicating that there is a low probability that the protein can elicit any allergic reaction. In fact, hydrolyzed ingested proteins are less likely to reach the intestine and therefore less likely to be absorbed and recognized by the immune system, decreasing the likelihood that they could be allergenic. Furthermore, by a bioinformatics analysis we predicted that brazzein would be hydrolyzed by trypsin and chymotrypsin, providing other evidences of the extensive protein degradation in the gastrointestinal tract. It is also important to bear in mind that the indigenous population of West Africa has safely used the natural source of brazzein to sweeten foods for many years, suggesting that brazzein protein does not pose any unusual risk to health (Lamphear *et al.*, 2005).

In conclusion, based on our preliminary allergological data (i.e. no history of allergenicity from human consumption, no similarity with known allergens, and ready hydrolysis by pepsin) we can conclude that brazzein is likely to be safe for human consumption.

5.2. Wheat Ice Structuring Protein

One of the main challenges of the frozen food industry is the control of the ice crystals formation and propagation.

Among frozen foods, the quality of edible ices (i.e. ice cream, including dairy ice cream, fruit ice, ice lollies, sorbets, and frozen desserts) is the most affected by the crystals size and shape, since they are consumed in a frozen state.

The three key structural components of ice cream are air bubble, fat globules, and ice crystals, which are distributed throughout an unfrozen serum phase. The aim of ice cream manufacturing (in particular of formulation, freezing and hardening), is to generate and maintain a large number of small ice crystals (<40 μm), in order to create a creamy and smooth product. One of the main problems concerning this point is the recrystallization of ice caused by temperature fluctuation during transportation, retailing, and home storage, that cause the formation of large ice crystals and the deterioration of the texture and taste experience of ice cream (and in general of frozen foods).

The discovery of the ISPs ability to inhibit the recrystallization of ice, has provided an opportunity to influence the ice crystals growth during manufacture and storage. Therefore, ISPs are proposed as natural recrystallization control agents, thus providing smoother ice creams and higher quality products compared to the current available products. In fact, the use of ISPs in the edible ices manufacture results in several benefits to consumers. First of all, it is possible to improve the nutritional profile and the final 'healthiness' of the products by lowering the quantity of fat and sugars (that are normally added in large amount to obtain a creamy texture), thus providing a low-calorie product. Moreover, by improving the ice cream stability, the use of ISPs allows for the production of an ice cream with an high fruit content; until now, this wasn't possible since an high amount of fruits affects the texture of ice cream, making difficult the formulation process. Also the organoleptic properties will be improved by the addition of ISPs, resulting in a creamy and smooth texture, and in an enhanced flavor delivery; in fact, stability and size of ice crystals influence flavor perception by modifying how the ice cream warms during consumption, and so how taste and aroma components are released. Last but not least, ISPs addition enhances the temperature stability throughout the whole supply chain, making the product less sensitive to temperature fluctuations. On this ground, we would like to underline that by providing a reduced dependence from temperature fluctuations, the use of ISPs is important not only from a quality point of view, but also from an economic one, since higher freezer storage temperature can be used with no effects on ice cream quality.

We decided to work with plant ISPs for several reasons, especially for their greatest ice recrystallization inhibition activity compared to other ISPs (e.g. fish ISPs) (Griffith *et al.*, 2004). This characteristic allows plants ISPs to work at very low concentration (e.g. 10 μg protein/ml for a *Lolium perenne* ISP; Sidebottom *et al.*, 2000), also avoiding problems related to aftertaste perception. Moreover, as reported in 1.2.5, despite the highest knowledge about fish ISPs, the use of proteins from this source presents both ethical (i.e. vegetarian consumers) and market (i.e. people think to eat "fishy" taste products) problems. Among plant ISPs, wheat (*Triticum aestivum*) ISPs present interesting proprieties (see 1.2.4.3). We focused our attention on a promising wheat ISP isolated and characterized by Kontogiorgos and coworkers (2007). They showed that this protein is responsible for the ice recrystallization inhibition activity in wheat extract; moreover, it is stable under pasteurization conditions, which make it a potential candidate as a food ingredient.

To perform preliminary studies we expressed this protein with an N-term His-tag sequence in different strains of *E. coli* (C41, BL21, and Origami2); however, all the tested strains produced a low quantity of the recombinant protein, which precipitated in the pellet during the purification protocol.

Therefore, in order to obtain high levels of soluble recombinant ISP, we moved to the *P. pastoris* expression system. We successfully cloned a synthetic codon-optimized DNA fragment coding for the wheat ISP in place of the brazzein gene in the constitutive expression plasmid pGAPZαA-BRA vector, to generate pGAPZαA-ISP. The latter plasmid was then modified to express the protein with an histidin-tag at the C-terminus (pGAPZαA-ISPht). Both pGAPZαA-ISP and pGAPZαA-ISPht vectors contain the native *S. cerevisiae* α-factor secretion signal, which allows for efficient protein secretion in *P. pastoris*. However, in literature is reported that some proteins have been expressed and secreted by *P. pastoris* using the native signal sequence of the protein itself (e.g. thaumatin; Ide *et al.*, 2007). The wheat ISP sequence analysis suggested that the protein contains a 22-amino acids N-terminal signal peptide that targets the protein to the secretory pathway. Hence, we delete the α-factor secretion signal sequence from the pGAPZαA-ISP and the pGAPZαA-ISPht plasmids in order to obtain the pGAPZA-ISP cutα and the pGAPZA-ISPht cutα ones.

All the expression plasmids were transformed into the yeast *P. pastoris* by electroporation. Single selected colonies were then screened in experiments on a small scale performed at different temperatures in order to evaluate the expression level for each protein form and to determine the best temperature condition. From these experiments we determined that only the wild type protein

with the α-factor was expressed after 5 days at 30 °C or after 2 days at 18 °C. Moreover, at 18 °C the presence of lower contaminants in the supernatant would facilitate the successive purification protocol. As reported by Li and coworkers for a fish ISP (2001), the improved protein expression at 18 °C could be explained by two reasons. Firstly, decreasing the temperatures reduces the rate of protein synthesis, leading to a higher rate of correctly folded proteins (Zhao *et al.*, 2008). The wheat ISP may be subjected to misfolding due to the presence of eight intermolecular disulfide bonds. Therefore, its expression at lower temperature may lead to a reduction of protein misfolding and so, to the production of an higher level of correctly folded protein that is secreted into the culture medium. Besides enhancing the proper folding pathway, it was demonstrated (Li *et al.*, 2001; Wang *et al.*, 2009) that another benefit of lowering expression temperature is the reduction of the proteolytic degradation of the secreted recombinant protein.

The produced wheat ISP has an observed molecular weight of 23.5 kDa, which is closed to the expected one of 23.6 kDa. Future development will be the scale-up of the process, the optimization of a purification protocol, and the characterization of the produced protein. Moreover, we want to express the protein without its native 22-amino acids secretion signal peptide (i.e. only with the α-factor secretion signal), in order to evaluate a possible interference with the *P. pastoris* secretion pathway.

To assess the wheat ISP potential allergenicity we analyzed its primary amino acid sequence and we determined that there was homology with twelve known allergens. Moreover, Sotovsky and coworkers (2011) demonstrate that this wheat ISP shown positive IgE reaction with sera from patients with a suspect history of wheat allergy. All together, these results indicate that the wheat ISP is likely to be allergenic. However, this result doesn't mean that we can not use this protein as food ingredient, but that the use of ISP preparation has to be specified in the food label of any products that were produced using it.

Finally, in order to study the possible applications of an ISP as ingredient in the food industry or as cryoprotectant in medicine (another scope for ISPs application), we set up an experimental approach to evaluate the ice recrystallization inhibition (RI) activity and the cryopreservation ability of different ISP sources.

We investigate the RI activity of different protein sources (wheat extract, and type I and II fish ISPs) in comparison with a sucrose solution by analyzing the ice crystal sizes by a cold-stage microscope and image analysis. From this experiments we found that only the addition of fish ISPs type I and II resulted in a significant reduction of the ice crystal size. Compared to the control (sucrose

30 %), ISP type I-containing sample presents a 44 % reduction of the mean area value, instead of the 36 % shown by the ISP type II-containing sample.

The application of the ISPs requires the optimization not only of the dimension, but also of the size distribution of the ice crystals, in order to obtain a uniform population of small ice crystals. Therefore, we also considered the peak width at half the peak height to evaluate the ice crystals size distribution. Fish ISP type I sample presents the narrowest peak, index of an homogeneous, small, population of ice crystals. For the fish ISP type II-containing sample we notice a larger peak width than the type I sample.

We also analyzed the different shape conformation of ice crystals: for samples containing the wheat extract I at both concentrations a lengthened conformation was observed instead of the circular one of the other samples. To evaluate the possible effects of the ice crystal shape on the texture and mouthfeel of a product (e.g. ice cream), we plan to prepare samples with the ISP source under consideration and to perform a sensory evaluation experiment.

We also investigate the ice crystals size in ice cream containing 0 % (SE0305) and 0.3 % (ICE PRO) of propylene glycol monostearate (PGMS), a known ice recrystallization inhibition agents. As expected, compared to the SE0305, ICE PRO sample presents a 82 % reduction of the mean area value, bestowing a smooth texture to the ice cream.

The set-up of an accurate method to quantify the dimension and size distribution of ice crystals in solution or in ice cream would be useful not only for our research purposes, but also for quality control and product development in the food industry. Moreover, since to date the only way to identify an ISP is by directly assaying its ability to interact with ice inhibiting the recrystallization process (Griffith *et al.*, 2004), this method can also be utilized to discover new promising ISPs.

In literature is reported that ISPs are potential cryoprotectant (see 1.2.5.2). Therefore, these proteins present interesting applications in the medical field where they could be utilized to enhance organs and tissues preservation for transplant or transfusion, or to increase viability of cells destined for cold or frozen storage. Hence, we evaluated the preservation ability of two different ISP sources (wheat extract and TypeI ISP from fish), compared with that of BSA (Bovine Serum Albumin, a known cryoprotective agent), at 4 °C at different time points. Cell survival was determined with the trypan blue method. From our preliminary results we can see that, using BSA as control, the wheat extract (10 mg/ml) and the TypeI ISP (20 mg/ml) exhibit a cells protective activity in the 4°C preservation process. Future research will focus on experimental determination of the compound/s present in the wheat extract responsible for the

protective effect. Moreover, we will evaluate the ISP protective effect also on cells cryopreservation.

Appendix I

Abbreviations

ABA	Abscisic Acid
ADFS	Allergen Database for Food Safety
Aoc and Roo	Active open-close and Resting open-open form of the sweet taste receptor
AR	Aspect Ratio
AWWE	Acclimated Winter Wheat Extract
BMG	Buffered Minimal Glycerol
BMI	Body Mass Index
BMM	Buffered Minimal Methanol
BRA Δ1M	Brazzein without the first amino acid (Met)
BSA	Bovine Serum Albumin
CFU	Colony Forming Units
CHT	Chitinases
CRD	Cysteine-Rich Domain
Des-pGlu1	Brazzein without its first amino acid (Glu)
DMSO	Dimethyl sulfoxide
DNA	Desoxyribonucleic acid
DO	Dissolved Oxygen concentration
DSC	Differential Scanning Calorimetry
DTT	Dithiothreitol
EFSA	European Food Safety Authority
FDA	Food and Drug Administration
GAP	Glyceraldehydes-3-phosphate dehydrogenase promoter
GLU	β-1,3-Glucanases
GMO	Genetically Modified Organism
GPCR	G-Protein Coupled Receptor
GRAS	Generally Recognize As Safe
HEL	Hen Egg white Lysozyme
HPLC	High Performance Liquid Chromatography
hT1R2/hT1R3	human Taste type 1 Receptor 2 or 3
IBS	Ice Binding Site
IP	Isoelectric Point
IPTG	Isopropyl-β-D-thiogalactopyranoside

ISGP	Ice structuring Glycoprotein
ISP	Ice Structuring Protein
LAB	Lactic Acid Bacteria
LB	Luria-Bertani media
MCS	Multiple Cloning Site
NICE	Nisin-Controlled Expression system
NMR	Nuclear Magnetic Resonance
(N)MWCO	(Nominal) Molecular Weight Cut Off
OD	Optical Density
PBS	Phosphate Buffered Saline
PCR	Polymerase Chain Reaction
PGMS	Propylene Glycol Monostearate
PR	Pathogenesis Related protein
RI	Recrystallization Inhibition activity
SA	Salicylic Acid
SCF	Scientific Committee on Food
SDS-PAGE	Sodium Dodecyl Sulphate-Polyacrylamide Gel electrophoresis
SOC	Super Optimal broth with Catabolite repression
SUMO	Small Ubiquitin-related Modifier
TAE	Tris-Acetate EDTA
TH	Thermal Hysteresis
TLP	Thaumatin-Like Protein
TMD	Transmembrane Domain
TP	Total Protein
(U)LMW	(Ultra) Low Molecular Weight
VFTM	Venus Flytrap Module
WPE	Wheat Protein Extract
YNB	Yeast Nitrogen Base
YPD	Yeast Peptone Dextrose media
YPDS	Yeast Peptone Dextrose media additioned with Sorbitol

Bibliography

Brazzein as low-calorie sweetener

Ager, D.J., Pantaleone, D.P., Henderson, S.A., Katritzky, A.R., Prakash, I., and Walters, D.E. (1998). Commercial, Synthetic Nonnutritive Sweeteners. Angewandte Chemie International Edition 37, 1802-1817.

Assadi-Porter, F.M., Maillet, E.L., Radek, J.T., Quijada, J., Markley, J.L., and Max, M. (2010). Key amino acid residues involved in multi-point binding interactions between brazzein, a sweet protein, and the T1R2-T1R3 human sweet receptor. J Mol Biol 398, 584-599.

Assadi-Porter, F.M., Tonelli, M., Maillet, E.L., Markley, J.L., and Max, M. (2010)I. Interactions between the human sweet-sensing T1R2–T1R3 receptor and sweeteners detected by saturation transfer difference NMR spectroscopy. Biochimica et Biophysica Acta (BBA) - Biomembranes 1798, 82-86.

Assadi-Porter, F.M., Patry, S., and Markley, J.L. (2008). Efficient and rapid protein expression and purification of small high disulfide containing sweet protein brazzein in *E. coli*. Protein Expr Purif 58, 263-268.

Assadi-Porter, F.M., Abildgaard, F., Blad, H., Cornilescu, C.C., and Markley, J.L. (2005). Brazzein, a small, sweet protein: effects of mutations on its structure, dynamics and functional properties. Chem Senses 30 Suppl 1, i90-91.

Assadi-Porter, F.M., Abildgaard, F., Blad, H., and Markley, J.L. (2003). Correlation of the sweetness of variants of the protein brazzein with patterns of hydrogen bonds detected by NMR spectroscopy. J Biol Chem 278, 31331-31339.

Assadi-Porter, F.M., Aceti, D.J., Cheng, H., and Markley, J.L. (2000). Efficient production of recombinant brazzein, a small, heat-stable, sweet-tasting protein of plant origin. Arch Biochem Biophys 376, 252-258.

Assadi-Porter, F.M., Aceti, D.J., and Markley, J.L. (2000). Sweetness determinant sites of brazzein, a small, heat-stable, sweet-tasting protein. Arch Biochem Biophys 376, 259-265.

Bellisle, F., and Drewnowski, A. (2007). Intense sweeteners, energy intake and the control of body weight. Eur J Clin Nutr 61, 691-700.

Berlec, A., and Strukelj, B. (2009). Large increase in brazzein expression achieved by changing the plasmid /strain combination of the NICE system in *Lactococcus lactis*. Lett Appl Microbiol 48, 750-755.

Berlec, A., Tompa, G., Slapar, N., Fonovic, U.P., Rogelj, I., and Strukelj, B. (2008). Optimization of fermentation conditions for the expression of sweet-tasting protein brazzein in *Lactococcus lactis*. Lett Appl Microbiol 46, 227-231.

Berlec, A., Jevnikar, Z., Majhenic, A.C., Rogelj, I., and Strukelj, B. (2006). Expression of the sweet-tasting plant protein brazzein in *Escherichia coli* and *Lactococcus lactis*: a path toward sweet lactic acid bacteria. Appl Microbiol Biotechnol 73, 158-165.

Betz, S.F. (1993). Disulfide bonds and the stability of globular proteins. Protein Sci 2, 1551-1558.

Caldwell, J.E., Abildgaard, F., Dzakula, Z., Ming, D., Hellekant, G., and Markley, J.L. (1998). Solution structure of the thermostable sweet-tasting protein brazzein. Nat Struct Biol 5, 427-431.

Caldwell, J.E., Abildgaard, F., Ming, D., Hellekant, G., and Markley, J.L. (1998). Complete 1H and partial 13C resonance assignments at 37 and 22 degrees C for brazzein, an intensely sweet protein. J Biomol NMR 11, 231-232.

Cardello, H., Da Silva, M., and Damasio, M.H. (1999). Measurement of the relative sweetness of stevia extract, aspartame and cyclamate/saccharin blend as compared to sucrose at different concentrations. Plant Food Hum. Nutr. 54, 119-130.

Clauss, K., Luck, E., and von Rymon Lipinski, G.W. (1976). Acetosulfam, a new sweetener. 1. synthesis and properties (author's transl). Zeitschrift fur Lebensmittel-Untersuchung und -Forschung 162, 37-40.

Cloninger, M.R., and Baldwin, R.E. (1970). Aspartylphenylalanine methyl ester: a low-calorie sweetener. Science (New York, NY) 170, 81-82.

deRuyter, P., Kuipers, O.P., and deVos, W.M. (1996). Controlled gene expression systems for *Lactococcus lactis* with the food-grade inducer nisin. Appl. Environ. Microbiol. 62, 3662-3667.

Dounias, E. (2008). *Pentadiplandra brazzeana* Baill. PROTA.

Faus, I. (2000). Recent developments in the characterization and biotechnological production of sweet-tasting proteins. Appl Microbiol Biotechnol 53, 145-151.

FAO/WHO, 2001. Evaluation of Allergenicity of Genetically modified Foods. Report of a Joint FAO/WHO Expert consultation. World Health Organization, Geneva.

Gao, G., Dai, J., Ding, M., Hellekant, G., Wang, J., and Wang, D. (1999). Studies on solution NMR structure of brazzein: Secondary structure and molecular scaffold. Sci China C Life Sci 42, 409-419.

Gao, G.H., Dai, J.X., Ding, M., Hellekant, G., Wang, J.F., and Wang, D.C. (1999). Solution conformation of brazzein by 1H nuclear magnetic resonance: resonance assignment and secondary structure. Int J Biol Macromol 24, 351-359.

Glasel, J.A. (1995). Validity of Nucleic Acid Purities Monitored by A260/A280 Absorbance Ratios. Biotechniques 18, 62-63.

Hellekant, G., and Danilova, V. (2005). Brazzein a small, sweet protein: discovery and physiological overview. Chem Senses 30 Suppl 1, i88-89.

Ibrahim, H.R., Aoki, T., and Pellegrini, A. (2002). Strategies for new antimicrobial proteins and peptides: Lysozyme and aprotinin as model molecules. Curr Pharm Design 8, 671-693.

Ide, N., Sato, E., Ohta, K., Masuda, T., and Kitabatake, N. (2009). Interactions of the Sweet-Tasting Proteins Thaumatin and Lysozyme with the Human Sweet-Taste Receptor. J Agric Food Chem 57, 5884-5890.

Izawa, H., Ota, M., Kohmura, M., and Ariyoshi, Y. (1996). Synthesis and characterization of the sweet protein brazzein. Biopolymers 39, 95-101.

Jenner, M.R., Waite, D., Jackson, G., Williams, J.C. (1982). Process for the preparation of 4,1',6'-trichloro-4,1',6'-trideoxygalactosucrose (United States).

Jin, Z., Danilova, V., Assadi-Porter, F.M., Aceti, D.J., Markley, J.L., and Hellekant, G. (2003). Critical regions for the sweetness of brazzein. FEBS Lett 544, 33-37.

Jin, Z., Danilova, V., Assadi-Porter, F.M., Markley, J.L., and Hellekant, G. (2003)I. Monkey electrophysiological and human psychophysical responses to mutants of the sweet protein brazzein: delineating brazzein sweetness. Chem Senses 28, 491-498.

Jorda, J., and Yeates, T.O. (2011). Widespread Disulfide Bonding in Proteins from Thermophilic Archaea. Archaea, 9.

Kant, R. (2005). Sweet proteins--potential replacement for artificial low calorie sweeteners. Nutrition journal 4, 5.

Kim, S.H., Devos, A., and Ogata, C. (1988). Crystal structures of 2 intensely sweet proteins. Trends BiochemSci 13, 13-15.

Klug, C., Lipinski, G.W.V., and Bottger, D. (1992). Backing stability of acesulfame-K. Z Lebensm-Unters-Forsch 194, 476-478.

Lamphear, B.J., Barker, D.K., Brooks, C.A., Delaney, D.E., Lane, J.R., Beifuss, K., Love, R., Thompson, K., Mayor, J., Clough, R., et al. (2005). Expression of the sweet protein brazzein in maize for production of a new commercial sweetener. Plant Biotechnol J 3, 103-114.

Li, D.F., Jiang, P.H., Zhu, D.Y., Hu, Y.L., Max, M., and Wang, D.C. (2008). Crystal structure of Mabinlin II: A novel structural type of sweet proteins and the main structural basis for its sweetness. J Struct Biol 162, 50-62.

Liu, Y.D., Goetze, A.M., Bass, R.B., and Flynn, G.C. (2011). N-terminal Glutamate to Pyroglutamate Conversion in Vivo for Human IgG2 Antibodies. Journal of Biological Chemistry 286, 11211-11217.

Liu, X.Z., Maeda, S.J., Hu, Z., Aiuchi, T., Nakaya, K., and Kurihara, Y. (1993). Purification, complete amino-acid-sequence and structural characterization of the heat stable sweet protein, Mabinlin-II. Eur J Biochem 211, 281-287.

Maehashi, K., and Udaka, S. (1998). Sweetness of lysozymes. Biosci Biotechnol Biochem 62, 605-606.

Masschalck, B., and Michiels, C.W. (2003). Antimicrobial properties of lysozyme in relation to foodborne vegetative bacteria. Crit Rev Microbiol 29, 191-214.

Masuda, T., and Kitabatake, N. (2006). Developments in biotechnological production of sweet proteins. J. Biosci. Bioeng. 102, 375-389.

Masuda, T., Ueno, Y., and Kitabatake, N. (2005). High yield secretion of the sweet-tasting protein lysozyme from the yeast *Pichia pastoris*. Protein Expr. Purif. 39, 35-42.

Mattes, R.D., and Popkin, B.M. (2009). Nonnutritive sweetener consumption in humans: effects on appetite and food intake and their putative mechanisms. Am J Clin Nutr 89, 1-14.

Mierau, I., and Kleerebezem, M. (2005). 10 years of the nisin-controlled gene expression system (NICE) in *Lactococcus lactis*. Appl. Microbiol. Biotechnol. 68, 705-717.

Ming, D., and Hellekant, G. (1994). Brazzein, a new high-potency thermostable sweet protein from *Pentadiplandra brazzeana* B. FEBS Lett 355, 106-108.

Morini, G., Bassoli, A., and Temussi, P.A. (2005). From small sweeteners to sweet proteins: Anatomy of the binding sites of the human T1R2_T1R3 receptor. J. Med. Chem. 48, 5520-5529.

Morris, J.A., and Cagan, R.H. (1972). Purification of monellin, the sweet principle of *Dioscoreophyllum cumminsii*. Biochimica et biophysica acta 261, 114-122.

Moynihan, P., and Petersen, P.E. (2004). Diet, nutrition and the prevention of dental diseases. Public Health Nutr 7, 201-226.

Muto, T., Tsuchiya, D., Morikawa, K., and Jingami, H. (2007). Structures of the extracellular regions of the group II/III metabotropic glutamate receptors. Proc. Natl. Acad. Sci. U. S. A. 104, 3759-3764.

Nakajima, K., Asakura, T., Maruyama, J., Morita, Y., Oike, H., Shimizu-Ibuka, A., Misaka, T., Sorimache, H., Arai, S., Kitamoto, K., et al. (2006). Extracellular production of neoculin, a sweet-tasting heterodimeric protein with taste-modifying activity, by *Aspergillus oryzae*. Appl. Environ. Microbiol. 72, 3716-3723.

Oberto, J., and Davison, J. (1985). Expression of chicken egg-white lysozyme by *Saccharomyces cerevisiae*. Gene 40, 57-65.

Pfeiffer, J.F., Boulton, R.B., and Noble, A.C. (2000). Modeling the sweetness response using time-intensity data. Food Quality and Preference 11, 129-138.

Pijl, H. (2011). Obesity: evolution of a symptom of affluence. How food has shaped our existence. Neth J Med 69, 159-166.

Poulsen, L.K. (2004). Allergy assessment of foods or ingredients derived from biotechnology, gene-modified organisms, or novel foods. Molecular Nutrition & Food Research 48, 413-423.

Price, J.M., Biava, C.G., Oser, B.L., Vogin, E.E., Steinfeld, J., and Ley, H.L. (1970). Bladder tumors in rats fed cyclohexylamine or high doses of a mixture of cyclamate and saccharin. Science (New York, NY) 167, 1131-1132.

Ranney, R.E., Oppermann, J.A., Muldoon, E., McMahon, F.G. (1976). Comparative metabolism of aspartame in experimental animals and humans. J Toxicol Environ Health 2(2), 441-451.

Sakaguchi, M., Takezawa, M., Nakazawa, R., Nozawa, K., Kusakawa, T., Nagasawa, T., Sugahara, Y., and Kawakita, M. (2008). Role of disulphide bonds

in a thermophilic serine protease aqualysin I from *Thermus aquaticus* YT-1. J Biochem 143, 625-632.

Stein, J. (2002). UW–Madison professor makes a sweet discovery. Wisconsin State Journal.

Stevens, S.S. (1956). The direct estimation of sensory magnitudes-loudness. The American journal of psychology 69, 1-25.

Stone, H., and Oliver, S.M. (1969). Measurement of the Relative Sweetness of Selected Sweeteners and Sweetener Mixtures. Journal of Food Science 34, 215-222.

Suzuki, M., Kurimoto, E., Nirasawa, S., Masuda, Y., Hori, K., Kurihara, Y., Shimba, N., Kawai, M., Suzuki, E.I., and Kato, K. (2004). Recombinant curculin heterodimer, exhibits taste-modifying and sweet-tasting activities. FEBS Lett. 573, 135-138.

Tandel, K.R. (2011). Sugar substitutes: Health controversy over perceived benefits. Journal of pharmacology & pharmacotherapeutics 2, 236-243.

Temussi, P.A. (2011). Determinants of sweetness in proteins: a topological approach. Journal of molecular recognition : JMR 24, 1033-1042.

Temussi, P.A. (2009). Sweet, bitter and umami receptors: a complex relationship. Trends Biochem.Sci. 34, 296-302.

Temussi, P.A. (2006). The history of sweet taste: not exactly a piece of cake. Journal of Molecular Recognition 19, 188-199.

Temussi, P.A. (2006). Natural sweet macromolecules: how sweet proteins work. Cell. Mol. Life Sci. 63, 1876-1888.

Temussi, P.A. (2002). Why are sweet proteins sweet? Interaction of brazzein, monellin and thaumatin with the T1R2-T1R3 receptor. FEBS Lett 526, 1-4.

Theerasilp, S., and Kurihara, Y. (1988). Complete purification and characterization of the taste-modifying protein, Miraculin, from miracle fruit. Journal of Biological Chemistry 263, 11536-11539.

Tigerström, A. (2005). Thermostability of Proteins. Bios 76, 22-27

Vaclavik, V., Vaclavik, V.A., Christian, E.W. (2007). Essentials of food science. In, Springer, ed.

van der Wel, H., and Loeve, K. (1972). Isolation and characterization of thaumatin I and II, the sweet-tasting proteins from Thaumatococcus daniellii Benth. European journal of biochemistry / FEBS 31, 221-225.

Vermunt, S.H.F., Pasman, W.J., Schaafsma, G., and Kardinaal, A.F.M. (2003). Effects of sugar intake on body weight: a review. Obesity Reviews 4, 91-99.

Walters, D.E., and Hellekant, G. (2006). Interactions of the sweet protein brazzein with the sweet taste receptor. J Agric Food Chem 54, 10129-10133.

Wetzel, R., Perry, L.J., Baase, W.A., and Becktel, W.J. (1988). Disulfide bonds and thermal stability in T4 lysozyme. Proc Natl Acad Sci U S A 85, 401-405.

Whitehouse, C.R., Boullata, J., and McCauley, L.A. (2008). The Potential Toxicity of Artificial Sweeteners. Aaohn J 56, 251-259.

Wintjens, R., Tran, M., Mbosso, E., and Huet, J. (2011). Hypothesis/review: The structural basis of sweetness perception of sweet-tasting plant proteins can be deduced from sequence analysis. Plant Sci. 181, 347-354.

World Health Organization, (2011). Global status report on noncommunicable diseases 2010.

Xu, H., Staszewski, L., Tang, H.X., Adler, E., Zoller, M., and Li, X.D. (2004). Different functional roles of T1R subunits in the heterormeric taste receptors. Proc. Natl. Acad. Sci. U. S. A. 101, 14258-14263.

Xue, W.F., Szuepankiewicz, O., Thulin, E., Linse, S., and Carey, J. (2009). Role of protein surface charge in monellin sweetness. BBA-Proteins Proteomics 1794, 410-420.

Yamashita, H., Theerasilp, S., Aiuchi, T., Nakaya, K., Nakamura, Y., and Kurihara, Y. (1990). Purification and complete amino-acid-sequence of a new type of sweet protein with taste-modifying activity, curculin. Journal of Biological Chemistry 265, 15770-15775.

Yan, Y.L., Orcutt, S.J., and Strickler, J.E. (2009). The use of SUMO as a fusion system for protein expression and purification. Chim. Oggi-Chem. Today 27, 42-47.

Yoon, S.Y., Kong, J.N., Jo, D.H., and Kong, K.H. (2011). Residue mutations in the sweetness loops for the sweet-tasting protein brazzein. Food Chem. 129, 1327-1330.

Web site:

- http://www.idf.org/diabetesatlas/
- http://allergen.nihs.go.jp/ADFS/index.jsp
- http://www.expasy.org/tools/peptidecutter

Ice structuring proteins (ISPs)

Aleong, J.M., Frochot, S., and Goff, H.D. (2008). Ice Recrystallization Inhibition in Ice Cream by Propylene Glycol Monostearate. Journal of Food Science 73, E463-E468.

Amir, G., Rubinsky, B., Basheer, S.Y., Horowitz, L., Jonathan, L., Feinberg, M.S., Smolinsky, A.K., and Lavee, J. (2005). Improved viability and reduced apoptosis in sub-zero 21-hour preservation of transplanted rat hearts using anti-freeze proteins. J Heart Lung Transplant 24, 1915-1929.

Antson, A.A., Smith, D.J., Roper, D.I., Lewis, S., Caves, L.S., Verma, C.S., Buckley, S.L., Lillford, P.J., and Hubbard, R.E. (2001). Understanding the mechanism of ice binding by type III antifreeze proteins. J Mol Biol 305, 875-889.

Arav, A., Shehu, D., and Mattioli, M. (1993). Osmotic and cytotoxic study of vitrification of immature bovine oocytes. J Reprod Fertil 99, 353-358.

Atici, O., and Nalbantoglu, B. (2003). Antifreeze proteins in higher plants. Phytochemistry 64, 1187-1196.

Barrett, J. (2001). Thermal hysteresis proteins. Int J Biochem Cell Biol 33, 105-117.

Beck, E.H., Fettig, S., Knake, C., Hartig, K., and Bhattarai, T. (2007). Specific and unspecific responses of plants to cold and drought stress. J Biosci 32, 501-510.

Beirao, J., Zilli, L., Vilella, S., Cabrita, E., Schiavone, R., and HerrÃ¡ez, M.P. (2011). Improving Sperm Cryopreservation with Antifreeze Proteins: Effect on Gilthead Seabream (*Sparus aurata*) Plasma Membrane Lipids. Biology of Reproduction.

Bernard, A., and Fuller, B.J. (1996). Cryopreservation of human oocytes: a review of current problems and perspectives. Human Reproduction Update 2, 193-207.

Bishop, J.G., Dean, A.M., and Mitchell-Olds, T. (2000). Rapid evolution in plant chitinases: molecular targets of selection in plant-pathogen coevolution. Proc Natl Acad Sci U S A 97, 5322-5327.

Bouvet, V., and Ben, R.N. (2003). Antifreeze glycoproteins: structure, conformation, and biological applications. Cell Biochem Biophys 39, 133-144.

Breton, G., Danyluk, J., Ouellet, F., and Sarhan, F. (2000). Biotechnological applications of plant freezing associated proteins. Biotechnol Annu Rev 6, 59-101.

Brockbank, K.G., Campbell, L.H., Greene, E.D., Brockbank, M.C., and Duman, J.G. (2011). Lessons from nature for preservation of mammalian cells, tissues, and organs. In Vitro Cell Dev Biol Anim 47, 210-217.

Carpenter, J.F., and Hansen, T.N. (1992). Antifreeze protein modulates cell survival during cryopreservation: mediation through influence on ice crystal growth. Proc Natl Acad Sci U S A 89, 8953-8957.

Chakravarty, S., and Varadarajan, R. (2000). Elucidation of determinants of protein stability through genome sequence analysis. FEBS Lett 470, 65-69.

Chao, H., Davies, P.L., and Carpenter, J.F. (1996). Effects of antifreeze proteins on red blood cell survival during cryopreservation. J Exp Biol 199, 2071-2076.

Chen, L.R., Huang, W. Y., Luoh Y. S., Wu, M. C. (1995). Cryopreservation of porcine oocytes before and after polar body formation by antifreeze protein type III. J Taiwan Livestock Res 28, 169-179.

Crevel, R.W., Fedyk, J.K., and Spurgeon, M.J. (2002). Antifreeze proteins: characteristics, occurrence and human exposure. Food Chem Toxicol 40, 899-903.

Damodaran, S. (2007). Inhibition of ice crystal growth in ice cream mix by gelatin hydrolysate. J Agric Food Chem 55, 10918-10923.

Davies, P.L., and Hew, C.L. (1990). Biochemistry of fish antifreeze proteins. FASEB J 4, 2460-2468.

Deng, G., Andrews, D.W., and Laursen, R.A. (1997). Amino acid sequence of a new type of antifreeze protein, from the longhorn sculpin *Myoxocephalus octodecimspinosis*. FEBS Letters 402, 17-20.

Deng, G., and Laursen, R.A. (1998). Isolation and characterization of an antifreeze protein from the longhorn sculpin, *Myoxocephalus octodecimspinosis*. Biochimica et Biophysica Acta (BBA) - Protein Structure and Molecular Enzymology 1388, 305-314.

DeVries, A.L., Komatsu, S.K., and Feeney, R.E. (1970). Chemical and physical properties of freezing point-depressing glycoproteins from Antarctic fishes. J Biol Chem 245, 2901-2908.

DeVries, A.L., and Wohlschlag, D.E. (1969). Freezing resistance in some Antarctic fishes. Science 163, 1073-1075.

Donhowe, D.P., Hartel, R.W., and Bradley, R.L. (1991). Determination of Ice Crystal Size Distributions in Frozen Desserts. Journal of dairy science 74, 3334-3344.

Duman, J.G., and de Vries, A.L. (1976). Isolation, characterization, and physical properties of protein antifreezes from the winter flounder, *Pseudopleuronectes americanus*. Comp Biochem Physiol B 54, 375-380.

Duman, J.G., and DeVries, A.L. (1975). The role of macromolecular antifreezes in cold water fishes. Comp Biochem Physiol A Comp Physiol 52, 193-199.

Duman, J.G., Li, N., Verleye, D., Goetz, F.W., Wu, D.W., Andorfer, C.A., Benjamin, T., and Parmelee, D.C. (1998). Molecular characterization and sequencing of antifreeze proteins from larvae of the beetle *Dendroides canadensis*. Journal of Comparative Physiology B: Biochemical, Systemic, and Environmental Physiology 168, 225-232.

Duman, J.G., Wu, D.W., Xu, L., Tursman, D., Olsen, T.M. (1991). Adaptations of Insects to Subzero Temperatures. The Quarterly Review of Biology 66, 387-410

Ewart, K.V., Lin, Q., and Hew, C.L. (1999). Structure, function and evolution of antifreeze proteins. Cell Mol Life Sci 55, 271-283.

FAO/WHO, 2001. Evaluation of Allergenicity of Genetically modified Foods. Report of a Joint FAO/WHO Expert consultation. World Health Organization, Geneva.

Fletcher, G.L., Hew, C.L., and Davies, P.L. (2001). Antifreeze proteins of teleost fishes. Annu Rev Physiol 63, 359-390.

Garnham, C.P., Campbell, R.L., and Davies, P.L. (2011). Anchored clathrate waters bind antifreeze proteins to ice. Proc Natl Acad Sci U S A 108, 7363-7367.

Goff, H.D. (2005). Food at subzero temperatures. In Soft Materials Structure and Dynamics, M.A.G. Dutcher J.R., ed. (New York, Marcel Dekker Inc.), pp. 229-320.

Graether, S.P., Kuiper, M.J., Gagne, S.M., Walker, V.K., Jia, Z., Sykes, B.D., and Davies, P.L. (2000). [beta]-Helix structure and ice-binding properties of a hyperactive antifreeze protein from an insect. Nature 406, 325-328.

Graham, L.A., and Davies, P.L. (2005). Glycine-rich antifreeze proteins from snow fleas. Science 310, 461.

Griffith, M., Ala, P., Yang, D.S., Hon, W.C., and Moffatt, B.A. (1992). Antifreeze protein produced endogenously in winter rye leaves. Plant Physiol 100, 593-596.

Griffith, M., and Ewart, K.V. (1995). Antifreeze proteins and their potential use in frozen foods. Biotechnology Advances 13, 375-402.

Griffith, M., and Yaish, M.W. (2004). Antifreeze proteins in overwintering plants: a tale of two activities. Trends Plant Sci 9, 399-405.

Grondin, M., Hamel, F., Sarhan, F., and Averill-Bates, D.A. (2008). Metabolic activity of cytochrome p450 isoforms in hepatocytes cryopreserved with wheat protein extract. Drug Metab Dispos 36, 2121-2129.

Hagiwara, T., and Hartel, R.W. (1996). Effect of Sweetener, Stabilizer, and Storage Temperature on Ice Recrystallization in Ice Cream. Journal of dairy science 79, 735-744.

Hamel, F., Grondin, M., Denizeau, F., Averill-Bates, D.A., and Sarhan, F. (2006). Wheat extracts as an efficient cryoprotective agent for primary cultures of rat hepatocytes. Biotechnol Bioeng 95, 661-670.

Harding, M.M., Ward, L.G., and Haymet, A.D.J. (1999). Type I 'antifreeze' proteins. European Journal of Biochemistry 264, 653-665.

Hays, L.M., Feeney, R.E., Crowe, L.M., Crowe, J.H., and Oliver, A.E. (1996). Antifreeze glycoproteins inhibit leakage from liposomes during thermotropic phase transitions. Proceedings of the National Academy of Sciences 93, 6835-6840.

Hew, C.L., Ewart, K.V (2002). Fish antifreeze proteins (World Scientific publishing).

Hew, C.L., and Yang, D.S.C. (1992). Protein interaction with ice. European Journal of Biochemistry 203, 33-42.

Hightower, R., Baden, C., Penzes, E., Lund, P., and Dunsmuir, P. (1991). Expression of antifreeze proteins in transgenic plants. Plant Mol Biol 17, 1013-1021.

Hirano, Y., Nishimiya, Y., Matsumoto, S., Matsushita, M., Todo, S., Miura, A., Komatsu, Y., and Tsuda, S. (2008). Hypothermic preservation effect on mammalian cells of type III antifreeze proteins from notched-fin eelpout. Cryobiology 57, 46-51.

Huang, V., Barrier, WA., Leake, LH., Wittinger, SG. (1992). Frozen dessert compositions and products, pp. 426-565.

Ide, N., Masuda, T., and Kitabatake, N. (2007). Effects of pre- and pro-sequence of thaumatin on the secretion by *Pichia pastoris*. Biochem Biophys Res Commun 363, 708-714.

Inglis, S.R., Turner, J.J., and Harding, M.M. (2006). Applications of type I antifreeze proteins: studies with model membranes & cryoprotectant properties. Curr Protein Pept Sci 7, 509-522.

Jia, Z., and Davies, P.L. (2002). Antifreeze proteins: an unusual receptor-ligand interaction. Trends Biochem Sci 27, 101-106.

Jia, Z., DeLuca, C.I., Chao, H., and Davies, P.L. (1996). Structural basis for the binding of a globular antifreeze protein to ice. Nature 384, 285-288.

Jo, J.W., Jee, B.C., Lee, J.R., and Suh, C.S. (2011). Effect of antifreeze protein supplementation in vitrification medium on mouse oocyte developmental competence. Fertil Steril 96, 1239-1245.

Jorov, A., Zhorov, B.S., and Yang, D.S. (2004). Theoretical study of interaction of winter flounder antifreeze protein with ice. Protein Sci 13, 1524-1537.

Julien, J. (1985). Ice cream. Dairy Science and Technology: Principles and Applications. (Quebec, QC, Canada, Laval Univ. Press).

Knight, C.A., Cheng, C.C., and DeVries, A.L. (1991). Adsorption of alpha-helical antifreeze peptides on specific ice crystal surface planes. Biophys J 59, 409-418.

Kontogiorgos, V., Regand, A., Yada, R.Y., and Goff, H.D. (2007). Isolation and characterization of ice structuring proteins from cold-acclimated winter wheat grass extract for recrystallization inhibition in frozen foods. Journal of Food Biochemistry 31, 139-160.

Kristiansen, E., and Zachariassen, K.E. (2005). The mechanism by which fish antifreeze proteins cause thermal hysteresis. Cryobiology 51, 262-280.

Kuwabara, C., Takezawa, D., Shimada, T., Hamada, T., Fujikawa, S., and Arakawa, K. (2002). Abscisic acid- and cold-induced thaumatin-like protein in winter wheat has an antifungal activity against snow mould, Microdochium nivale. Physiol Plant 115, 101-110.

Lee, C.Y., Rubinsky, B., Fletcher, G.L (1992). Hypothermic preservation of whole mammalian liver with antifreeze proteins. Cryo Lett 13, 59-66.

Li, Z.J., Xiong, F., Lin, Q.S., d'Anjou, M., Daugulis, A.J., Yang, D.S.C., and Hew, C.L. (2001). Low-temperature increases the yield of biologically active herring antifreeze protein in *Pichia pastoris*. Protein Expr Purif 21, 438-445.

Madura, J.D., Baran, K., and Wierzbicki, A. (2000). Molecular recognition and binding of thermal hysteresis proteins to ice. J Mol Recognit 13, 101-113.

Mao, Y., and Ba, Y. (2006). Ice-surface adsorption enhanced colligative effect of antifreeze proteins in ice growth inhibition. J Chem Phys 125, 091102.

Miroux, B., and Walker, J.E. (1996). Over-production of proteins in *Escherichia coli*: Mutant hosts that allow synthesis of some membrane proteins and globular proteins at high levels. J Mol Biol 260, 289-298.

Modig, K., Qvist, J., Marshall, C.B., Davies, P.L., and Halle, B. (2010). High water mobility on the ice-binding surface of a hyperactive antifreeze protein. Phys Chem Chem Phys 12, 10189-10197.

Moffatt, B., Ewart, V., and Eastman, A. (2006). Cold comfort: plant antifreeze proteins. Physiologia Plantarum 126, 5-16.

Morris, H.R., Thompson, M.R., Osuga, D.T., Ahmed, A.I., Chan, S.M., Vandenheede, J.R., and Feeney, R.E. (1978). Antifreeze glycoproteins from the blood of an antarctic fish. The structure of the proline-containing glycopeptides. J Biol Chem 253, 5155-5162.

Ng, N.F., and Hew, C.L. (1992). Structure of an antifreeze polypeptide from the sea raven. Disulfide bonds and similarity to lectin-binding proteins. J Biol Chem 267, 16069-16075.

O'Neil, L., Paynter, S.J., Fuller, B.J., Shaw, R.W., and DeVries, A.L. (1998). Vitrification of mature mouse oocytes in a 6 M Me_2SO solution supplemented with antifreeze glycoproteins: the effect of temperature. Cryobiology 37, 59-66.

Panadero, J., Randez-Gil, F., and Prieto, J.A. (2005). Heterologous Expression of Type I Antifreeze Peptide GS-5 in Baker's Yeast Increases Freeze Tolerance and Provides Enhanced Gas Production in Frozen Dough. Journal of Agricultural and Food Chemistry 53, 9966-9970.

Payne, S.R., Sandford, D., Harris, A., and Young, O.A. (1994). The effects of antifreeze proteins on chilled and frozen meat. Meat Science 37, 429-438.

Pentelute, B.L., Gates, Z.P., Tereshko, V., Dashnau, J.L., Vanderkooi, J.M., Kossiakoff, A.A., and Kent, S.B. (2008). X-ray structure of snow flea antifreeze protein determined by racemic crystallization of synthetic protein enantiomers. J Am Chem Soc 130, 9695-9701.

Prathalingam, N.S., Holt, W.V., Revell, S.G., Mirczuk, S., Fleck, R.A., and Watson, P.F. (2006). Impact of antifreeze proteins and antifreeze glycoproteins on bovine sperm during freeze-thaw. Theriogenology 66, 1894-1900.

Raymond, J.A., and DeVries, A.L. (1977). Adsorption inhibition as a mechanism of freezing resistance in polar fishes. Proc Natl Acad Sci U S A 74, 2589-2593.

Regand, A., and Goff, H.D. (2005). Freezing and Ice Recrystallization Properties of Sucrose Solutions Containing Ice Structuring Proteins from Cold-Acclimated Winter Wheat Grass Extract. Journal of Food Science 70, E552-E556.

Regand, A., and Goff, H.D. (2006). Ice recrystallization inhibition in ice cream as affected by ice structuring proteins from winter wheat grass. J Dairy Sci 89, 49-57.

Rubinsky, B., Arav, A., and Devries, A.L. (1992). The cryoprotective effect of antifreeze glycopeptides from antarctic fishes. Cryobiology 29, 69-79.

Scotter, A.J., Marshall, C.B., Graham, L.A., Gilbert, J.A., Garnham, C.P., and Davies, P.L. (2006). The basis for hyperactivity of antifreeze proteins. Cryobiology 53, 229-239.

Sidebottom, C., Buckley, S., Pudney, P., Twigg, S., Jarman, C., Holt, C., Telford, J., McArthur, A., Worrall, D., Hubbard, R., et al. (2000). Heat-stable antifreeze protein from grass. Nature 406, 256.

Smolin, N., and Daggett, V. (2008). Formation of ice-like water structure on the surface of an antifreeze protein. J Phys Chem B 112, 6193-6202.

Sotkovsky, P., Sklenar, J., Halada, P., Cinova, J., Setinova, I., Kainarova, A., Golias, J., Pavlaskova, K., Honzova, S., and Tuckova, L. (2011). A new approach to the isolation and characterization of wheat flour allergens. Clin Exp Allergy 41, 1031-1043.

Tablin, F., Oliver, A.E., Walker, N.J., Crowe, L.M., and Crowe, J.H. (1996). Membrane phase transition of intact human platelets: correlation with cold-induced activation. J Cell Physiol 168, 305-313.

Tomczak, M.M., Hincha, D.K., Estrada, S.D., Wolkers, W.F., Crowe, L.M., Feeney, R.E., Tablin, F., and Crowe, J.H. (2002). A mechanism for stabilization of membranes at low temperatures by an antifreeze protein. Biophys J 82, 874-881.

Tomczak, M.M., Crowe J.H. (2002)I. The Interaction of Antifreeze Proteins with Model Membranes and Cells. In Fish antifreeze proteins, W.S. publishing., ed., pp. 187-212.

Tomczak, M.M., Hincha, D.K., Estrada, S.D., Feeney, R.E., and Crowe, J.H. (2001). Antifreeze proteins differentially affect model membranes during freezing. Biochimica et Biophysica Acta (BBA) - Biomembranes 1511, 255-263.

Urrutia, M.E., Duman, J.G., and Knight, C.A. (1992). Plant thermal hysteresis proteins. Biochim Biophys Acta 1121, 199-206.

Venketesh, S., and Dayananda, C. (2008). Properties, Potentials, and Prospects of Antifreeze Proteins. Critical Reviews in Biotechnology 28, 57-82.

Wang, Y., Wang, Z., Xu, Q., Du, G., Hua, Z., Liu, L., Li, J., and Chen, J. (2009). Lowering induction temperature for enhanced production of polygalacturonate lyase in recombinant *Pichia pastoris*. Process Biochemistry 44, 949-954.

Warren, G., Mueller, GM., Mckown, RL. (1992). Ice crystal growth suppression polypeptides and method of making, pp. 350-530.

Wathen, B., Kuiper, M., Walker, V., and Jia, Z. (2004). New Simulation Model of Multicomponent Crystal Growth And Inhibition. Chemistry – A European Journal 10, 1598-1605.

Winfield, M.O., Lu, C., Wilson, I.D., Coghill, J.A., and Edwards, K.J. (2010). Plant responses to cold: transcriptome analysis of wheat. Plant Biotechnology Journal 8, 749-771.

Wu, Y., and Fletcher, G.L. (2001). Efficacy of antifreeze protein types in protecting liposome membrane integrity depends on phospholipid class. Biochimica et Biophysica Acta (BBA) - General Subjects 1524, 11-16.

Yaish, M.W., Doxey, A.C., McConkey, B.J., Moffatt, B.A., and Griffith, M. (2006). Cold-active winter rye glucanases with ice-binding capacity. Plant Physiol 141, 1459-1472.

Yang, D.S., Hon, W.C., Bubanko, S., Xue, Y., Seetharaman, J., Hew, C.L., and Sicheri, F. (1998). Identification of the ice-binding surface on a type III antifreeze protein with a "flatness function" algorithm. Biophys J 74, 2142-2151.

Yeh, Y., and Feeney, R.E. (1996). Antifreeze Proteins: Structures and Mechanisms of Function. Chem Rev 96, 601-618.

Younis, A.I., Rooks, B., Khan, S., and Gould, K.G. (1998). The effects of antifreeze peptide III (AFP) and insulin transferrin selenium (ITS) on cryopreservation of chimpanzee (*Pan troglodytes*) spermatozoa. J Androl 19, 207-214.

Yue, C.W., and Zhang, Y.Z. (2009). Cloning and expression of *Tenebrio molitor* antifreeze protein in *Escherichia coli*. Mol Biol Rep 36, 529-536.

Zhao, H., Xue, C., Wang, Y., Yao, X., and Liu, Z. (2008). Increasing the cell viability and heterologous protein expression of *Pichia pastoris* mutant deficient in PMR1 gene by culture condition optimization. Applied Microbiology and Biotechnology 81, 235-241.

Web site:

- http://www.its.caltech.edu/~atomic/snowcrystals/ice/ice.htm
- http://www.lsbu.ac.uk/water/ice1h.html
- http://www.cbs.dtu.dk/services/TargetP
- http://allergen.nihs.go.jp/ADFS/index.jsp